

## CHAPTER 6

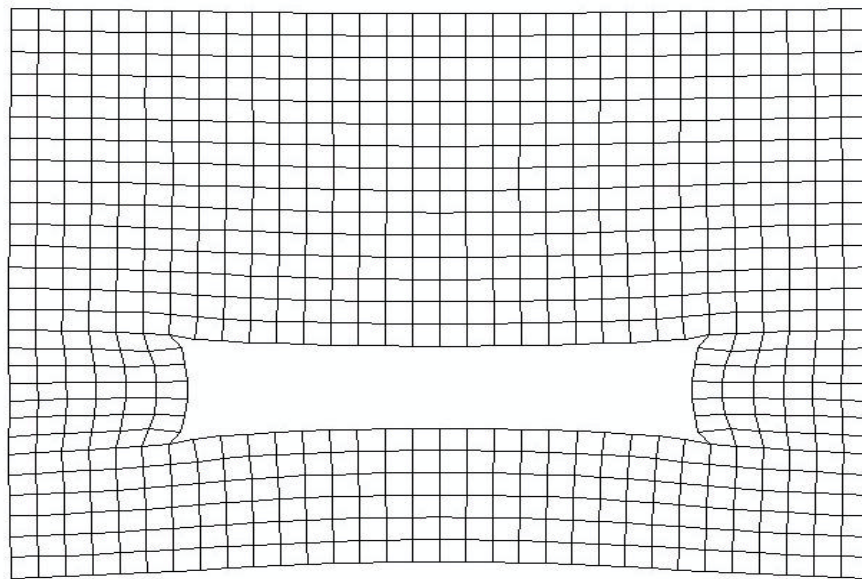
# ROOF STRESS WITH INTERFACE SLIDING BETWEEN LAYERS

### 6.1 Introduction

Field measurements have confirmed that roof failure is more likely to occur in a laminated weak roof subjected to high horizontal stress. Since there are weak interfaces between the laminated layers, these layers may slide and separate. Over the years, some researchers have studied the slip between coalbeds and surrounding roof rocks and the separation between the roof layers using numerical methods. For example, the effects of roof and floor interface slip on coal pillar behavior were analyzed using a numerical software, called FLAC, by Iannacchione (1990). However, since the interfaces between roof/floor and coal and among the roof layers become discontinuous during the numerical analysis, many numerical softwares can not handle them. In addition, a coal pillar will move toward an entry under a high horizontal stress. Up to now, researches about sliding and separating between roof layers and coal seam in a high horizontal stress have been scarce. Consequently, it is still relatively unknown regarding how the interfaces influence the stress in the immediate roof of an entry, especially under a high horizontal stress.

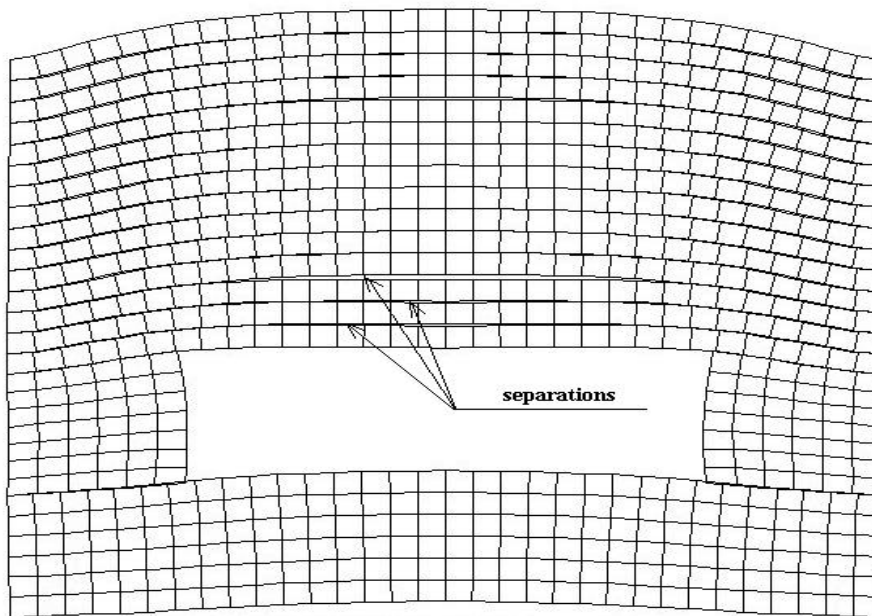
Figs. 6-1 and 6-2 show the strata deformations, simulated by means of the finite element method, around an entry in different situations. They indicate that the strata deformations with the interfaces between the coal and roof/floor and among roof layers are more reasonable, no matter if a horizontal stress occurs. These figures also show that the results of the finite element analysis are more reasonable when the interfaces are taken into account. Without the interfaces, the roof bolt functions can not be simulated by using the numerical analysis methods. Therefore, in this chapter, the effects of the roof and coal interface slip and the different layer interface slip in the roof on the roof stress are analyzed by using the finite element analysis software named ABAQUS.

Since there are some technical problems in the three-dimensional finite element analysis involving the finite sliding between two deformable bodies, the two-dimensional finite element analysis (plane strain) is used in this study.



DISPLACEMENT MAGNIFICATION FACTOR = 100.

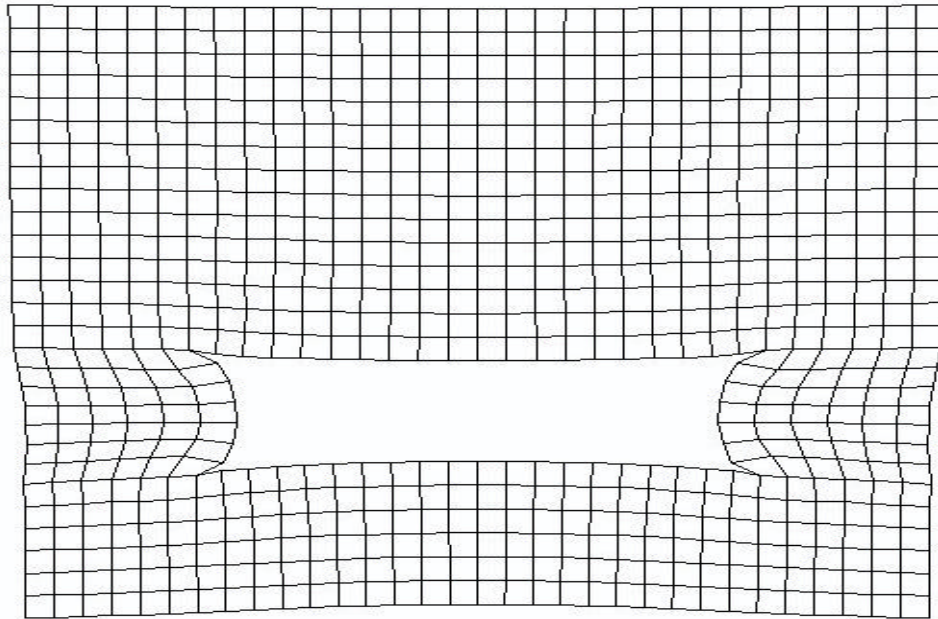
**(a) Deformation without Sliding**



DISPLACEMENT MAGNIFICATION FACTOR = 100.

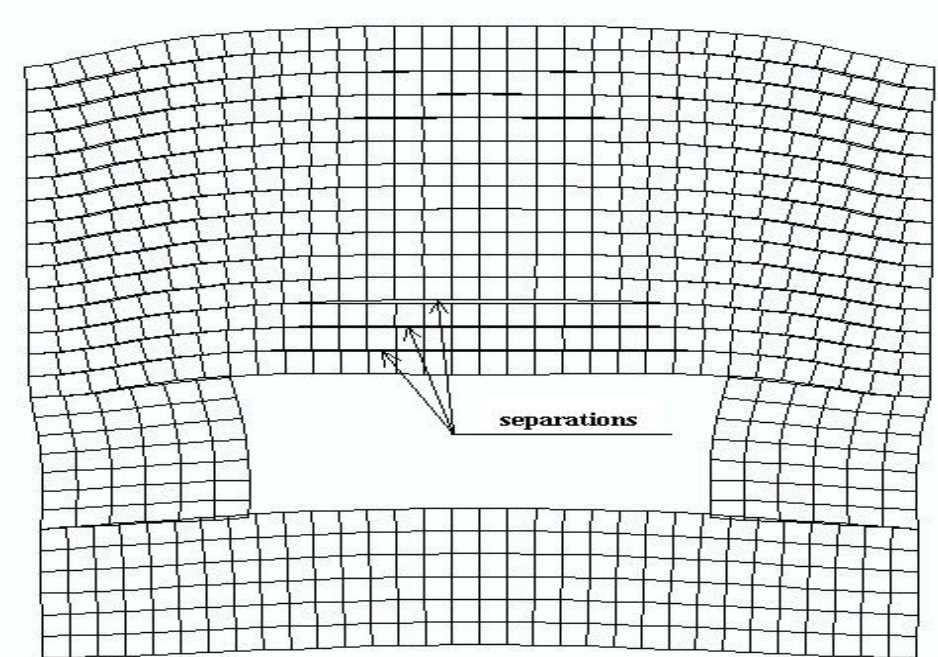
**(b) Deformation with Sliding**

**Fig. 6-1 Strata Deformations without/with Sliding between Roof/Floor and Coal and between Roof Layers without Horizontal Stress**



DISPLACEMENT MAGNIFICATION FACTOR = 100.

(a) Deformation without sliding



DISPLACEMENT MAGNIFICATION FACTOR = 100.

(b) Deformation with Sliding

**Fig. 6-2 Strata Deformations without/with Sliding between Roof/Floor and Coal and between Roof Layers with Horizontal Stress**

## 6.2 Research Scope and Methods

### 6.2.1 Research Scope

Generally, the following factors may control the effects of the interfaces between the roof/floor and coal and among the roof layers on the stress in the immediate roof:

- a. the cohesion and coefficients of friction in the interfaces;
- b. the thickness of the roof layers;
- c. the roof properties; and
- d. the vertical and horizontal stresses

The interface between coal and surrounding roof/floor rocks always represents a sharp change in lithology. The surface is usually smooth. The cohesion in this type of interface is small. The cohesion in the interfaces in the laminated roof is also small. Therefore, it is assumed in this study that the cohesion in all interfaces is zero. The coefficient of friction in the interfaces is 0.1, 0.2, 0.3, 0.4, 0.5, 0.6, 0.7, and 0.8, respectively.

Field measurements have confirmed that the roof failures often occur in the laminated roof, where the roof consists of numerous thin rock layers. Generally, the thinner the roof layer is, the more easily the roof layer fails. In this study, the thickness of each roof layer is equal to 1 ft. Assume that the maximum height of the laminated roof is 10 ft.

Although the roof properties are important, they have little effect on the pattern of stress distributions in the roof, as analyzed in the previous chapters. Therefore, in this chapter, only the weak roof is used.

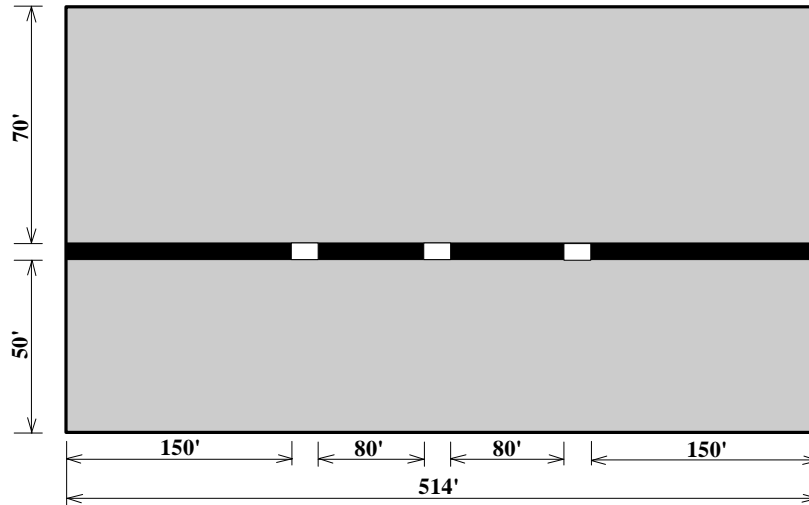
Previous stress measurements have shown that in the eastern United States, the magnitude of the maximum horizontal stress is typically three times greater than the vertical stresses<sup>[28]</sup>. In addition, some field measurements (Table 2) showed that the ratio of horizontal stress to the vertical stress ranged from 4.0 to 7.0. In this study, the overburden depth is 800 ft. Therefore, the stress ratio (R) of the horizontal stress to the vertical stress in this study is 3.0, 4.0, 5.0, 6.0, and 7.0, respectively.

## 6.2.2 Finite Element Models

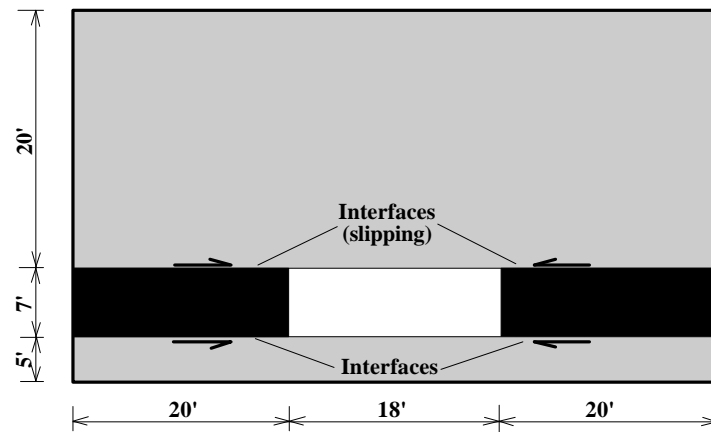
The models used in this study are shown in Fig. 6-3. There are two types of models, a global model and a submodel. In these models, the entry width is 18 ft and the coal thickness is 7 ft. In the global model, the thickness of the floor is 50 ft and the thickness of the roof is 70 ft. The total length of the global model is 514 ft, as shown in Fig. 6-3(a). In the submodel, the floor is 5 ft thick, the roof is 20 ft thick, and the model length is 38 ft, as shown in Fig. 6-3(b) and (c). In the global model, no interfaces are involved. The purpose of the global model is to determine the boundary conditions for the submodel. The element sizes in the global model are 1 ft by 1 ft, and 1ft by 2 ft. In the submodel shown in Fig. 6-3(b), the interfaces appear only between the coal and the roof/floor. In the other submodel, the interfaces between the coal and the roof/floor and among the roof layers are involved. The element size in the roof and coal seam is 0.5 ft by 0.5 ft, and in the floor, it is 1 ft by 1 ft. In the global model, there are three entries. Generally, the stress around the middle entry is larger than that around the other entries when a horizontal stress does not occur. When a horizontal stress exists, the stress around the two side entries is slightly larger than that around the middle one. In addition, the stress around the side entries is not symmetrical. Therefore, the submodels simulate one of the side entries (the right side entry). The rock properties used in this study are listed in Table 6-1.

**Table 6-1 Rock Properties Used in The Study**

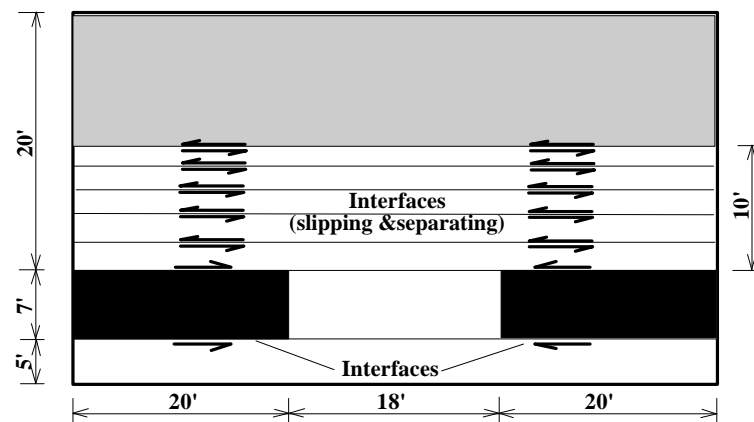
	Rock Type	Young's Modulus (x 10 <sup>6</sup> psi)	Poisson's Ratio	Uniaxial Comp. Strength (psi)	Cohesion (psi)	Friction Angle (°)
<b>Main Roof</b>	<b>Siltstone</b>	2.1	0.21	6,500	1,350	25
	<b>Shale</b>	1.5	0.22	5,500	1,200	28
	<b>Shale with sandstone</b>	1.68	0.22	5,200	1,630	30
<b>Immed. Roof</b>	<b>Weak shale</b>	0.55	0.25	3,500	1,000	32
<b>Seam</b>	<b>Coal</b>	0.35	0.30	1,200	900	35
<b>Immed. Floor</b>	<b>Shale</b>	1.5	0.22	5,500	1,200	26
<b>Main Floor</b>	<b>Claystone</b>	1.1	0.30	1,300	760	35
	<b>Shale with sandstone</b>	1.68	0.22	5,200	1,630	30



(a) Global Model



(b) Submodel with Interfaces between Coal Seam and Roof/Floor



(c) Submodel with Interfaces between Coal Seam and Roof/Floor and among Roof Layers

Fig. 6-3 Finite Element Models

In this study, four types of stress in the entry roof are analyzed: (1) the Von Mises stress, (2) the minimum principal stress, (3) the maximum principal stress, and (4) the stress along the horizontal direction. In order to study the stress distributions in the roof, the stresses will be discussed at three roof levels: at the roof line level (level 1), at 1ft-deep level (level 2), and at 5ft-deep level (level 3).

In this study, first the stresses in the roof are analyzed for the different stress ratios ( $R$ ) of the horizontal to the vertical stress and the different coefficients of friction when the interfaces between the coal and the roof/floor are involved. Then, the stresses in the roof are studied for the different situations when the interfaces occur between the coal and the roof/floor and between the roof layers. In this case, the thickness of each roof layer is 1 ft.

### **6.3 Roof Stress with Interfaces between Coal and Roof/Floor**

Generally, when the interfaces between the coal seam and the roof/floor occur, the stress in the roof decreases because of the slip of the coal seam (or pillar). The stress is different for the different coefficients of friction in the interfaces. In this section, the stress distributions in the roof are analyzed for the different coefficients of friction and different stress ratios.

#### **6.3.1 Von-Mises Stress in the Roof**

The Von-Mises stress at the roof line level is shown in Fig. 6-4 for different stress ratios ( $R$ ) and coefficients of friction ( $f$ ). In this figure, the horizontal axis represents the distance from one rib side of the entry while the vertical one is for the stress. In this figure, the capital letter  $R$  stands for the stress ratio of the horizontal to the vertical stress, and small letter  $f$  stands for the coefficient of friction in the interfaces between the coal seam and the roof/floor.

Fig. 6-4 indicates that the Von-Mises stress at the roof line level has the following characteristics:

- a. The patterns of the Von-Mises stress distributions in the roof with the interfaces are similar to that without the interfaces;
- b. The Von-Mises stress is concentrated at the two rib sides of the entry;
- c. The Von-Mises stress is not symmetrical. In this case, the stress at the left side is slightly larger than that at the other side because of the difference of movement between the two entry ribs;
- d. The Von-Mises stress relieves to some degree when the interface sliding between the coal seam and the roof/floor occurs;
- e. The Von-Mises stress increases with the coefficient of friction ( $f$ ) in the interfaces; and
- f. The bigger the stress ratio ( $R$ ) is, the larger the Von-Mises stress is.

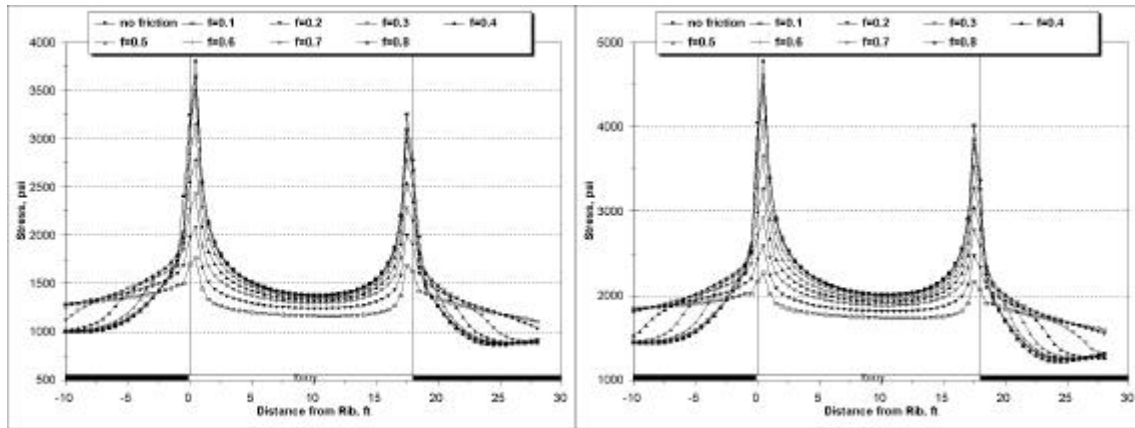
The typical Von-Mises stress distribution at the roof line level is shown in Fig. 6-5. It shows the Von-Mises stress in the half entry roof for different coefficients of friction. In this case, the stress ratio ( $R$ ) is equal to 3. It clearly indicates that the Von-Mises stress relieves to some degree when the interface sliding occurs. For example, the maximum Von-Mises stress at the roof line level is about 3,750 psi without interface sliding. It reduces to about 1,750 psi when the coefficient of friction in the interfaces is 0.1. In addition, the Von-Mises stress increases obviously with the coefficient of friction ( $f$ ). For instance, when the coefficient of friction ( $f$ ) increases to 0.5, the maximum Von-Mises stress at the roof reaches about 3,200 psi. Generally, the maximum stress in the roof occurs near the entry rib sides.

As the stress ratio ( $R$ ) of the horizontal to the vertical stress increases, the Von-Mises stress at the roof line level increases. Fig. 6-6 shows the Von-Mises stress at the rib sides for different stress ratios. Since the stress at the left side of the entry is slightly larger than that at the other side, the stress at the left side is mainly analyzed in the following.

At the different roof levels, the stress is different. In order to understand the stress distributions in the roof, the Von-Mises stress at other two roof levels (level 2 and level 3) is analyzed.

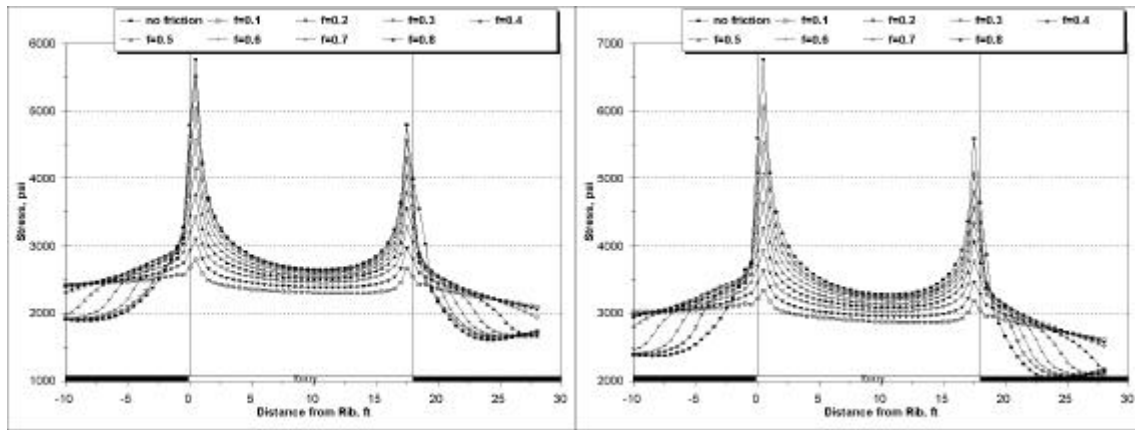
Fig. 6-7 shows the Von-Mises stress at level 2 and level 3. At level 2, the Von-Mises stress over the entry rib sides is less than that at level 1. But its pattern is similar to that at level 1. Over the entry center, the stress increases. At level 2, the maximum Von-Mises stress occurs over the entry rib sides. But, at level 3, the Von-Mises stress distribution is different from that at level 2. The stress over the entry rib sides is small. The stress at the other roof is larger. In addition, the Von-Mises stress at level 2 and level 3 increases with the stress ratio (R).

The Von-Mises stress distribution in the entry roof is influenced not only by the stress ratio (R) but also by the coefficient of friction (f). Fig. 6-8 shows the Von-Mises stress in the roof for different coefficients of friction, when the stress ratio is 5. Without the interface sliding between the coal seam and the roof/floor, the maximum Von-Mises stress occurs at level 1. At level 2 the stress at the rib sides is significantly less than that at level 1 and the stress distribution at level 3 is different, as shown in Fig. 6-8(a). When the interface sliding between the coal and the roof/floor occurs, the stress distributions are affected by the coefficient of friction (f). For example, if the coefficient of friction (f) is 0.1, the Von-Mises stress at the rib sides at level 2 is near the same as that at level 1, and the stress at level 3 changes significantly, as shown in Fig. 6-8(b). As the coefficient of friction (f) increases, the difference in the Von-Mises stress at the rib sides between these three levels increases while the difference of stress at the entry middle reduces, as shown in Fig. 6-8(c) & (d). In addition, the Von-Mises stress in the roof increases with the coefficient of friction (f).



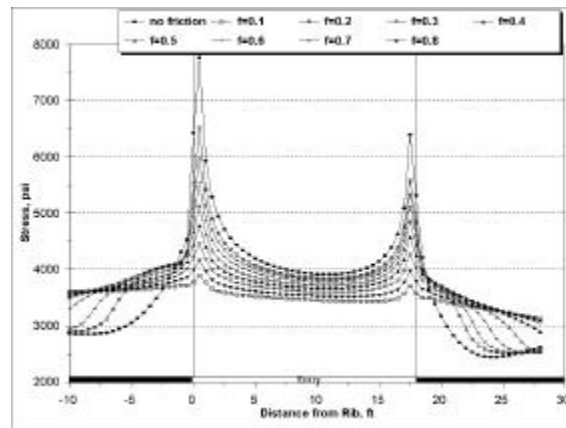
(a) R=3

(b) R=4



(a) R=5

(b) R=6



R=7

Fig. 6-4 Von-Mises Stress at the Roof Line Level (Level 1)

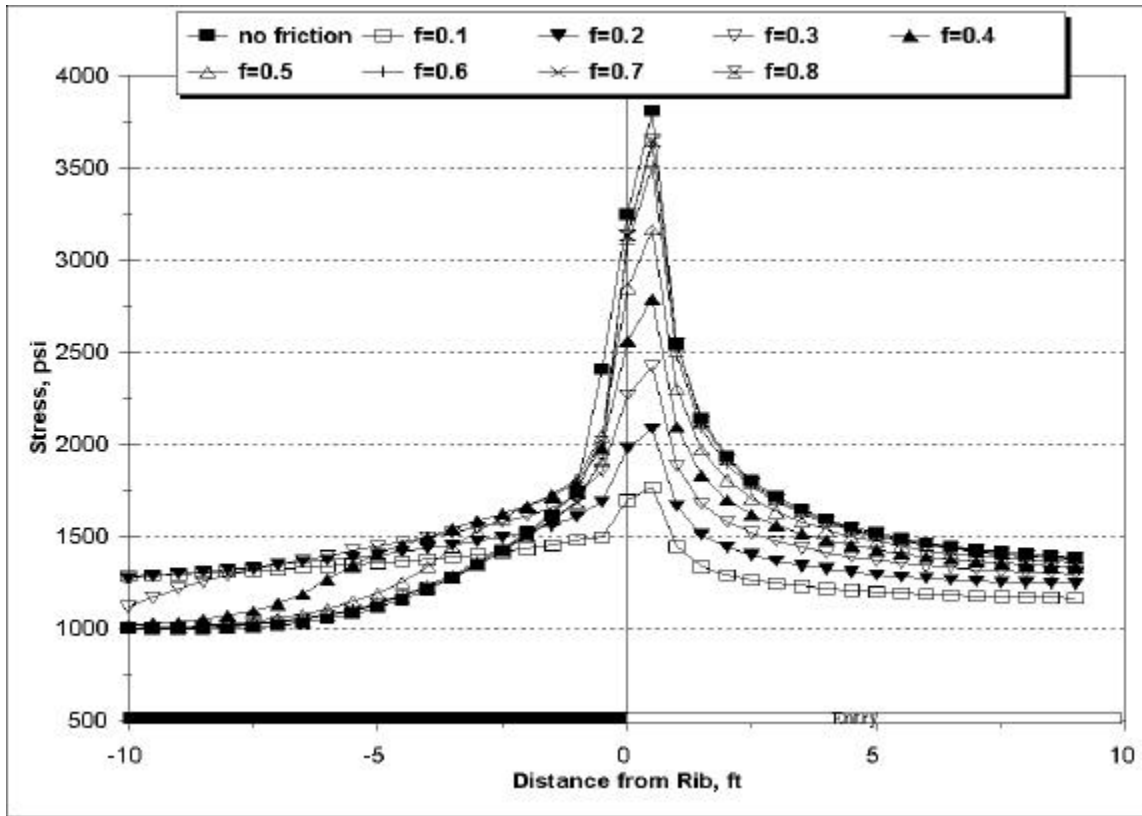


Fig. 6-5 Typical Von-Mises Stress Changes at the Roof Line Level with the Frictional Coefficient (R=3)

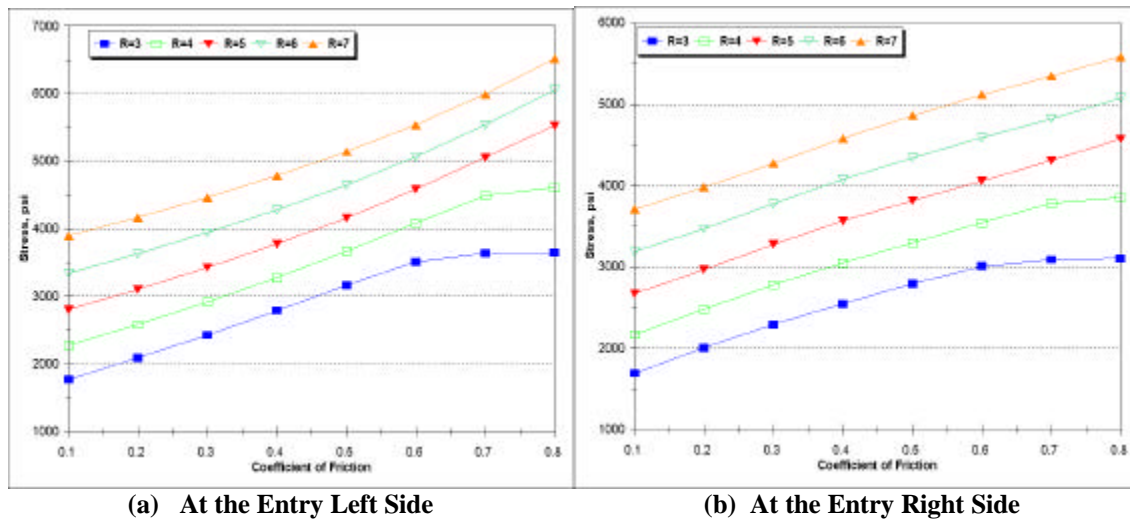
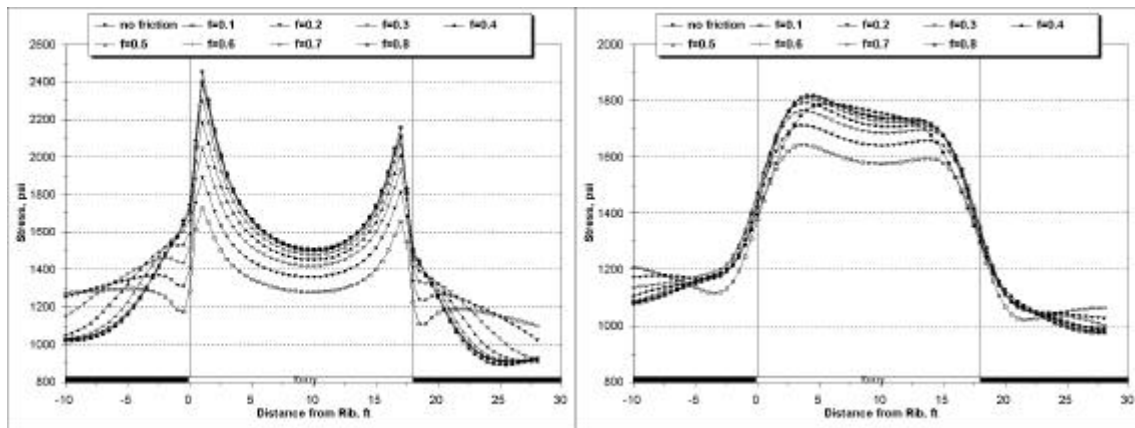
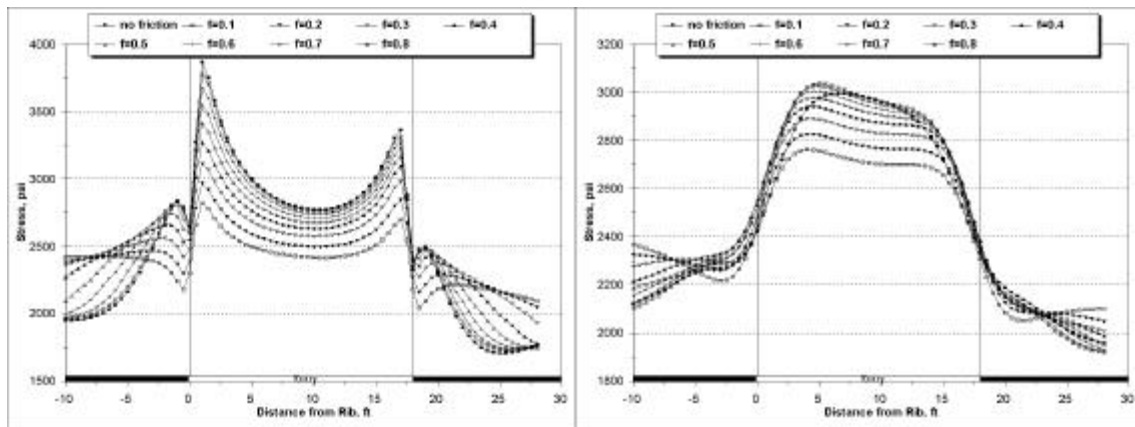


Fig. 6-6 Von-Mises Stress at Two Specified Points in the Roof For Different Stress Ratios (R=3~7)



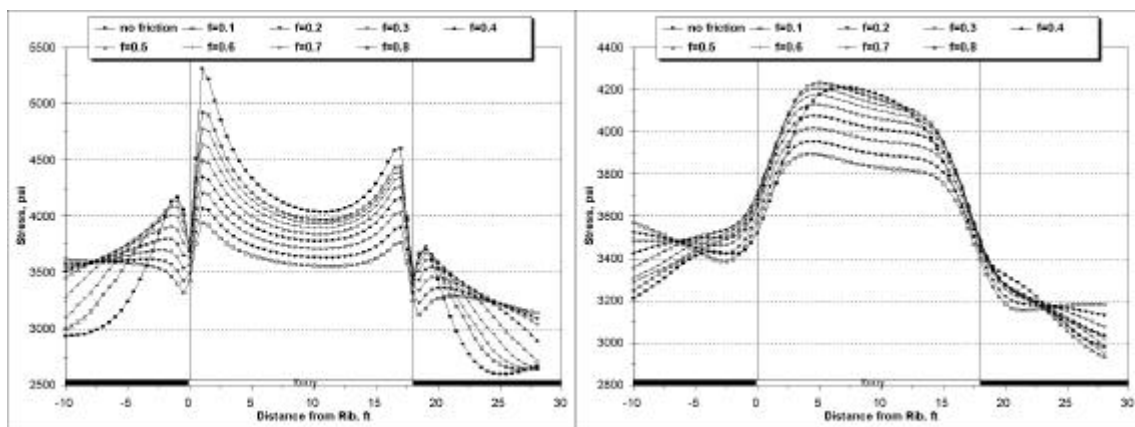
(a) At Level 2 (R=3)

(b) At Level 3 (R=3)



(c) At Level 2 (R=5)

(d) At Level 3 (R=5)



(e) At Level 2 (R=7)

(f) At Level 3 (R=7)

Fig. 6-7 Von-Mises Stress at Different Levels in the Roof

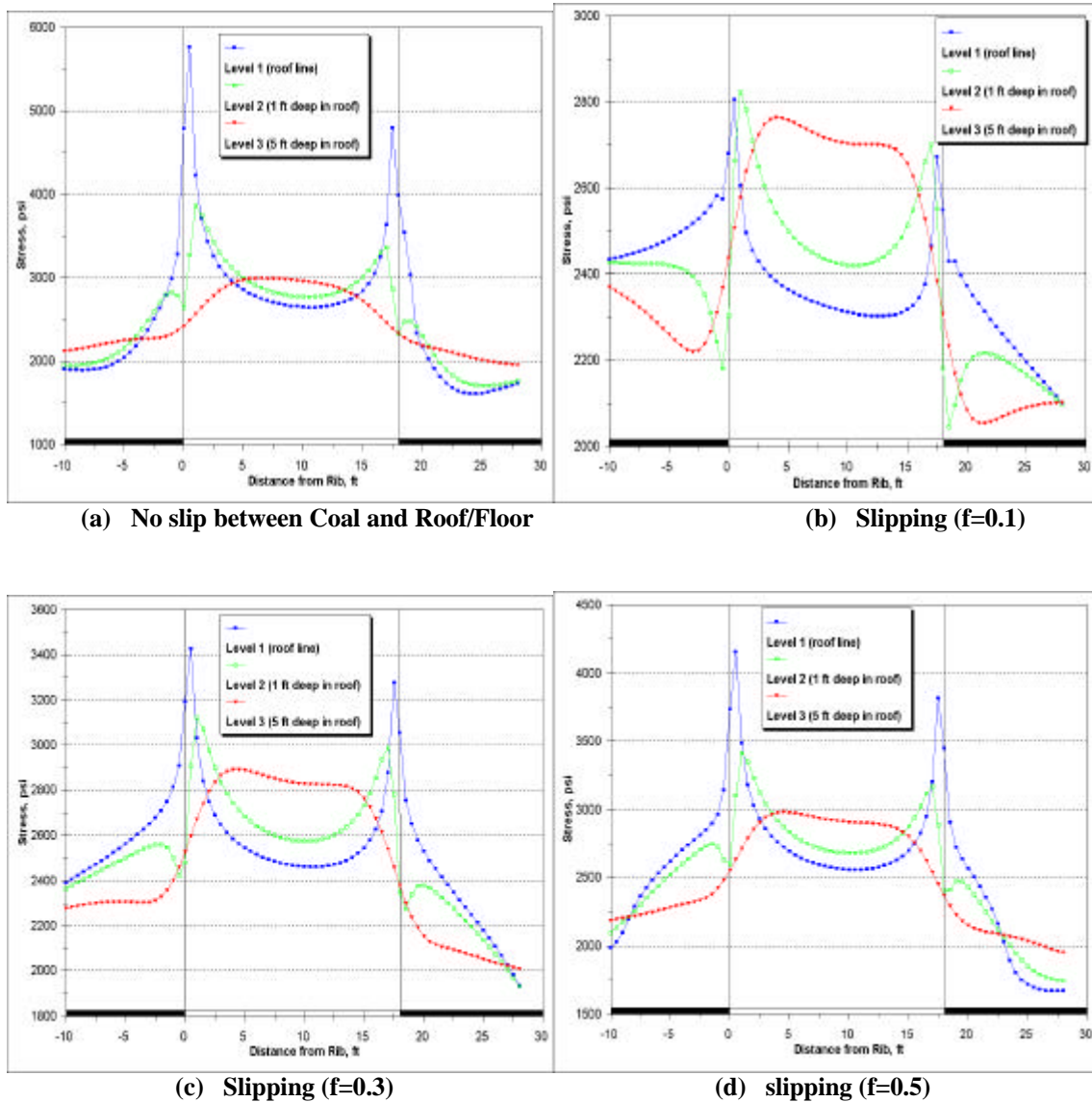


**Fig. 6-8 Typical Von-Mises Stress Distribution in the Roof For the Frictional Coefficient (R=5)**

### 6.3.2 Max. Principal Stress in the Roof

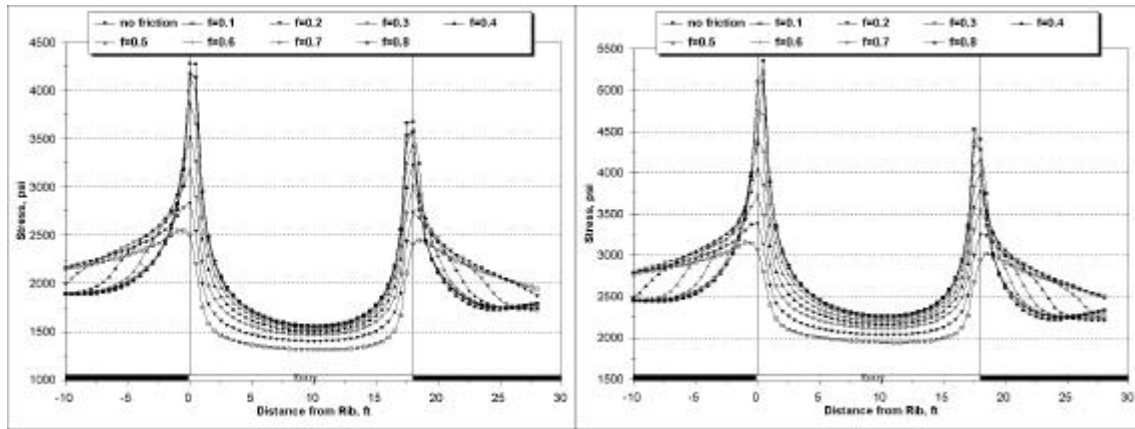
The maximum principal stress at the roof line level (level 1) is shown in Fig. 6-9. It indicates that the maximum principal stress relieves to some degree when the interface sliding between the coal seam and the roof/floor occurs, although the stress concentration also occurs at the two rib sides of the entry. In addition, the maximum principal stress increases with the coefficient of friction in the interfaces and the stress ratio (R) of the horizontal and the vertical stress. The distributions of the maximum principal stress at

level 1 are similar to those of the Von-Mises stress when there is no interface sliding between the coal and the roof/floor. But there is one difference between them; for the Von-Mises stress distribution, the maximum stress occurs at the points located near the entry corner, not just at the entry corner. For the maximum principal stress, the maximum stress occurs just at the entry corner when the stress ratio (R) is 3, as shown in Fig. 6-9(a). When the stress ratio (R) is larger than 3, the maximum Von-Mises stress and the maximum principal stress occur at some points near and at the entry corner, as shown in Fig. 6-9(b)~(e).

When the interface sliding between the coal and the roof/floor occurs, for the maximum principal stress, the location of the maximum stress at the roof line level depends both on the stress ratio (R) and on the coefficient of friction (f) in the interfaces. When the coefficient of friction (f) is equal to and less than 0.6, the maximum stress is located at the entry corner. When the coefficient of friction (f) is more than 0.6 and the stress ratio (R) is larger than 3, the maximum stress moves toward the entry center very slightly, as shown in Fig. 6-9.

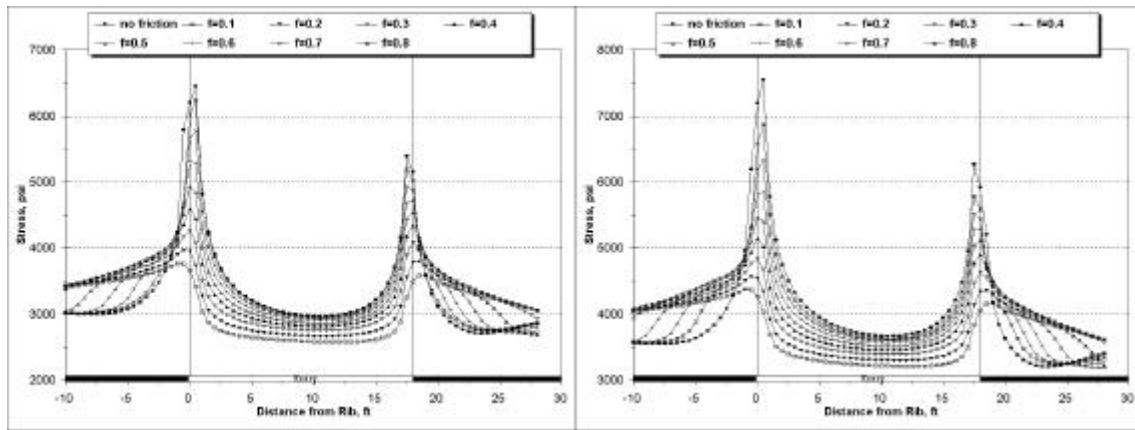
The typical maximum principal stress distributions at the roof line level (level 1) are shown in Fig. 6-10. These figures show the maximum principal stress change with the stress ratio (R) of the horizontal and the vertical stress and the coefficient of friction (f) in the interfaces. The maximum principal stress at the two points (P1 and P2) on the entry corner is shown in Fig 6-11. Generally, the maximum principal stress increases linearly with the stress ratio (R) and the coefficient of friction (f).

The maximum principal stress at the different roof levels is shown in Fig. 6-12. At level 2 and level 3, the maximum principal stress at the rib sides is always smaller than that at level 1 (the roof line level). But the principal stress at the other sections of the entry roof is larger. In addition, the coefficient of friction (f) affects the stress distributions in the roof. For example, without the interface sliding between the coal seam and the roof/floor, the stress difference at the entry center between level 1 and level 3 is small and the principal stress distribution at level 3 changes slightly. With interface sliding, the difference becomes significant. The larger the difference, the smaller the coefficient of friction.



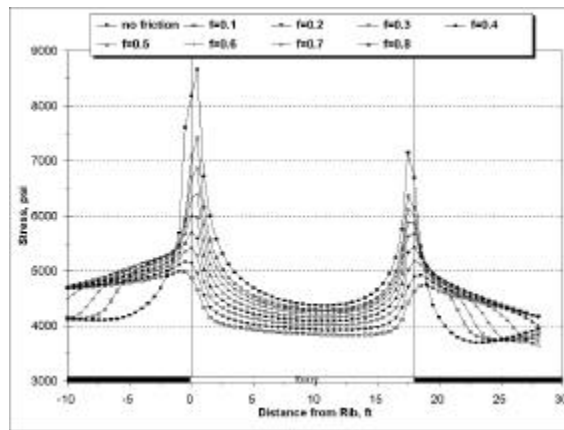
(a) R=3

(b) R=4



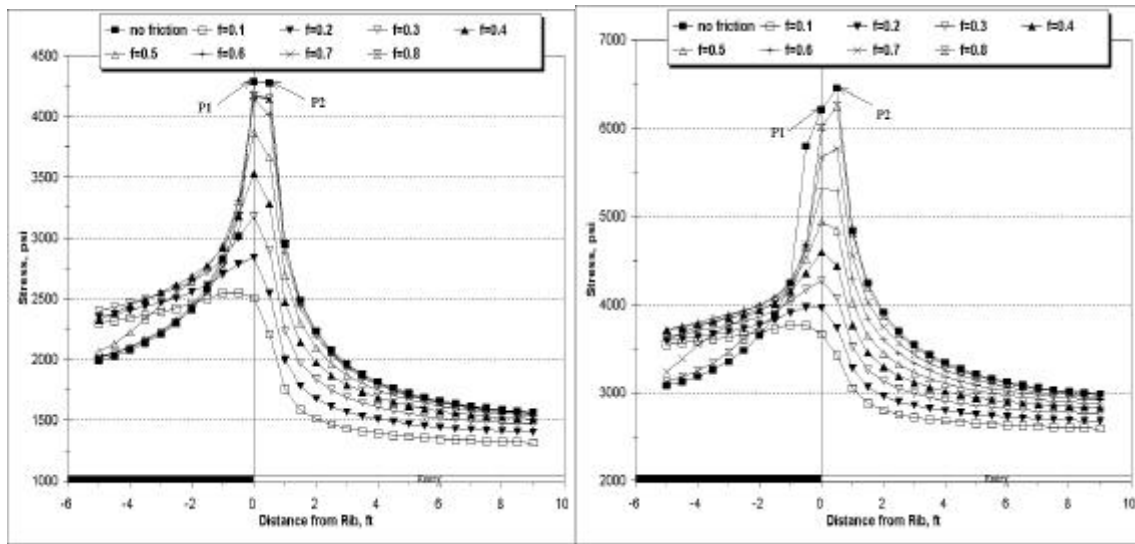
(c) R=5

(d) R=6



R=7

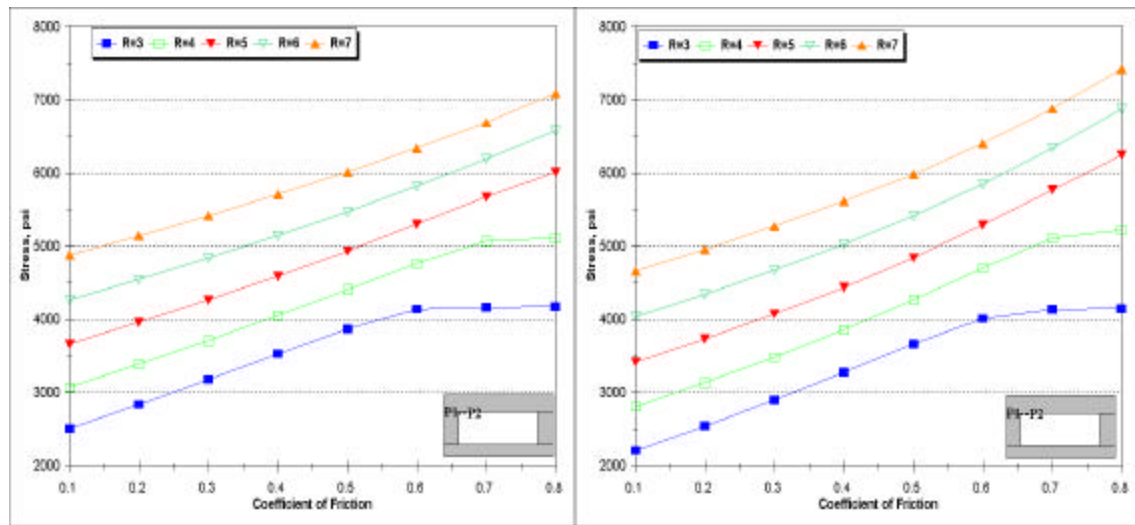
Fig. 6-9 Max. Principal Stress at the Roof Line Level  
 $(R = \sigma_h / \sigma_v ; \sigma_h - \text{Horizontal stress, } \sigma_v - \text{Vertical Stress})$



(a) R=3

(b) R=5

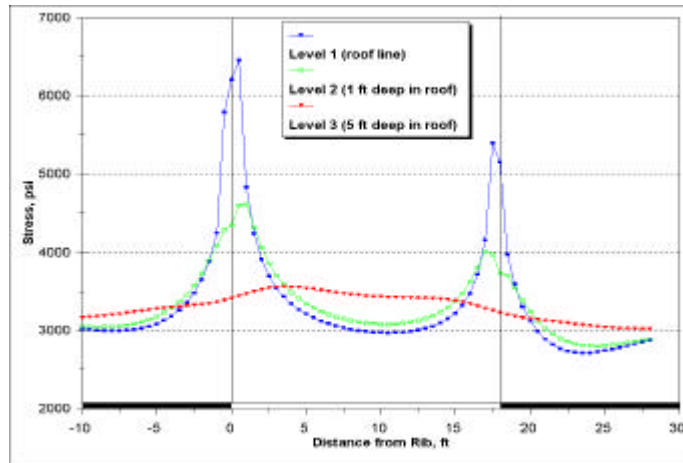
Fig. 6-10 Typical Max. Principal Stress Change at the Roof Line Level with Different Frictional Coefficients



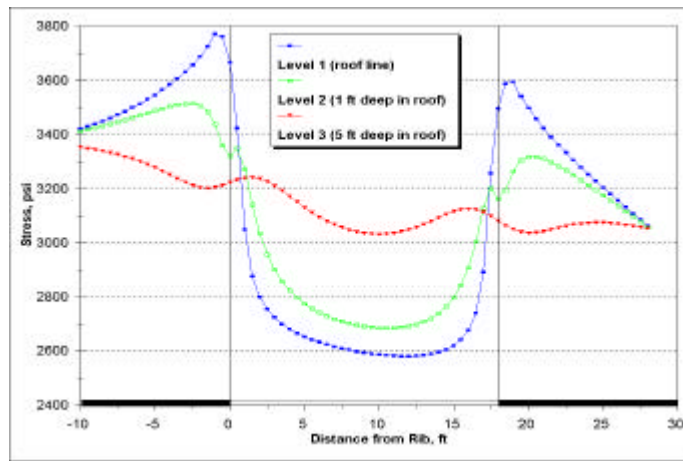
(a) at Point P1

(b) at Point P2

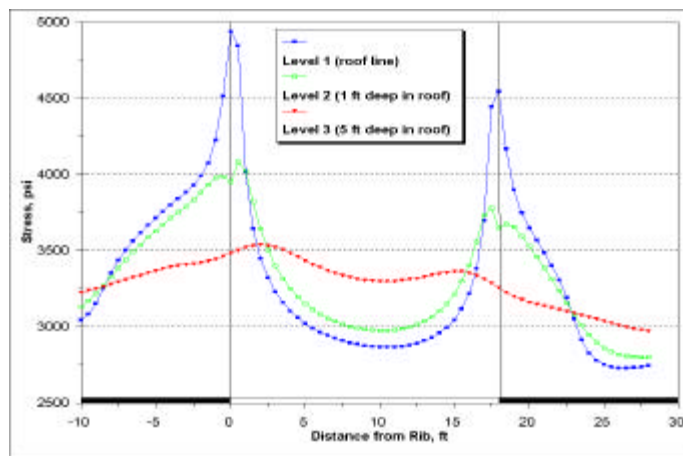
Fig. 6-11 Max. Principal Stress at the Specified Points



(a) No Slipping



(b) Slipping ( $f=0.1$ )



(c) Slipping ( $f=0.5$ )

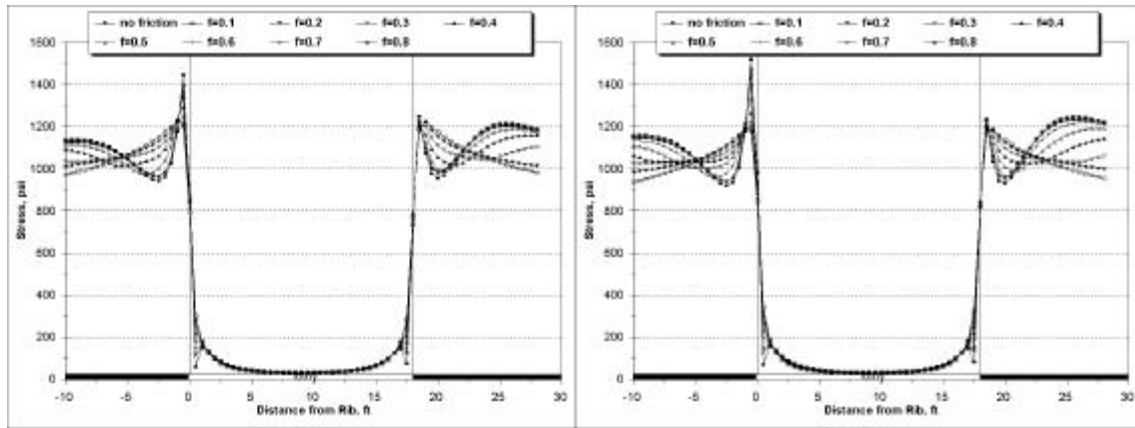
Fig. 6-12 Typical Max. Principal Stress Distribution at Different Levels (Stress Ratio  $R=5$ )

### 6.3.3 Min. Principal Stress in the Roof

The minimum principal stress at the roof line level (level 1) is shown in Fig. 6-13. When the interface sliding between the coal and the roof/floor occurs, the minimum principal stress at level 1 is different from that without interface sliding. Without interface sliding, the minimum principal stress near the entry rib sides is smaller. When the stress ratio ( $R$ ) of the horizontal to the vertical stress is small, the stress at the two rib sides is nearly the same as that at the entry center. This indicates that the tensile stress could more likely occur at the entry rib sides when there is no slip between the coal and the roof/floor.

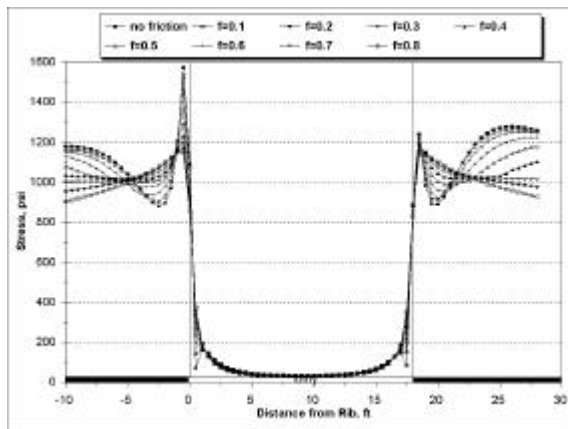
With interface sliding, the minimum principal stress distribution appears like that without horizontal stress. The minimum magnitude of the minimum principal stress always occurs at the entry center. The influence of the coefficient of friction in the interfaces on the minimum principal stress is very small, and can be ignored. In addition, the stress ratio ( $R$ ) has a little effect on the minimum principal stress at the roof line level.

Fig. 6-14 shows the typical distributions of the minimum principal stress at the different roof levels for stress ratio ( $R$ ) being 5. In the entry roof, the minimum principal stress increases with the depth. Generally, the minimum magnitude of the minimum principal stress occurs at the entry center, although the stress near the two rib sides is small when no interface sliding between the coal and the roof/floor is involved. These figures also indicate that the influences of the stress ratio and the coefficient of friction on the minimum principal stress at the roof line level is very small.

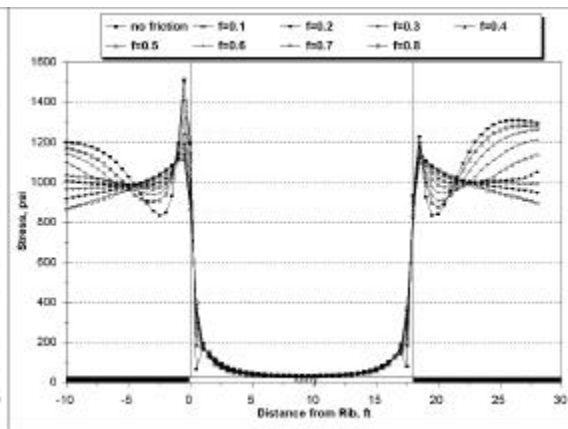


(a) R=3

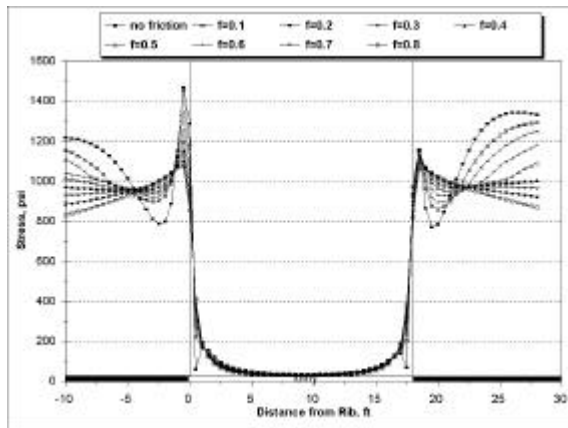
(b) R=4



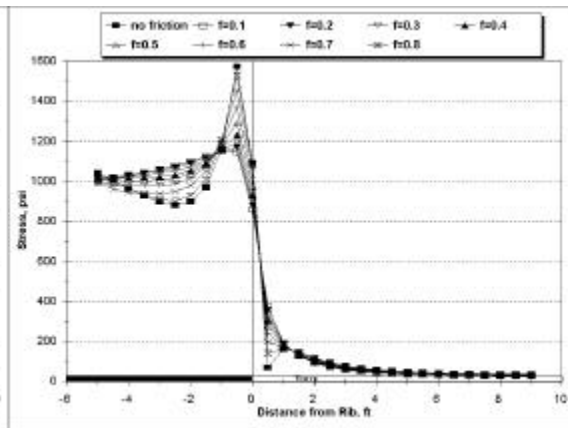
(c) R=5



(d) R=6

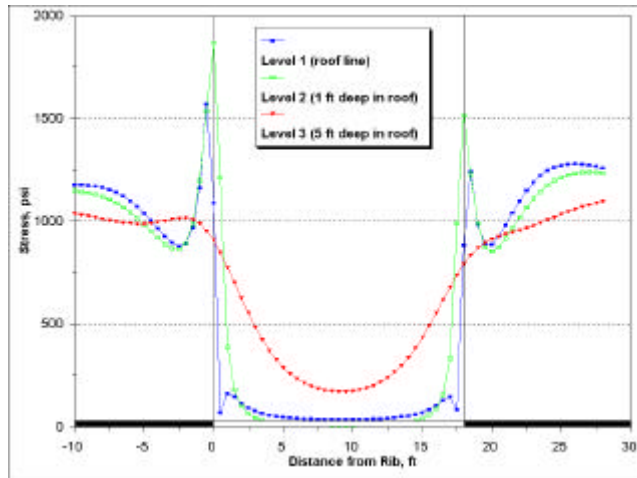


(e) R=7

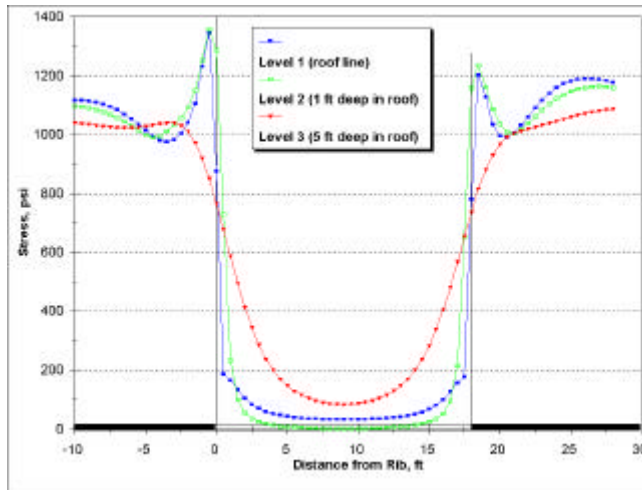


(f) Typical Distribution (R=5)

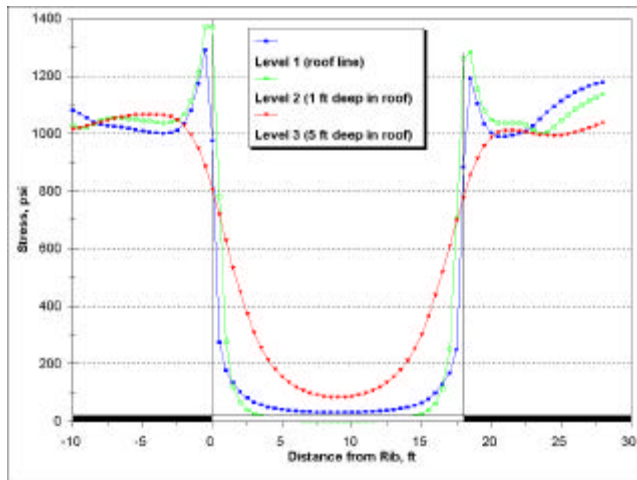
Fig. 6-13 Min. Principal Stress at the Roof Line Level



(a) No Slipping



(b) Slipping ( $f=0.1$ )



(b) Slipping ( $f=0.5$ )

Fig. 6-14 Typical Min. Principal Stress Distributions at Different Roof Levels (R=5)

#### 6.3.4 Stress along Horizontal Direction in the Roof

In a high horizontal stress field, the horizontal stress is much larger than the vertical stress. Traditionally, it is thought that the horizontal stress will redistribute around an entry. In order to study the stress redistribution in the entry roof, the stress along the horizontal direction in the entry roof is analyzed.

Fig. 6-15 shows the stress along the horizontal direction at the roof line level. It indicates that the stress distribution is similar to that of the maximum principal stress. When no interface sliding between the coal and the roof/floor is involved, the stress is larger. It increases with the stress ratio ( $R$ ). In addition, the maximum stress occurs near the two rib sides of the entry, not just at the two upper corners of the entry. For the maximum principal stress, the maximum stress is just at the two upper corners only when the stress ratio is less than 4 (Fig. 6-9). When the interface sliding is involved, the stress along the horizontal direction relieves to some degree. For example, when the coefficient of friction ( $f$ ) is 0.1, the maximum stress is about 3,500 psi if the stress ratio ( $R$ ) is 5. When the coefficient of friction ( $f$ ) is 0.5, it reaches about 4,700 psi.

The typical distribution of the stress along the horizontal direction at the roof line level is shown in Fig. 6-15(f). When the coefficient of friction ( $f$ ) in the interfaces is less than 0.6, the maximum stress occurs just at the entry corners. When the coefficient of friction ( $f$ ) is more than 0.6, the location of the maximum stress moves toward the entry slightly, not just at the entry corners. Generally, the stress along the horizontal direction at the roof line level is concentrated at the rib sides. It increases with the stress ratio ( $R$ ) and the coefficient of friction ( $f$ ). When a slip occurs between the coal and the roof/floor, the stress along the horizontal direction in the roof relieves to some degree. The smaller the coefficient of friction ( $f$ ) in the interfaces, the larger the degree of the stress relief.

The stress along the horizontal direction in the different roof levels is shown in Fig. 6-16. It is similar to the maximum principal stress. The stress distributions are affected by both the stress ratio ( $R$ ) and the coefficient of friction ( $f$ ).

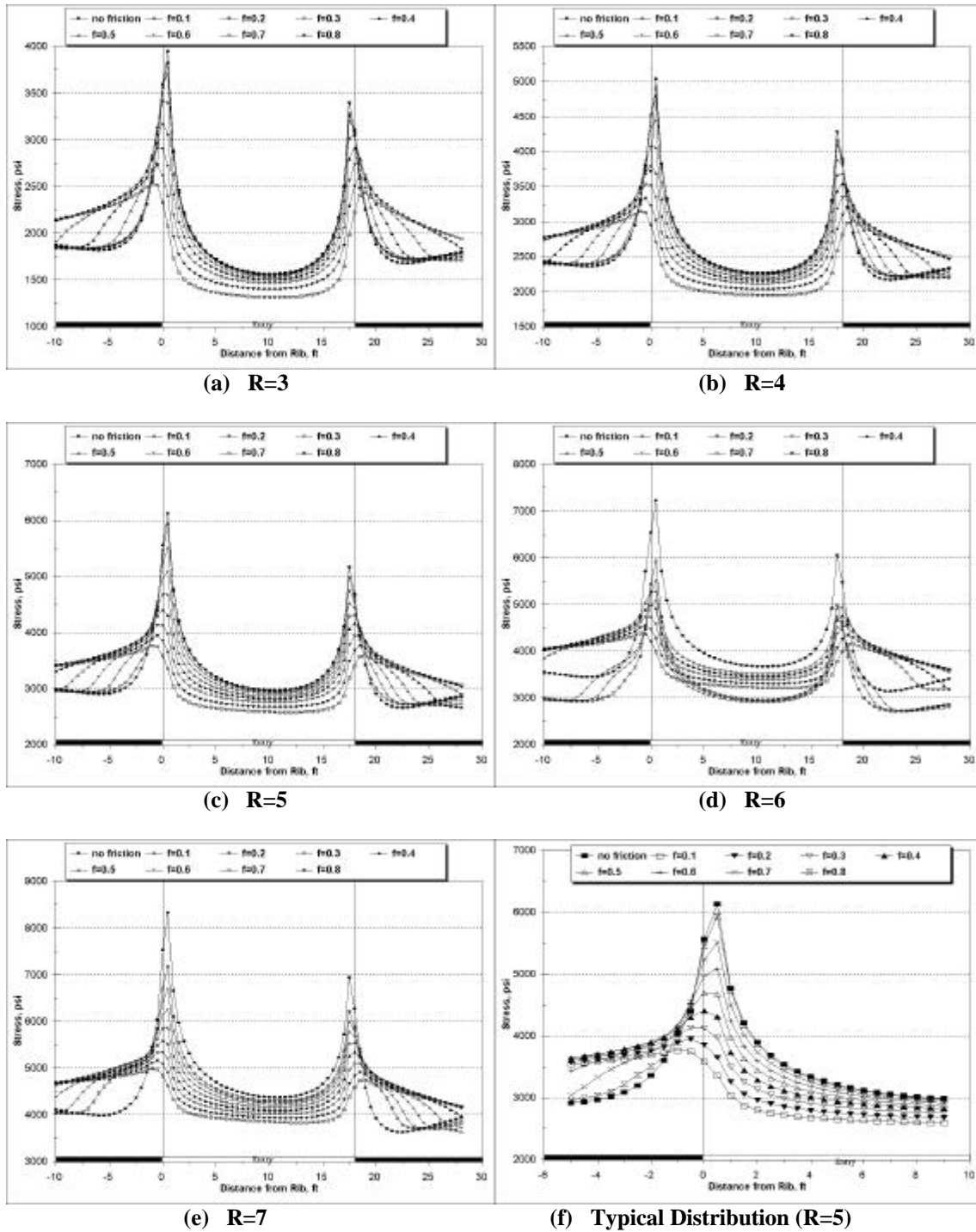
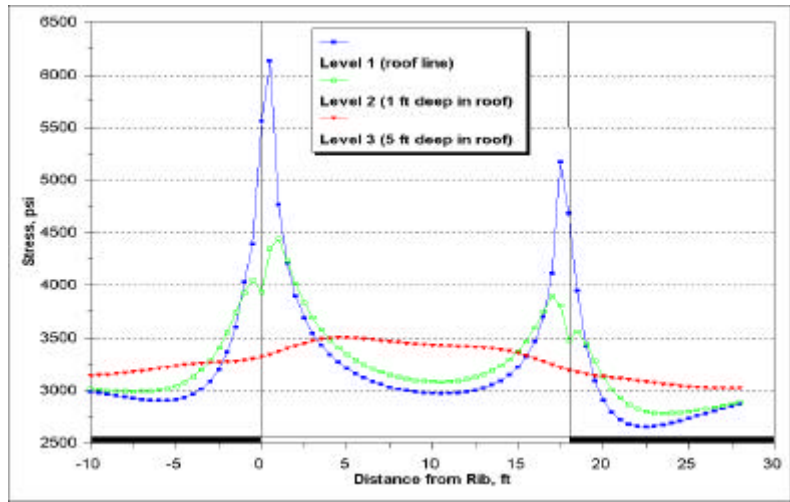
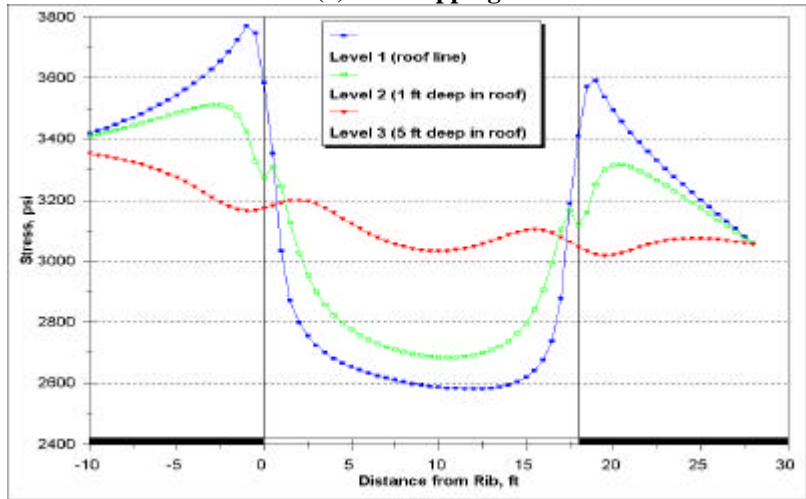


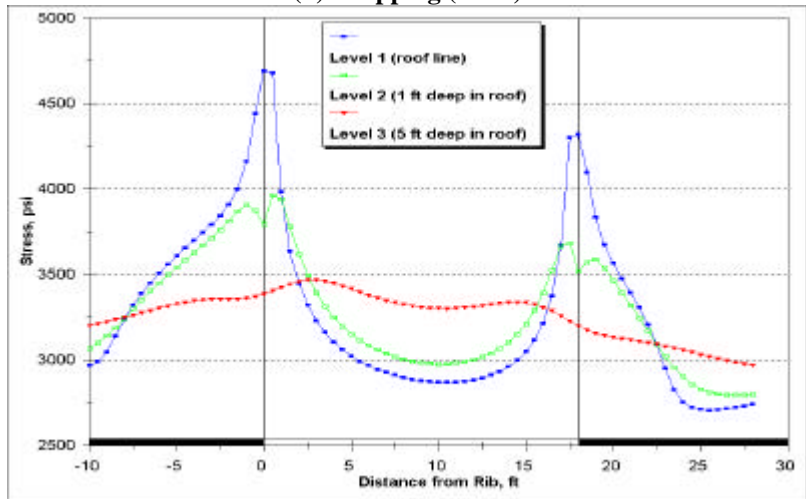
Fig. 6-15 Stress along the Horizontal Direction at the Roof Line Level



(a) No Slipping



(b) Slipping ( $f=0.1$ )



(c) Slipping ( $f=0.5$ )

Fig. 6-16 Typical Distribution of the Stress along Horizontal Direction in the Roof ( $R=5$ )

### 6.3.5 Summary

Based on the above stress analyses, it is found that the interface sliding between the coal seam and the roof/floor does have significant effects on the stress distributions in an entry roof. Without the interface sliding, the stress in the roof is larger. The stress in the roof relieves to some degree when the interface sliding is involved. The degree of stress relief depends on the coefficient of friction ( $f$ ) in the interfaces. The smaller the frictional coefficient ( $f$ ), the larger the degree of the stress relief.

Usually, the Von-Mises stress, the maximum principal stress, and the stress along the horizontal direction are larger at the roof line level. They increase with the coefficient of friction ( $f$ ) in the interfaces between the coal seam and the roof/floor and the stress ratio ( $R$ ) of the horizontal to the vertical stress. The maximum magnitudes of these stresses occur near the entry rib sides.

The minimum stress of the minimum principal stress may occur near the entry rib sides without the interface sliding between the coal seam and the roof/floor. When the interface sliding occurs, the minimum stress generally occurs at the entry center. In addition, the influence of the stress ratio ( $R$ ) on the minimum principal stress at the roof line level is very small.

## 6.4 Roof Stress with Interfaces Between Layers

In this study, the stress ratio ( $R$ ) of the horizontal to the vertical stress is 3, 5, and 7, respectively. For each stress ratio, the coefficient of friction ( $f_1$ ) between the coal seam and the roof/floor is 0.2, 0.4, and 0.6, respectively. Because the difference in the stress in the roof between with and without interface sliding is small when the coefficient of friction ( $f$ ) between the coal seam and the roof/floor is more than 0.6, based on the previous stress analysis. For each case, the coefficient of friction ( $f_2$ ) between the roof layers is 0.2, 0.3, 0.4, 0.5, and 0.6, respectively. Therefore, there are 45 cases in this study. The total cases are listed in Table 6-2. In addition, the thickness of each roof layer is 1 ft in this study. The Von-Mises stress, the maximum and minimum principal stresses, and the stress along the horizontal direction in the first, second, and fifth roof layers are studied. Since the stresses in the first layer are the largest, the stress distributions in this layer are mainly analyzed.

**Table 6-2 Coefficients of Friction Used in the Study**

Stress Ratio ( $R$ )	Coefficient of frictional * ( $f_1$ )	Coefficient of Friction between Roof Layers ( $f_2$ )				
		0.2	0.3	0.4	0.5	0.6
3	0.2	0.2	0.3	0.4	0.5	0.6
	0.4	0.2	0.3	0.4	0.5	0.6
	0.6	0.2	0.3	0.4	0.5	0.6
5	0.2	0.2	0.3	0.4	0.5	0.6
	0.4	0.2	0.3	0.4	0.5	0.6
	0.6	0.2	0.3	0.4	0.5	0.6
7	0.2	0.2	0.3	0.4	0.5	0.6
	0.4	0.2	0.3	0.4	0.5	0.6
	0.6	0.2	0.3	0.4	0.5	0.6

\* Coefficient of friction between the coal seam and the roof/floor

Since there is interface sliding between the roof layers, the stress in the roof and the roof displacement are different for those without the interface sliding. Generally, the roof separations occur. Fig. 6-17(a)~(c) shows the displacements of the first, second, and fifth roof layers. These figures indicate that the displacement of the first layer is the largest among all layers and that the difference of the displacements of the two opposite surfaces of a roof layer is very small. For example, in the first layer, the difference in the

displacements of its two opposite surfaces is about 0.03 in. In addition, a separation between the opposing surface of a interface occurs. For instance, the maximum separation between the opposing surface is about 0.1 in, as shown in Fig. 6-17(d).

Because of the roof separation, the stress in the entry roof will be different from that discussed previously. In the following, the Von-Mises stress, the maximum and minimum principal stresses, and the stress along the horizontal direction are analyzed.

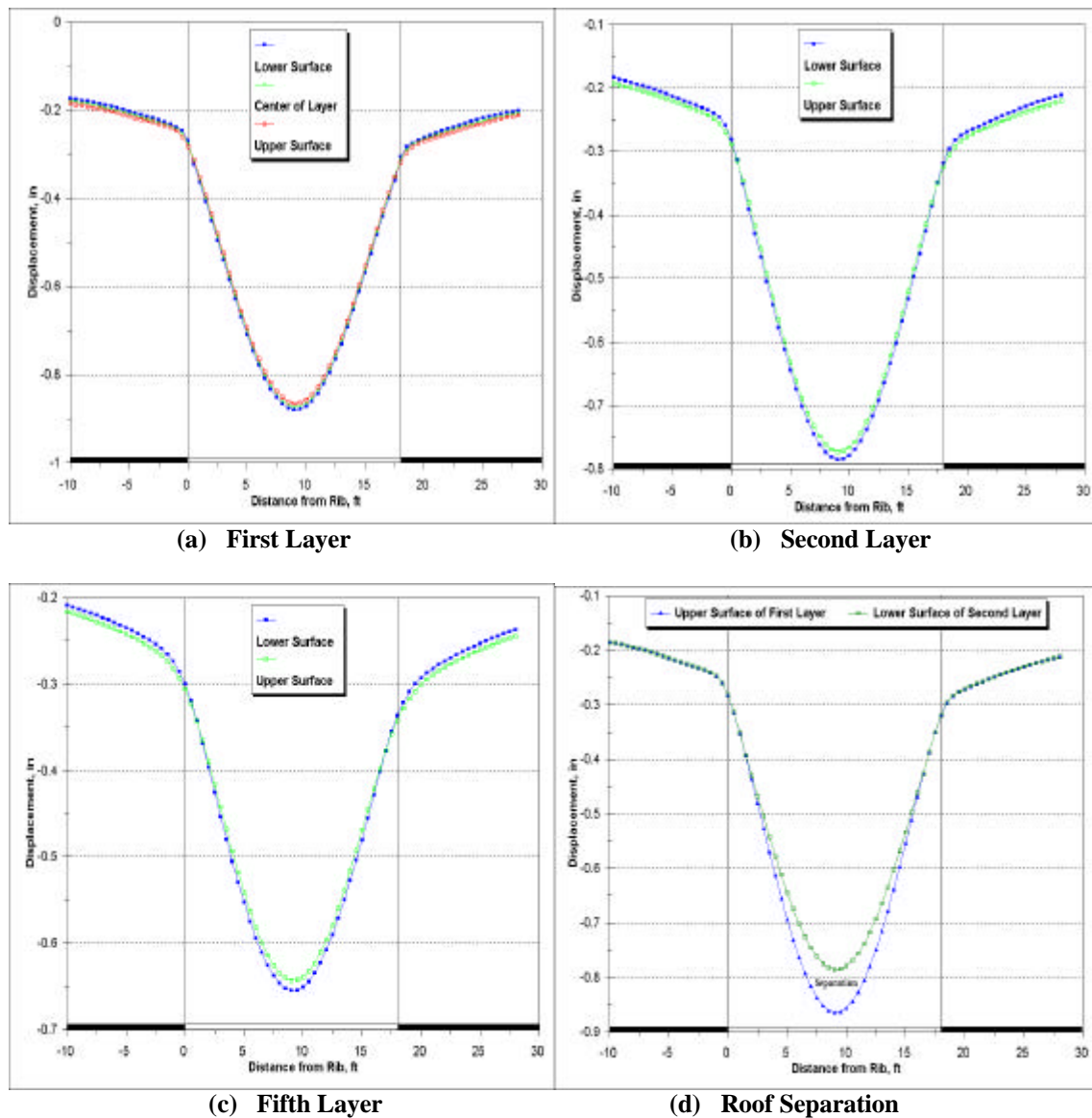


Fig. 6-17 Vertical Displacements in the Different Roof Layers ( $R=3$ ,  $f_1=0.4$ ,  $f_2=0.2$ )

#### 6.4.1 Von-Mises Stress in the Roof

Fig. 6-18 shows the typical distributions of the Von-Mises stress in the first, second, and fifth roof layers. The Von-Mises stress in the laminated roof has the following characteristics:

- a. The stress distribution in the lower surface of a layer is different from that in the upper surface. For example, the maximum Von-Mises stress on the lower surface of the first layer occurs near the two entry rib sides. But on its upper surface the maximum stress occurs at the entry center, as shown in Fig. 6-18(a). In addition, for any layer, the Von-Mises stress at the center is larger on the upper surface than that on the lower surface.
- b. The Von-Mises stress in the first layer is the largest in the roof layers. For instance, on its lower surface, the Von-Mises stress at the rib sides is about 3,000 psi while it is about 1,750 psi at the center. On its upper surface, it is about 2,700 psi at the center. This indicates that the roof failure, when it occurs, will begin at the first layer.
- c. The stress is concentrated at the two rib sides. Generally, the stress at one rib side is larger than that at the other side.
- d. Compared with the stress without roof separations (Fig. 6-5), the Von-Mises stress in the laminated roof is larger. For example, when the stress ratio is 3 and the coefficient of friction ( $f_1$ ) is 0.4, the maximum Von-Mises stress at the roof line level is about 2,700 psi. If a roof separation occurs, it is about 3,100 psi.

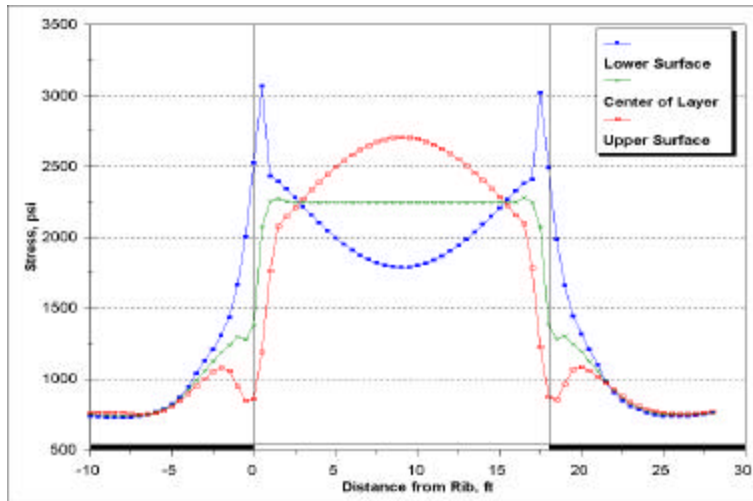
Since the stress at the roof line level (the lower surface of the first layer) is the largest in the roof layers, the Von-Mises stress at this level is analyzed for different cases in the following.

Fig. 6-19 show the Von-Mises stress at the roof line level when the stress ratio ( $R$ ) of the horizontal to the vertical stress is 3. It shows that the maximum stress occurs near the rib side, not just at the entry corner. In addition, the stress increases with the coefficient of friction ( $f_1$ ) in the interfaces between the coal seam and the roof/floor. But

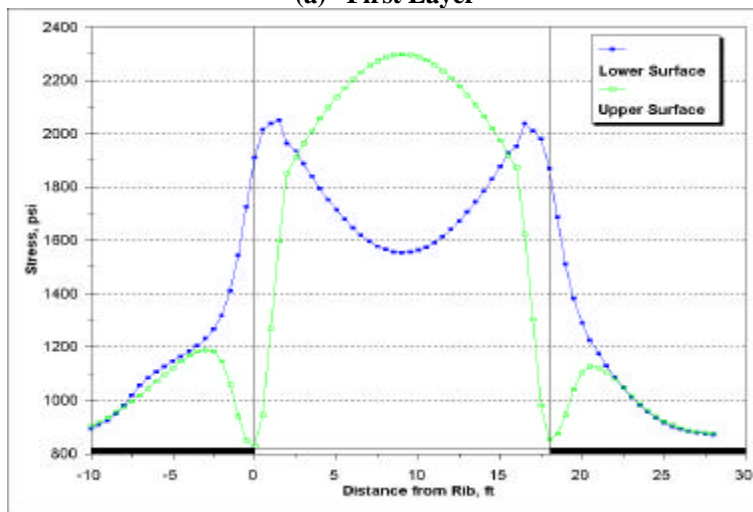
the stress decreases with the coefficient of friction ( $f_2$ ) in the interfaces between the roof layers, as shown in Fig. 6-19(d).

When the stress ratio ( $R$ ) increases, the Von-Mises stress also increases. Fig. 6-20 shows the Von-Mises stress at the roof line level when the stress ratio ( $R$ ) is 5. It is similar to Fig. 6-19. The maximum stress increases with the coefficient of friction ( $f_1$ ) and decreases with the coefficient of friction ( $f_2$ ). When the stress ratio ( $R$ ) reaches 7, the Von-Mises stress changes with the coefficients of friction ( $f_1$  and  $f_2$ ) in the interfaces significantly, as shown in Fig. 6-21. For example, when the coefficient of friction ( $f_1$ ) is 0.2, the stress decreases uniformly with the coefficient of friction ( $f_2$ ). When the coefficient of friction ( $f_1$ ) is 0.4 and 0.6, respectively, the stress decreases at a faster rate with the coefficient of friction ( $f_2$ ), as shown in Fig. 6-21(d).

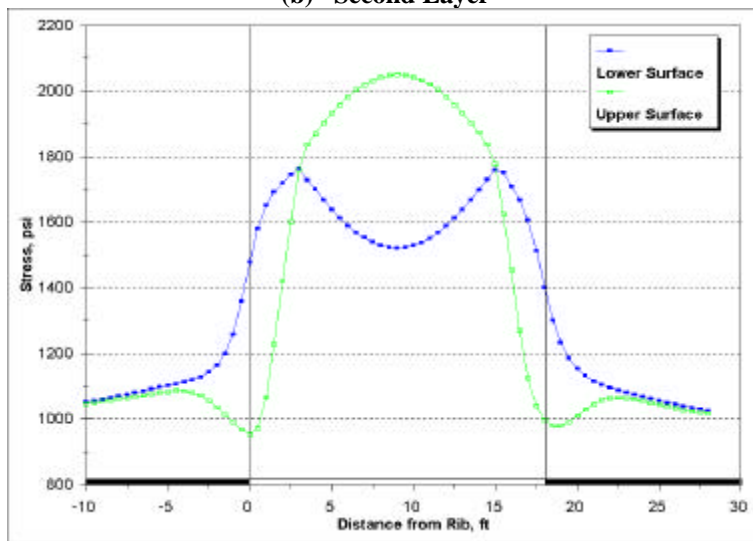
Generally, the Von-Mises stress at the roof line level increases with the coefficient of friction ( $f_1$ ) in the interfaces between the coal seam and the roof/floor, as discussed in the previous section. But, since the interface sliding between the roof layers occurs, the stress is larger than that when only the interface sliding occurs between the coal seam and the roof/floor. In addition, the Von-Mises stress increases with the stress ratio ( $R$ ). If the coefficient of friction ( $f_1$ ) and the stress ratio ( $R$ ) are fixed, the Von-Mises stress decreases with the coefficient of friction ( $f_2$ ) between the roof layers.



(a) First Layer

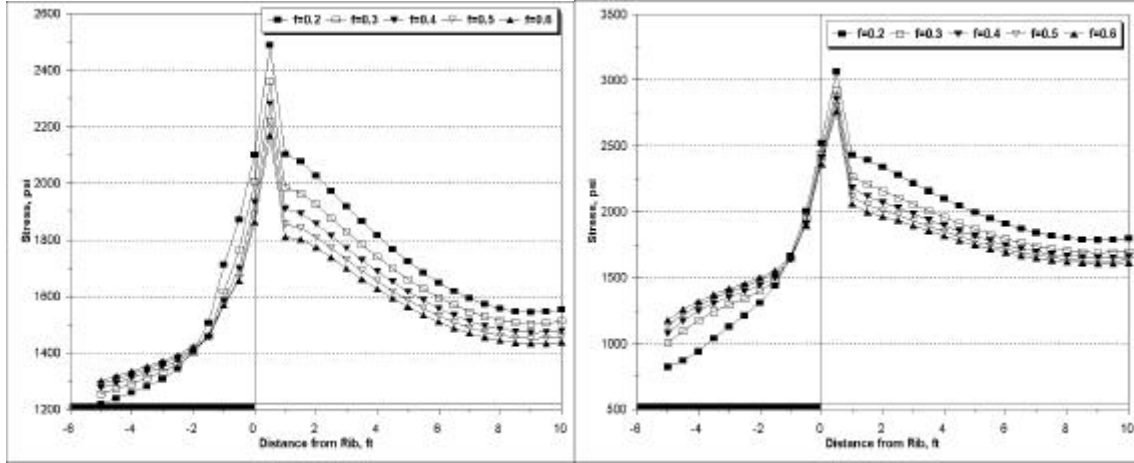


(b) Second Layer



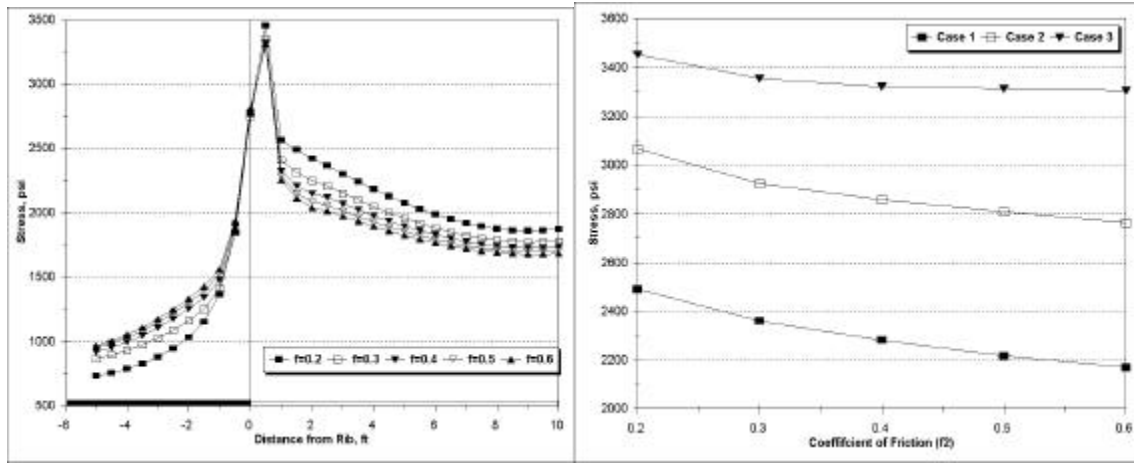
(c) Fifth Layer

Fig. 6-18 Von-Mises Stress in the Different Layers ( $R=3$ ,  $f_1=0.4$ ,  $f_2=0.2$ )



(a) Case 1:  $f_1=0.2$

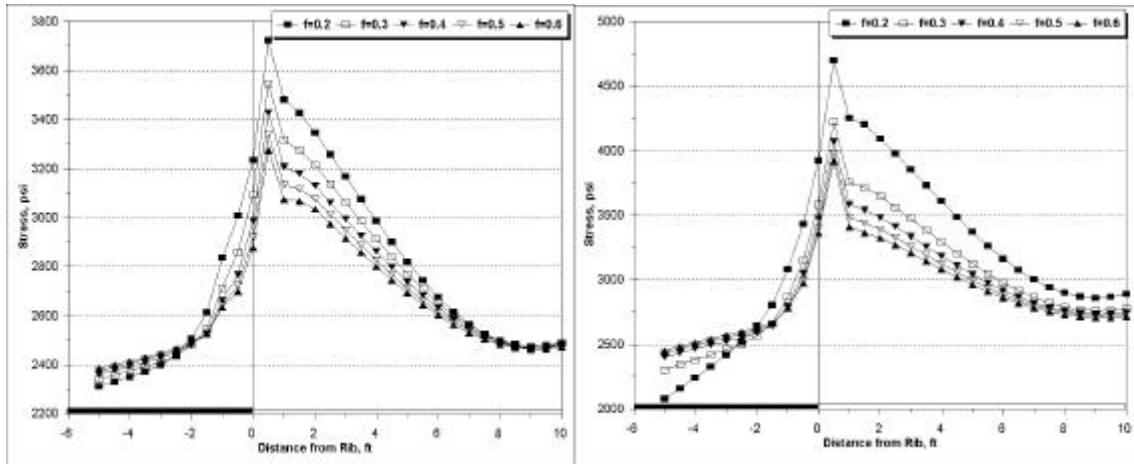
(b) Case 2:  $f_1=0.4$



(c) Case 3:  $f_1=0.6$

(d) Max. Stress with  $f_2$

Fig. 6-19 Von-Mises Stress at the Roof Line level for Different Cases (R=3)



(a) Case 1:  $f_1=0.2$

(b) Case 2:  $f_1=0.4$

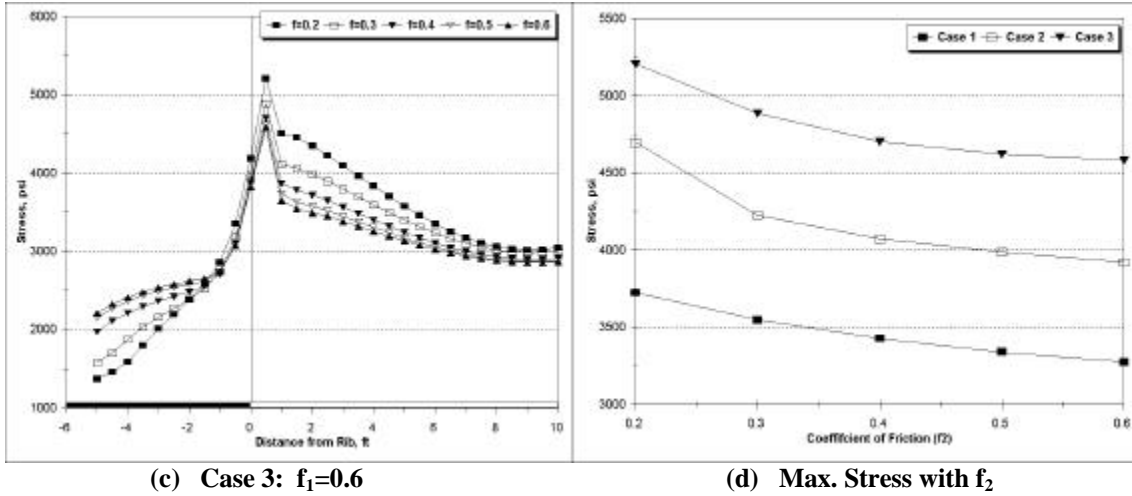


Fig. 6-20 Von-Mises Stress at the Roof Line level for Different Cases (R=5)

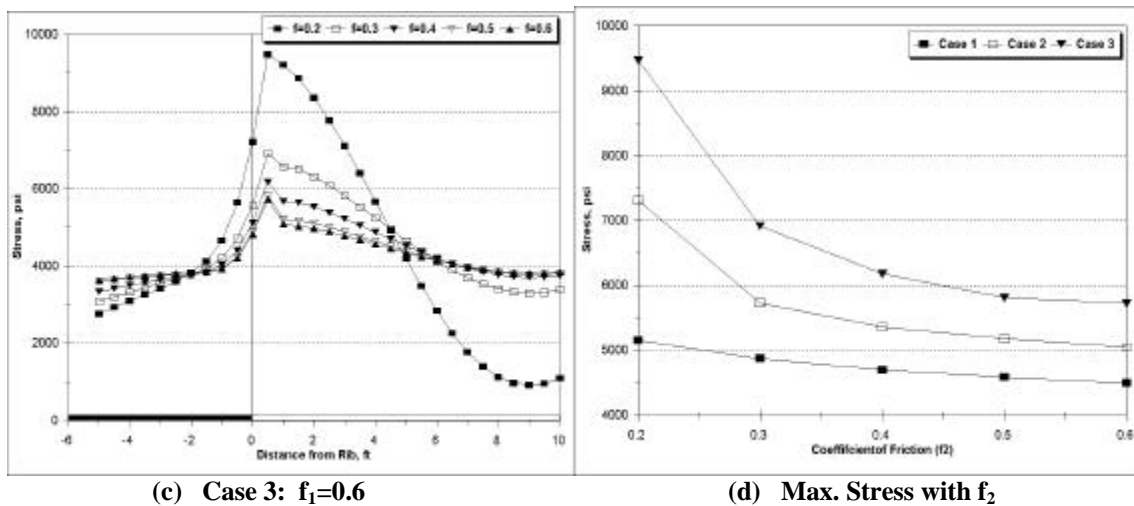
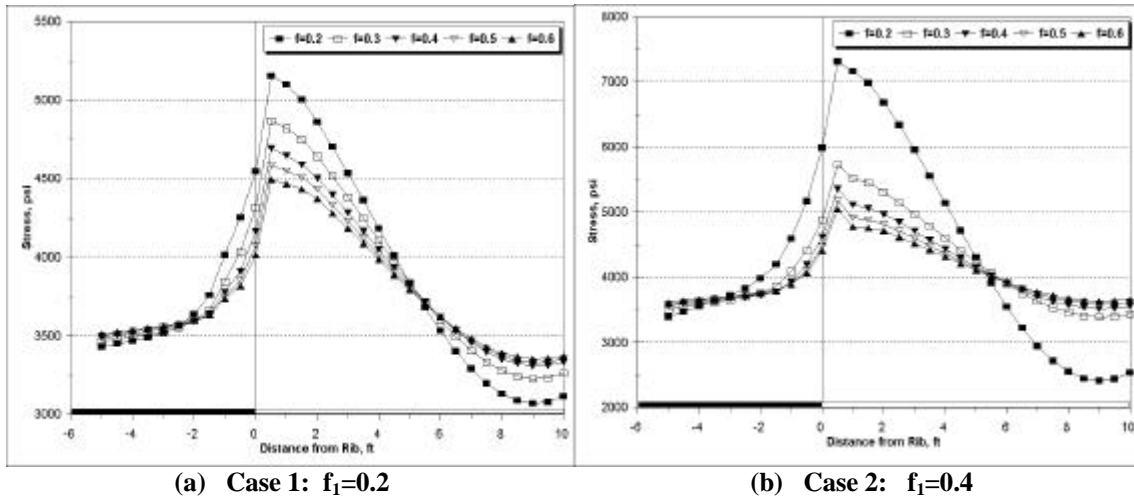


Fig. 6-21 Von-Mises Stress at the Roof Line level for Different Cases (R=7)

#### 6.4.2 Max. Principal Stress in the Roof

The maximum principal stress in the different roof layers is shown in Fig. 6-22. It shows the maximum principal stress in the first, second, and fifth layers when the stress ratio ( $R$ ) is 3 and the coefficient of friction ( $f_1$  and  $f_2$ ) are 0.4 and 0.2, respectively. For other cases, the stress distributions are similar to this figure. The maximum principal stress is concentrated at the two rib sides. In addition, the patterns of the stress distributions in these three layers are similar. On the lower surfaces of each layer, the maximum stress occurs at the rib sides while on the upper surface it occurs at/over the entry center. But the stress in the first layer is the largest in the roof layers. Therefore, the maximum principal stress is analyzed only at the roof line level (the lower surface of the first layer) in the following.

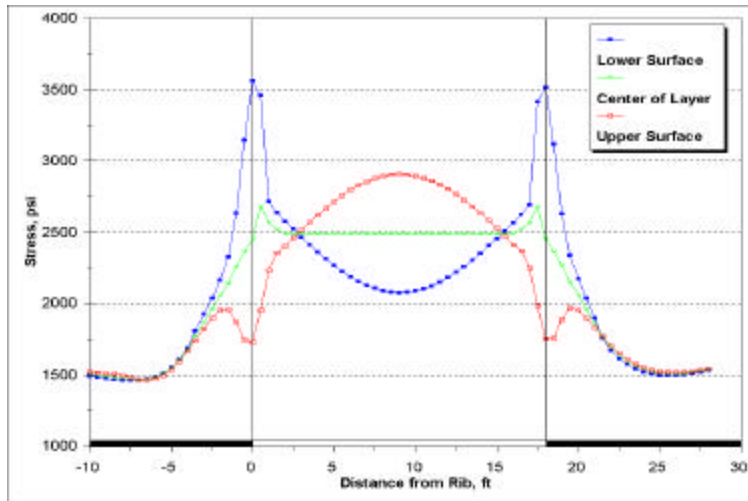
When the stress ratio ( $R$ ) is equal to 3, the maximum stress of the maximum principal stress at the roof line level is just on the rib sides. The stress increases with the coefficient of friction ( $f_1$ ) in the interfaces between the coal seam and the roof/floor and decreases slightly with the coefficient of friction ( $f_2$ ) in the interfaces between the roof layers, as shown in Fig. 6-23. When the coefficient of friction ( $f_1$ ) is equal to 0.6, the stress at point P1 (just at the rib side) is smaller than that at point P2 if  $f_2 = 0.2$ .

As the stress ratio ( $R$ ) increases, the maximum principal stress increases and the location of the maximum stress at the roof line level changes. When the stress ratio ( $R$ ) is equal to 5, the maximum principal stress is shown in Fig. 6-24. The stress increases with the coefficient of friction ( $f_1$ ) in the interfaces between the coal seam and the roof/floor and decreases slightly with the coefficient of friction ( $f_2$ ) in the interfaces between the roof layers. If the coefficient of friction ( $f_1$ ) is equal to 0.2, the maximum stress occurs just at the rib side (point P1). The maximum stress occurs at point P2 when the coefficient of friction ( $f_1$ ) is more than 0.2. The maximum stress moves toward the entry. At points P1 and P2, the maximum principal stress decreases with the coefficient of friction ( $f_2$ ), as shown in Fig. 6-24(d) and (e). The difference between these two cases is small.

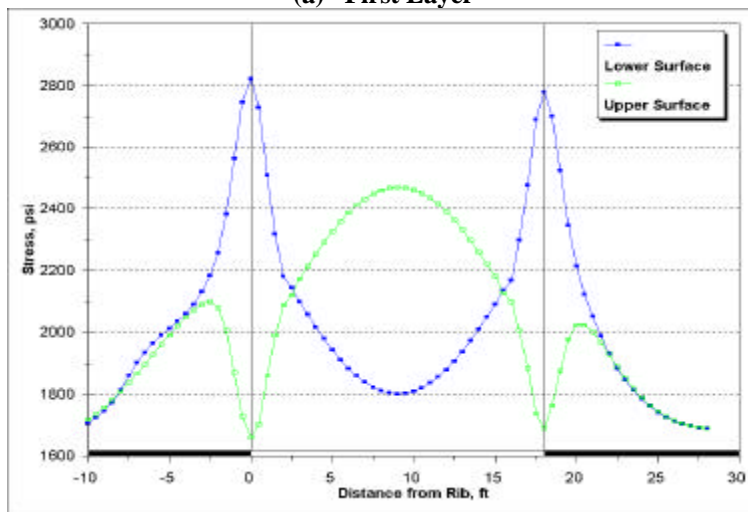
When the stress ratio ( $R$ ) is equal to 7, the maximum stress of the maximum principal stress generally occurs at point P2, as shown in Fig. 6-25. The stress changes

like the Von-Mises stress. The maximum principal stress increases with the coefficient of friction ( $f_1$ ) and decreases with the coefficient of friction ( $f_2$ ). If the coefficient of friction ( $f_1$ ) is equal to 0.2, the maximum stress of the maximum principal stress smoothly decreases with the coefficient of friction ( $f_2$ ). When the coefficient of friction ( $f_1$ ) is larger than 0.2, the maximum stress of the maximum principal stress decreases rapidly with the coefficient of friction ( $f_2$ ), as shown in Fig.6-25(d).

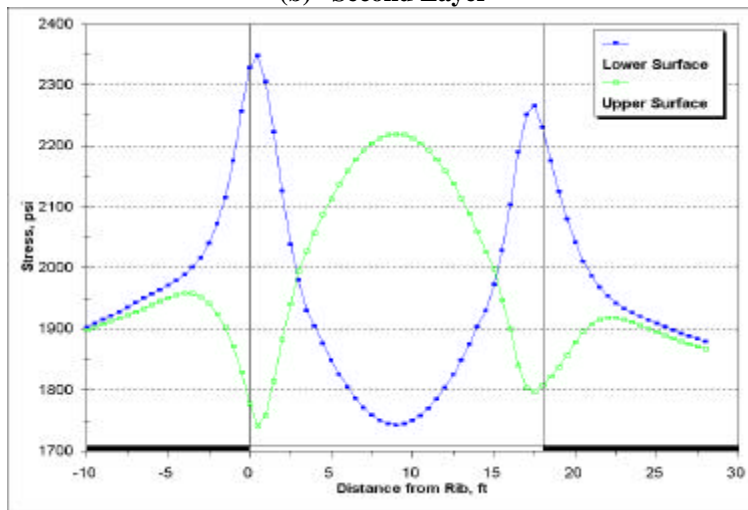
Usually, the maximum principal stress is distributed at the roof line level in the way like the Von-Mises stress. It increases with the stress ratio ( $R$ ) of the horizontal to the vertical stress and the coefficient of friction ( $f_1$ ) in the interfaces between the coal seam and the roof/floor and decreases with the coefficient of friction ( $f_2$ ) between the roof layers. In addition, the location of the maximum stress of the maximum principal stress depends on the stress ratio ( $R$ ) and the coefficient of friction ( $f_1$ ). Generally, if the stress ratio is equal to 0.2, the maximum stress occurs just at the rib side. When the stress ratio ( $R$ ) is equal to 5 or 7, it occurs just at the rib side if the coefficient of friction ( $f_1$ ) is equal to 0.2, or it moves toward the entry if the coefficient of friction ( $f_1$ ) is larger than 0.2.



(a) First Layer

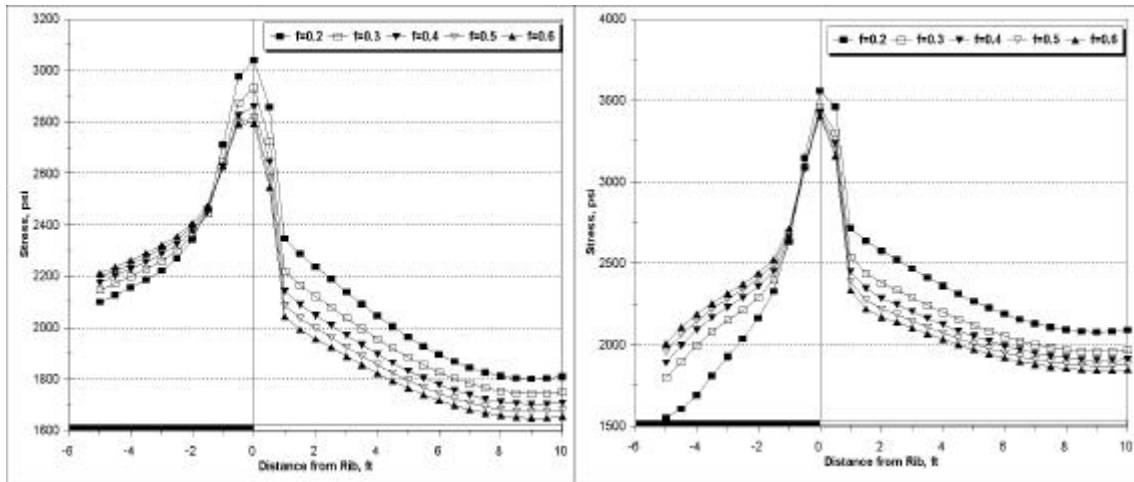


(b) Second Layer



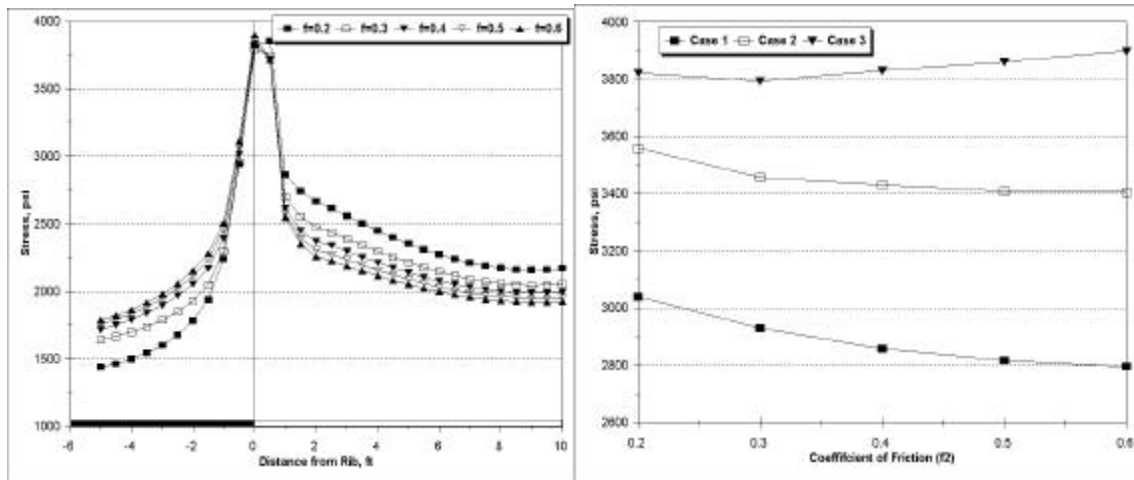
(c) Fifth Layer

Fig. 6-22 Max. Principal Stress in the Different Layers ( $R=3$ ,  $f_1=0.4$ ,  $f_2=0.2$ )



(a) Case 1:  $f_1=0.2$

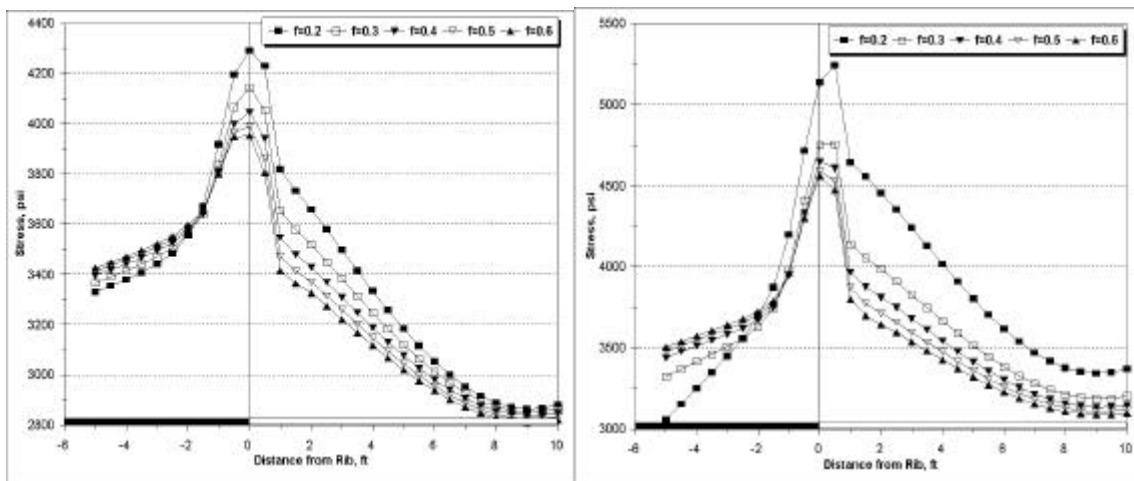
(b) Case 2:  $f_1=0.4$



(c) Case 3:  $f_1=0.6$

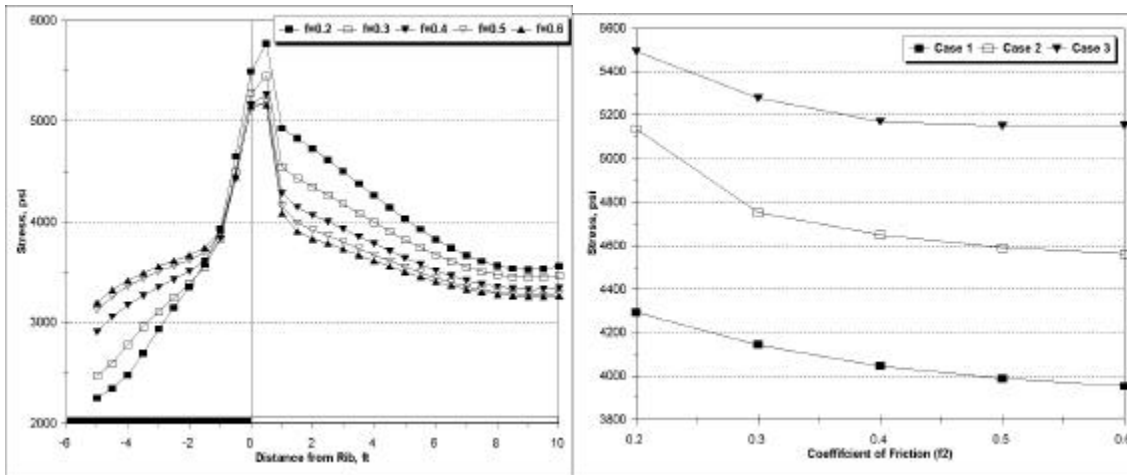
(d) Max. Stress with  $f_2$

Fig. 6-23 Max. Principal Stress at the Roof Line level for Different Cases (R=3)



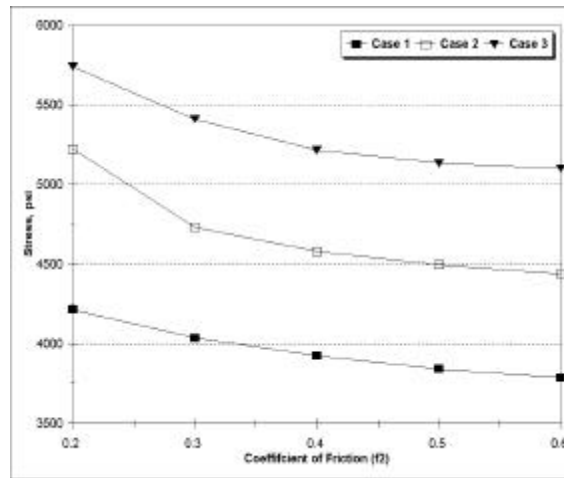
(a) Case 1:  $f_1=0.2$

(b) Case 2:  $f_1=0.4$



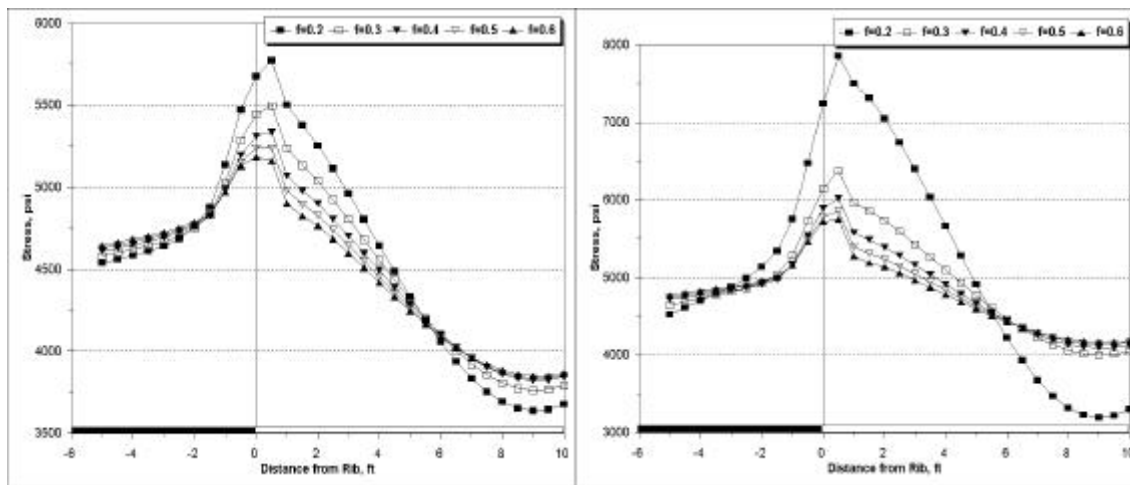
(c) Case 3:  $f_1=0.6$

(d) Max. Stress with  $f_2$  at P1



(e) Max. Stress with  $f_2$  at P2

Fig. 6-24 Max. Principal Stress at the Roof Line level for Different Cases (R=5)



(a) Case 1:  $f_1=0.2$

(b) Case 2:  $f_1=0.4$

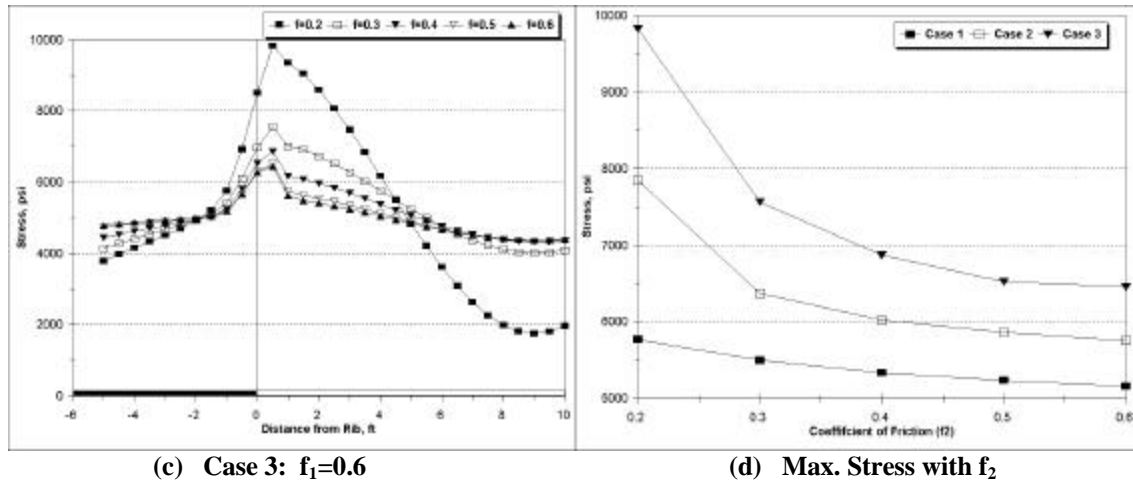


Fig. 6-25 Max. Principal Stress at the Roof Line level for Different Cases (R=7)

### 6.4.3 Min. Principal Stress in the Roof

When the interface sliding occurs between the roof layers, the distributions of the minimum principal stress in the roof are totally different from those without interface sliding. Without interface sliding, the minimum stress of the minimum principal stress generally occurs at the roof line level. However, when the interface sliding is involved and separations between the roof layers occur, the minimum principal stress in the roof is distributed in the different ways. Fig. 6-26 shows the typical distributions of the minimum principal stress in the first, second, and fifth layers. It is interesting that the minimum principal stress on the upper surface is smaller than that on the lower surface in each layer. This seems different from the traditional stress distributions in a bending beam. Without the horizontal stress, the lower surface of a roof layer is in tension while the upper surface is in compression along the horizontal direction. In this situation, the minimum principal stress on the lower surface is smaller. But, when the roof layers are subjected to high horizontal stress, the whole layer is in compression along the horizontal direction (in the next section, the stress along the horizontal direction will be analyzed). In this situation, the layer will deform along the vertical direction. Since there is a space (separation) between the roof layers and the stress along horizontal direction on the upper surface is larger than that on the lower surface, the minimum principal stress on the upper surface is smaller than that on the lower surface. The direction of the minimum principal stress is vertical.

At the roof line level, the minimum stress is smaller near the rib sides where the maximum Von-Mises stress and the maximum principal stress occur. Therefore, the minimum principal stress at the roof line level is analyzed in the following.

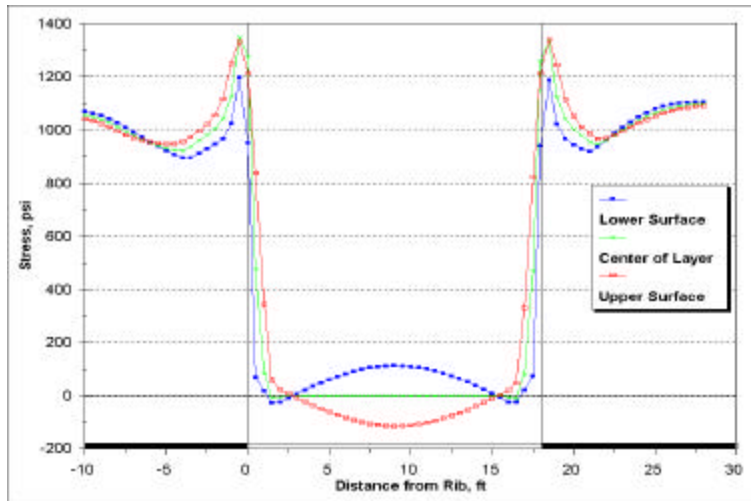
The minimum principal stress at the roof line level is shown in Fig. 6-27 when the stress ratio ( $R$ ) of the horizontal to the vertical stress is equal to 3. In the entry roof, the influence of the coefficients of friction ( $f_1$  and  $f_2$ ) in the interfaces between the coal seam and the roof/floor and among the roof layers on the minimum principal stress is very small. This influence can be ignored. But the influence of the coefficients of friction ( $f_1$  and  $f_2$ ) on the minimum principal stress in the pillar is significant. Since this study mainly analyzes the stress in the entry roof, this type of influence is not discussed here.

When the stress ratio ( $R$ ) is equal to 5, the minimum principal stress at the roof line level changes slightly, as shown in Fig. 6-28. Near the entry rib side, the minimum principal stress decreases slightly with the coefficient of friction ( $f_1$ ) in the interfaces between the coal seam and the roof/floor, but it increases slightly with the coefficient of friction ( $f_2$ ) in the interfaces between the roof layers. In this case, tensile stress along the vertical direction occurs. At the entry center, it reverses. The minimum principal stress increases slightly with the coefficient of friction ( $f_1$ ) and decreases slightly with the coefficient of friction ( $f_2$ ).

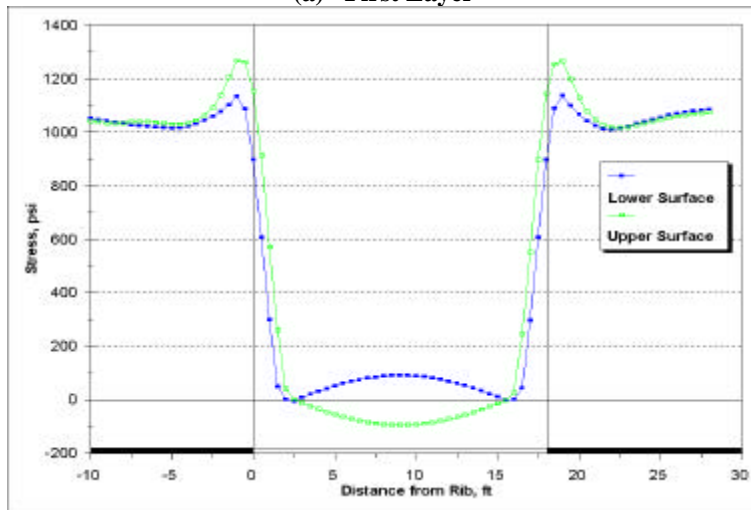
As the stress ratio ( $R$ ) increases, the minimum principal stress near the rib side decreases rapidly. Fig. 6-29 shows the stress distributions when the stress ratio ( $R$ ) is equal to 7. In this case, tensile stress along the vertical direction near the rib side increases significantly with the coefficient of friction ( $f_1$ ). But it reduces with the coefficient of friction ( $f_2$ ). At the entry center, the minimum principal stress increases slightly with the coefficient of friction ( $f_1$ ) between coal seam and roof/floor rock and decreases slightly with the coefficient of friction ( $f_2$ ) between roof layers.

Generally, the influence of the stress ratio ( $R$ ) on the minimum principal stress at the roof line level is not as significant as that on the Von-Mises stress and the maximum principal stress. The minimum principal stress at the roof line level is smaller near the rib sides. It decreases slightly with the coefficient of friction ( $f_1$ ) in the interfaces between

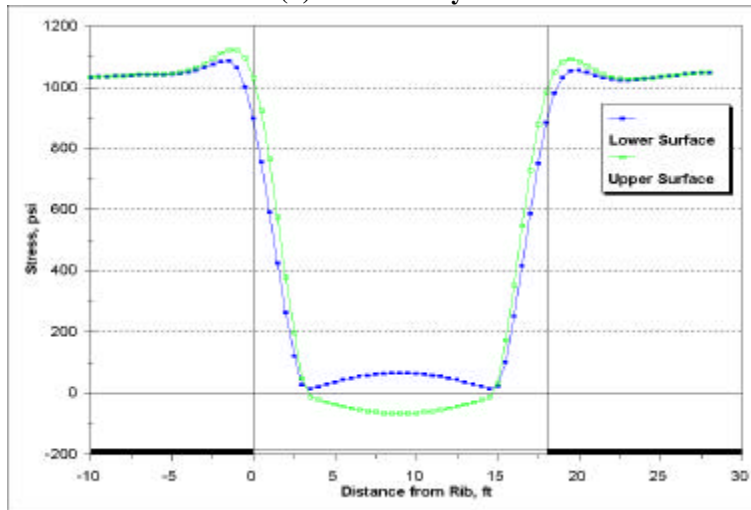
the coal seam and the roof/floor and increases slightly with the coefficient of friction ( $f_2$ ) in the interfaces between the roof layers. When the stress ratio ( $R$ ) is larger than 3, tensile stress along the vertical direction near the rib sides occurs. At the entry center, the minimum principal stress increase slightly with the stress ratio ( $R$ ) and the coefficient of friction ( $f_1$ ) between coal seam and roof/floor and decreases slightly with the coefficient of friction ( $f_2$ ) between roof layers.



(a) First Layer

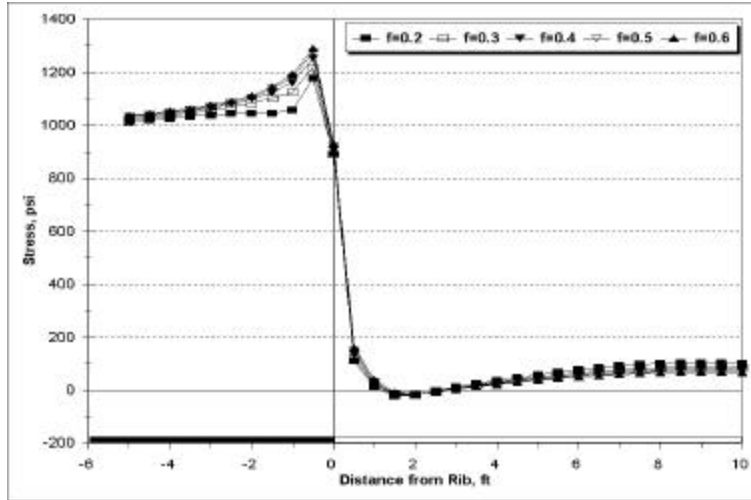


(b) Second Layer

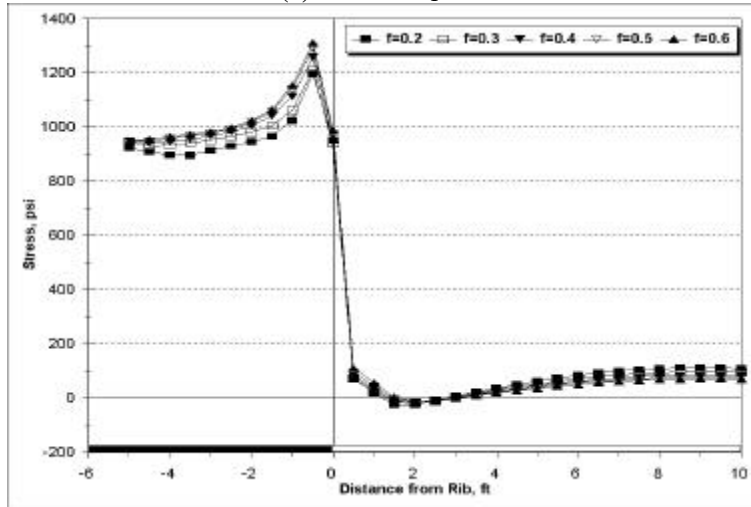


(c) Fifth Layer

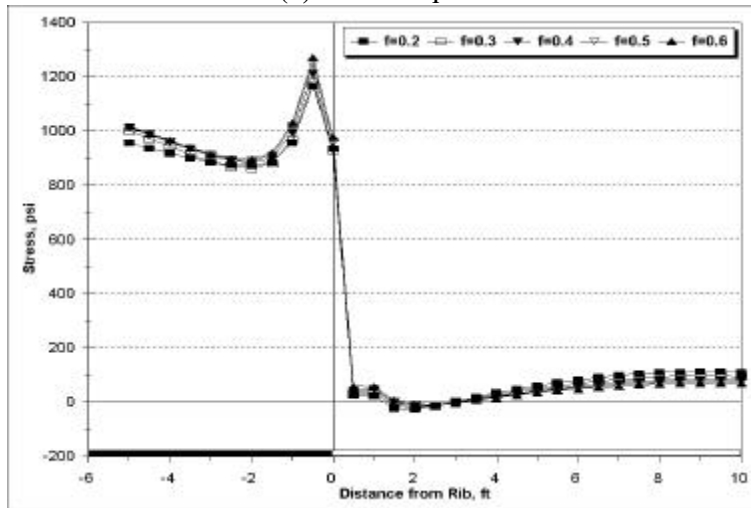
Fig. 6-26 Min. Principal Stress in the Different Layers ( $R=3$ ,  $f_1=0.4$ ,  $f_2=0.2$ )



(a) Case 1:  $f_1=0.2$

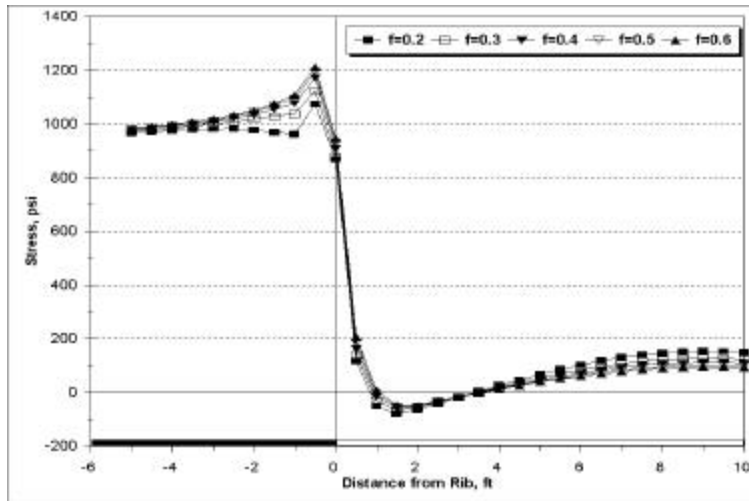


(b) Case 2:  $f_1=0.4$

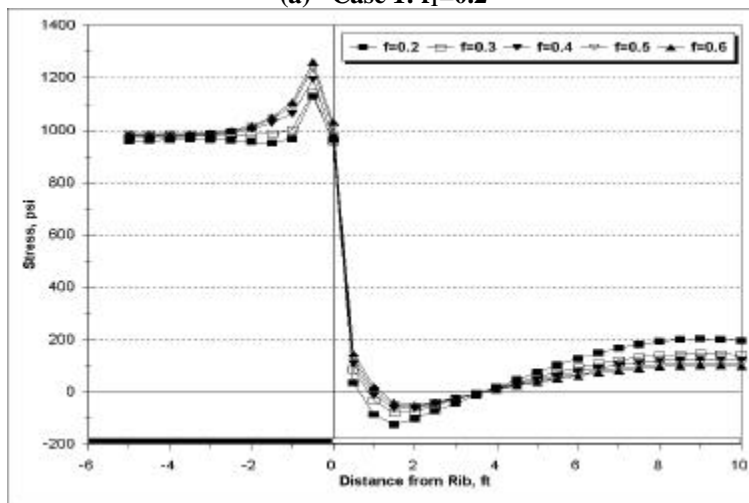


(c) Case 3:  $f_1=0.6$

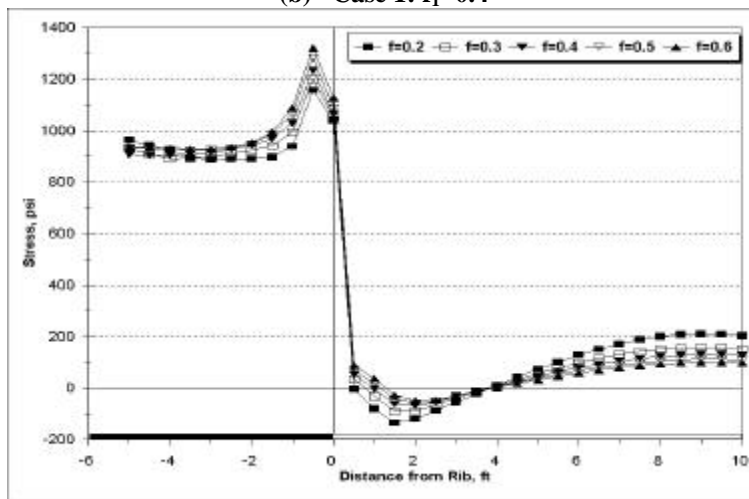
Fig. 6-27 Min. Principal Stress at the Roof Line Level (R=3)



(a) Case 1:  $f_1=0.2$

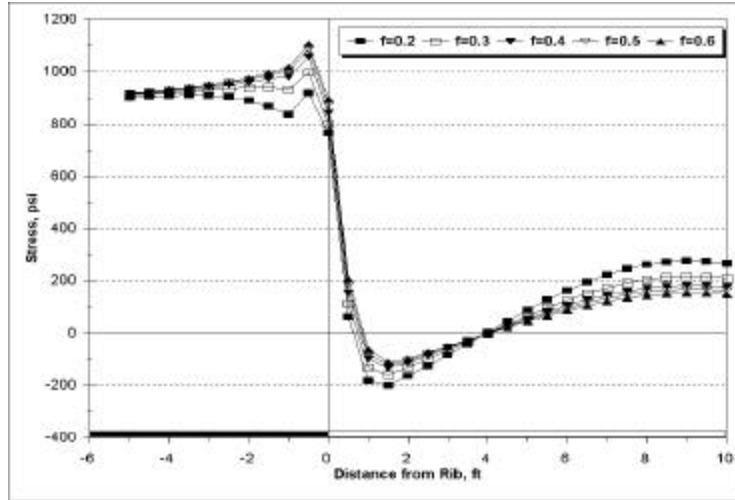


(b) Case 1:  $f_1=0.4$

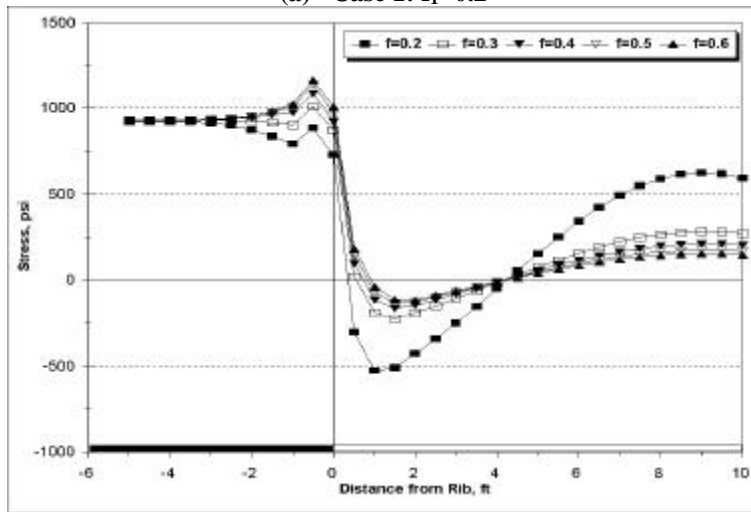


(c) Case 3:  $f_1=0.6$

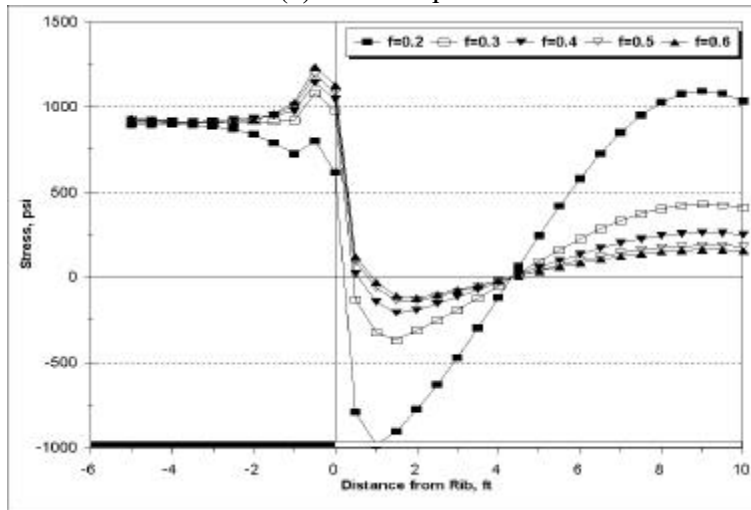
Fig. 6-28 Min. Principal Stress at the Roof Line Level (R=5)



(a) Case 1:  $f_1=0.2$



(b) Case 2:  $f_1=0.4$



(c) Case 3:  $f_1=0.6$

Fig. 6-29 Min. Principal Stress at the Roof Line Level (R=7)

#### 6.4.4 Stress along Horizontal Direction in the Roof

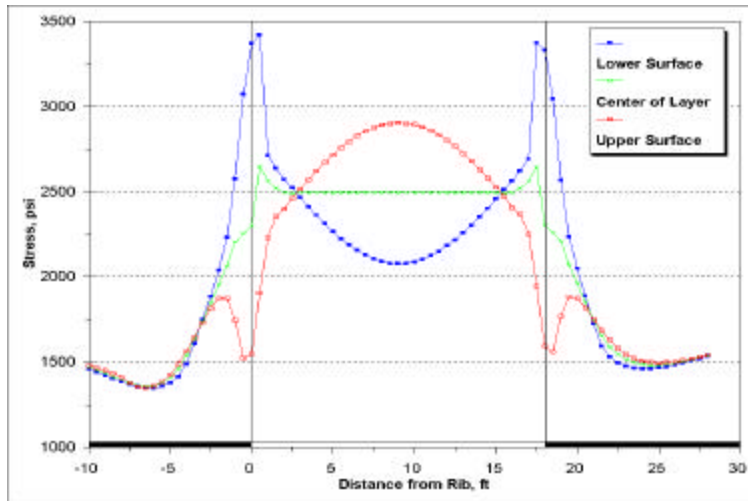
The typical stress distributions along the horizontal direction in the roof are shown in Fig. 6-30. They are similar to those of the maximum principal stress (Fig. 6-22). Generally, at the two rib sides, the stress along the horizontal stress on the lower surface of each roof layer is larger than that on the upper surface. At the entry center, the stress on the upper surface of each roof layer is larger than that on the lower surface. In addition, the stress along the horizontal direction in the first layer is the largest in the roof, and the maximum stress occurs at the roof line level. Therefore, the stress along the horizontal direction at the roof line level is analyzed in the following.

Fig. 6-31 shows the stress along the horizontal direction at the roof line level when the stress ratio ( $R$ ) is equal to 3. The stress increases with the coefficient of friction ( $f_1$ ), but decreases slightly with the coefficient of friction ( $f_2$ ). When the coefficient of friction ( $f_1$ ) is larger than 0.2, the maximum stress moves toward the entry, namely, the maximum stress occurs at point P2. The maximum stress changes with the coefficients of friction ( $f_1$  and  $f_2$ ) are shown in Fig. 6-31(d) and (e).

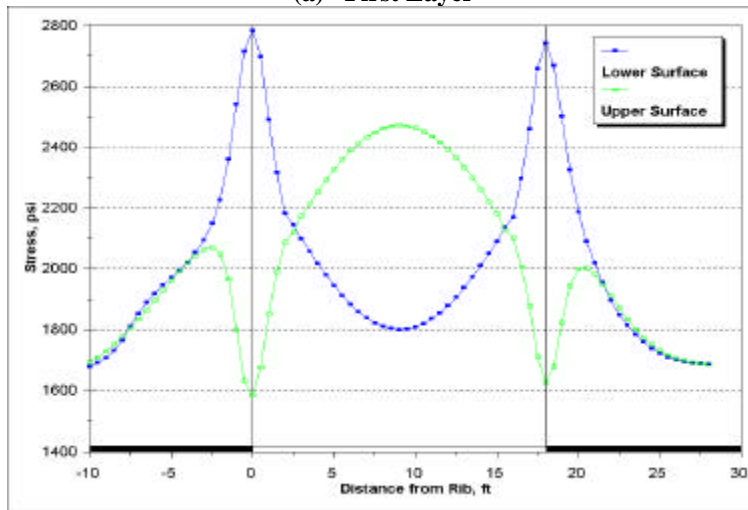
When the stress ratio ( $R$ ) is equal to 5, the stress distributions are similar to that when the stress ratio ( $R$ ) is 3, as shown in Fig. 6-32. The stress increases with the coefficient of friction ( $f_1$ ), but decreases slightly with frictional coefficient ( $f_2$ ).

As the stress ratio ( $R$ ) is equal to 7, the maximum stress always occurs at point P2, as shown in Fig. 6-33. Near the rib sides, the stress along the horizontal direction increases significantly with the coefficient of friction ( $f_1$ ) and decreases with the coefficient of friction ( $f_2$ ). But at the entry center, the stress increases with coefficient of friction ( $f_2$ ).

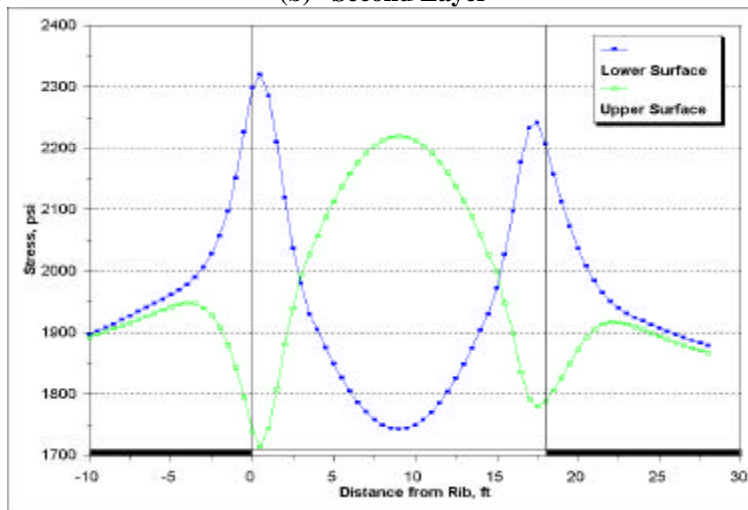
Usually, the stress along the horizontal direction is concentrated at the rib sides. It increases with the stress ratio ( $R$ ) and the coefficient of friction ( $f_1$ ) in the interfaces between the coal seam and the roof/floor and decreases slightly with the coefficient of friction ( $f_2$ ) in the interfaces between the roof layers. The maximum stress often occurs near the rib sides. On the upper surface of a roof layer, the maximum stress occurs at the center of the layer.



(a) First Layer

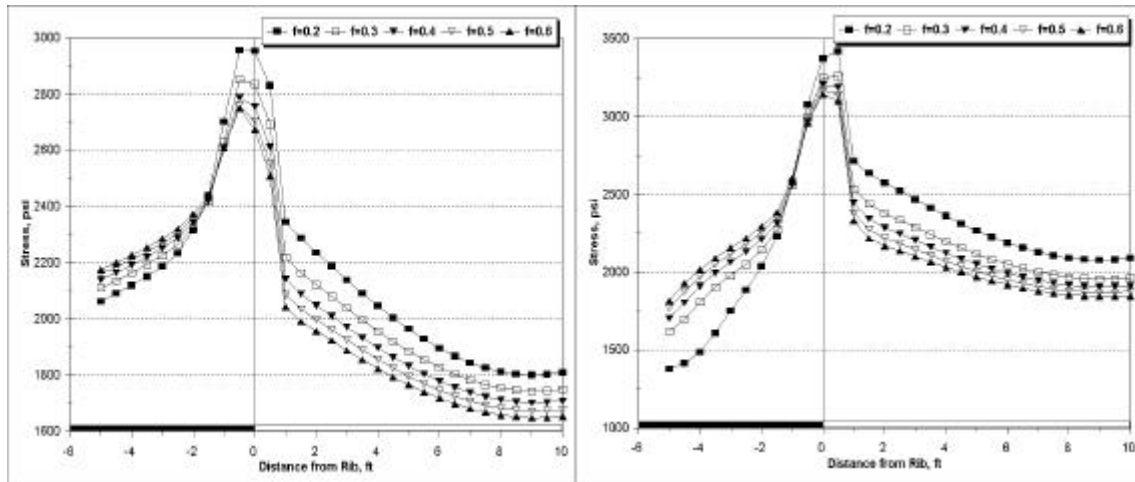


(b) Second Layer



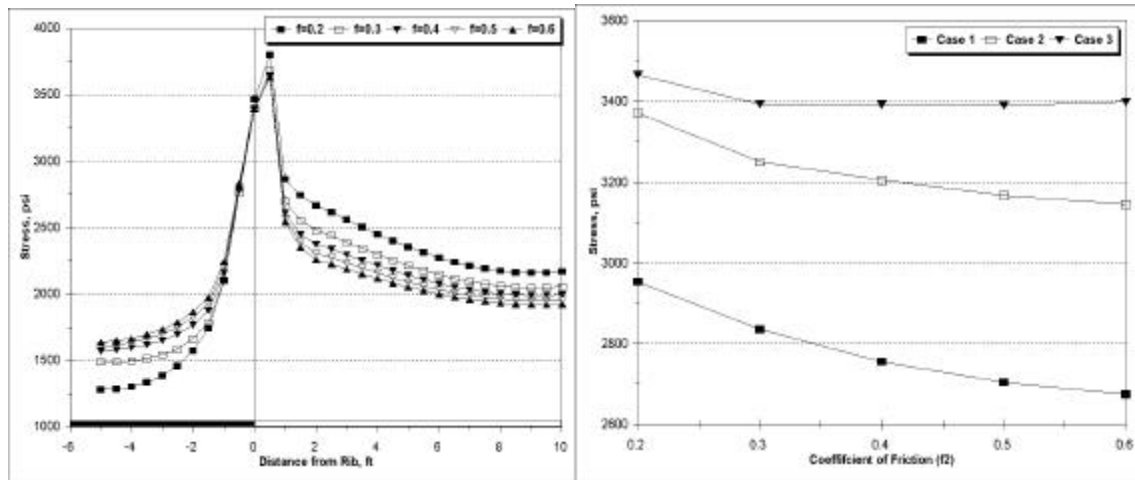
(c) Fifth Layer

Fig. 6-30 Stress along Horizontal Direction in the Different Layers ( $R=3$ ,  $f_1=0.4$ ,  $f_2=0.2$ )



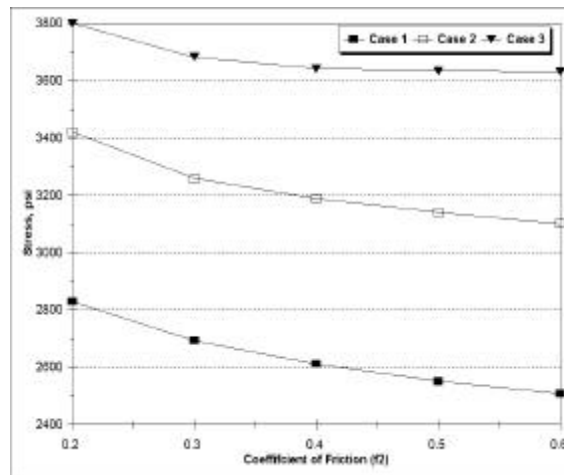
(a) Case 1:  $f_1=0.2$

(b) Case 2:  $f_1=0.4$



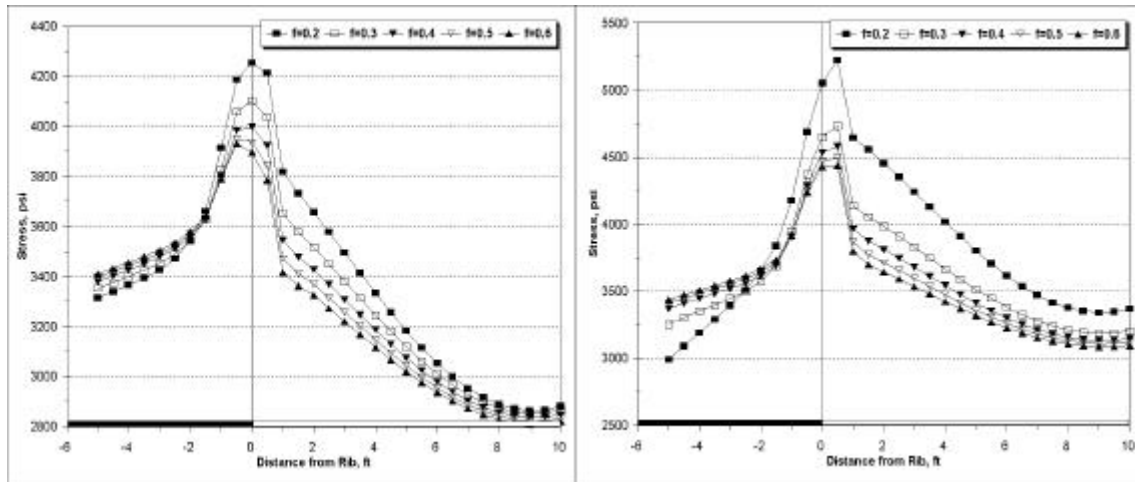
(c) Case 3:  $f_1=0.6$

(d) Max. Stress with  $f_2$  at P1



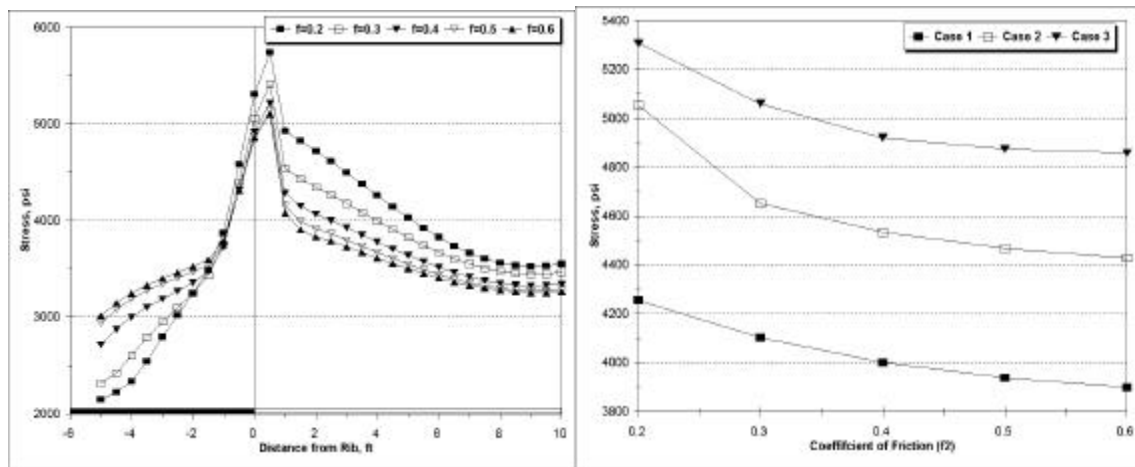
(e) Max. Stress with  $f_2$  at P2

Fig. 6-31 Stress along Horizontal Direction at the Roof Line Level (R=3)



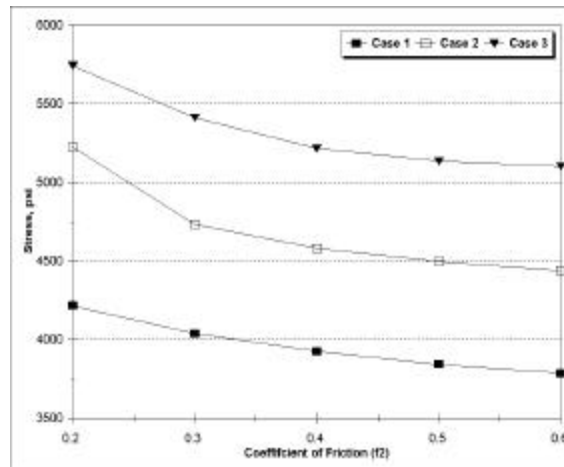
(a) Case 1:  $f_1=0.2$

(b) Case 2:  $f_1=0.4$



(c) Case 3:  $f_1=0.6$

(d) Max. Stress with  $f_2$  at P1



(e) Max. Stress with  $f_2$  at P2

Fig. 6-32 Stress along Horizontal Direction at the Roof Line Level (R=5)

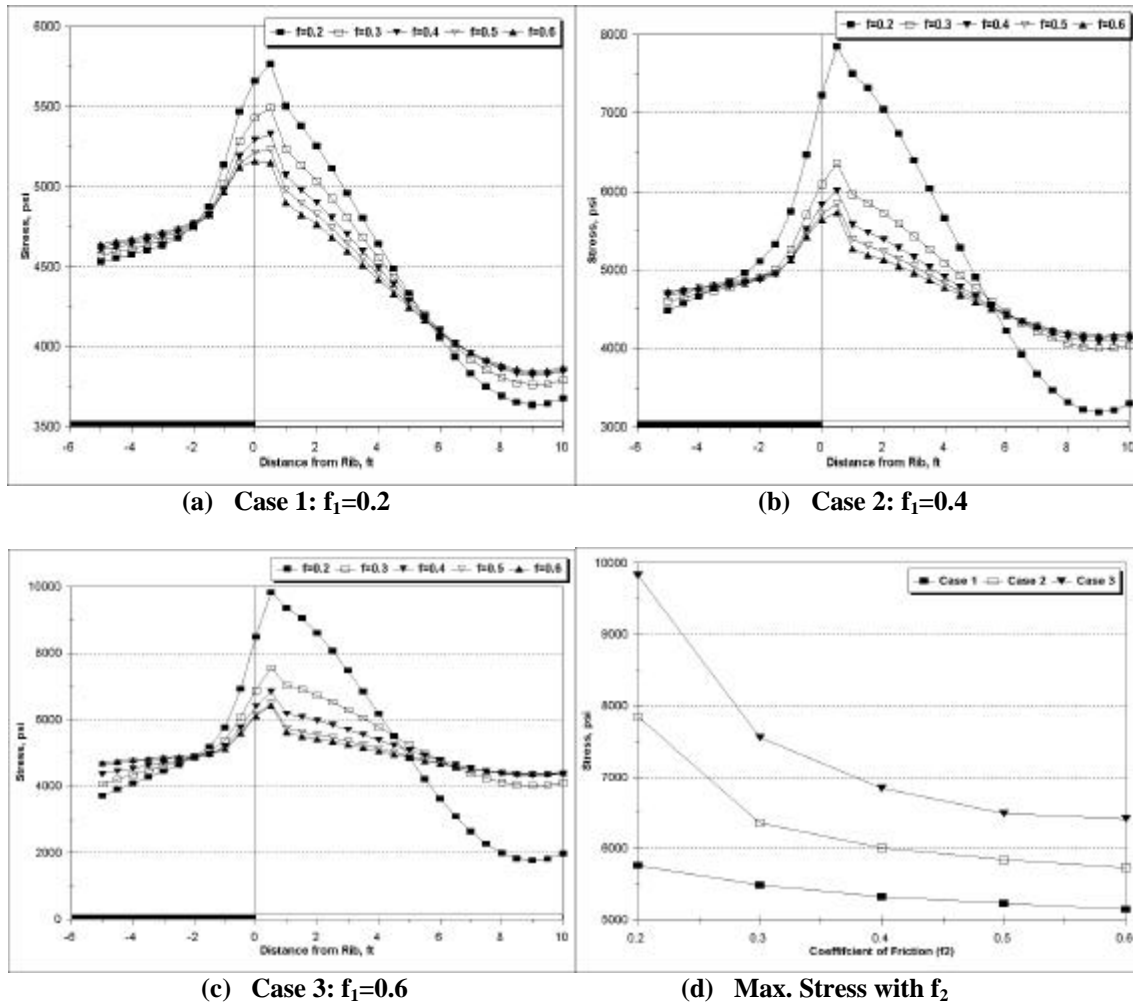


Fig. 6-33 Stress along Horizontal Direction at the Roof Line Level ( $R=7$ )

### 6.4.5 Summary

When the interface sliding between the roof layers occurs, the stress in the roof changes with the stress ratio ( $R$ ) of the horizontal and the vertical stress and the coefficients of friction ( $f_1$  and  $f_2$ ) between the coal seam and the roof/floor and between the roof layers. Generally, the stress distributions are the same regardless if the interface sliding between the roof layer occurs. However, when the interface sliding between the roof layers occurs, the Von-Mises stress, the maximum principal stress, and the stress along the horizontal direction are larger. The maximum magnitudes of these stresses occur near the entry rib sides. They decrease slightly with the coefficient of friction ( $f_2$ ) in the interfaces between the roof layers. The minimum principal stress changes slightly

with the stress ratio ( $R$ ) and the coefficients of friction ( $f_1$  and  $f_2$ ) in the interfaces between the coal seam and the roof/floor and between roof layers. At the roof line level, the minimum stress of the minimum principal stress occurs near the rib sides. But, on the upper surface of a roof layer, the minimum stress occurs in the entry center.

Based on the above stress analysis, it is found that the laminated roof is more likely to fail, because of the separations between the roof layers.

## 6.5 Discussion of Results

In this study, two cases are considered. In the first case, the interface sliding occurs only between the coal seam and the roof/floor. The slip between these interfaces occurs. In the other case, the interfaces both between the coal seam and the roof/floor and between the roof layers occur. The coal seam moves toward an entry, namely the slip occurs between coal seam and roof/floor. In addition, the slip also occurs between roof layers. Moreover, roof separations occur when the roof layer weight is larger than the cohesion in the interfaces and the tensile stress along the vertical direction caused by the high horizontal stress exceeds the tensile strength of the interface. Since the roof in these two cases deforms in the different ways, the stress in the roof is distributed differently. In addition, the stress at the roof line level is usually larger in the whole roof. Therefore, the stress at the roof line level is discussed for these two cases, respectively.

### 6.5.1 Sliding between Coal and Roof/Floor

When the interface sliding occurs between the coal seam and the roof/floor, the stress in an entry roof is relieved to some degree. Generally, the stress magnitude depends both on the stress ratio ( $R$ ) of the horizontal to the vertical stress and on the coefficient of friction ( $f$ ) in the interfaces.

#### Von-Mises Stress

The typical Von-Mises stress distribution is shown in Fig. 6-34. It shows that the Von-Mises stress relieves when sliding between the coal and the roof/floor occurs. In

addition, the stress increases with the stress ratio (R) and the coefficient of friction (f) in the interfaces. However, the pattern of the stress distributions is similar to that without the interfaces, in that the Von-Mises stress is still concentrated at the entry two rib sides. Generally, the maximum stress occurs at point P2 near the rib side. Table 6-3 lists the Von-Mises stress at points P1 and P2 for different situations. Point P1 is at the entry corner, while the distance between points P1 and P2 is 0.5 ft.

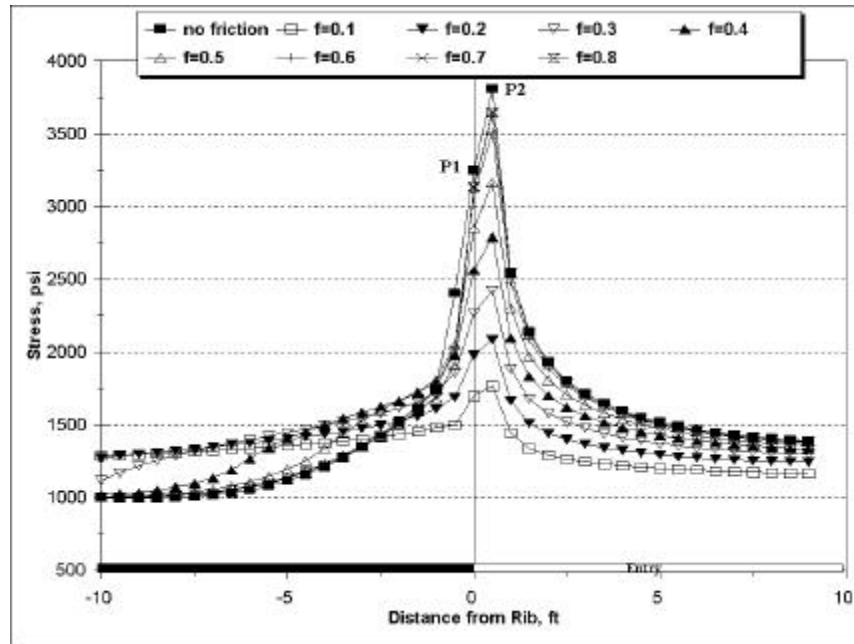


Fig. 6-34 Typical Von-Mises Stress at Roof Line Level

Table 6-3 Von-Mises Stress Near Rib Side

Point	Stress Ratio (R)	Coefficient of Friction between Coal and Roof/Floor (f)								No interfaces
		0.1	0.2	0.3	0.4	0.5	0.6	0.7	0.8	
P1	3	1700	1982	2270	2564	2851	3094	3130	3138	3249
	4	2168	2436	2713	2995	3288	3582	3849	3887	4048
	5	2681	2931	3192	3460	3738	4031	4333	4623	4793
	6	3220	3452	3694	3947	4207	4483	4778	5090	5603
	7	3773	3989	4214	4448	4692	4947	5221	5522	6428
P2	3	1769	2089	2427	2790	3166	3509	3639	3650	3810
	4	2276	2587	2920	3279	3672	4089	4495	4612	4781
	5	2805	3104	3428	3776	4161	4589	5054	5527	5768
	6	3348	3632	3943	4281	4650	5067	5538	6058	6764
	7	3899	4168	4464	4788	5144	5541	5996	6520	7767

### Maximum Principal Stress

The maximum principal stress at the roof line level is concentrated at the entry rib side. Its distribution is similar to that of the Von-Mises stress, as shown in Fig. 6-35. Generally, the maximum stress occurs at point P1 when the stress ratio (R) is equal to or less than 3. When the stress ratio (R) is larger than 3 and the coefficient of friction (f) is larger than 0.5, it occurs at point P2. The maximum principal stress at points P1 and P2 is listed in Table 6-4. Generally speaking, the maximum principal stress is relieved when the interface sliding between the coal seam and the roof/floor occurs.

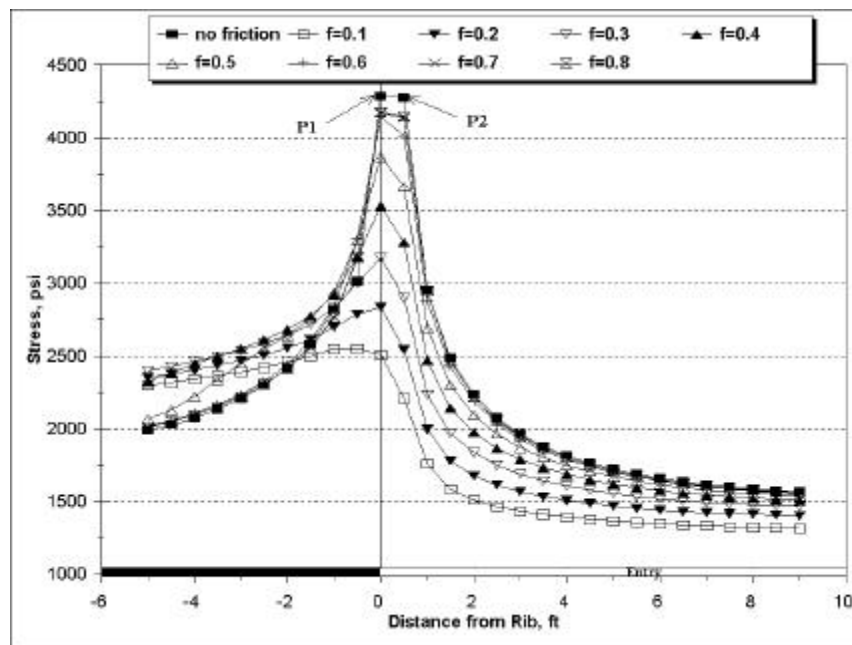


Fig. 6-35 Typical Max. Principal Stress at the Roof Line Level

Table 6-4 Max. Principal Stress Near Rib Side

Point	Stress Ratio (R)	Coefficient of Friction between Coal and Roof/Floor (f)								No interfaces
		0.1	0.2	0.3	0.4	0.5	0.6	0.7	0.8	
P1	3	2511	2839	3179	3532	3871	4142	4168	4176	4288
	4	3075	3388	3714	4056	4413	4766	5073	5111	4356
	5	3666	3962	4271	4595	4939	5304	5673	6013	6208
	6	4271	4549	4840	5147	5471	5822	6196	6583	7193
	7	4883	5145	5420	5707	6012	6339	6697	7085	8187
P2	3	2211	2546	2901	3281	3669	4014	4138	4149	4277
	4	2810	3137	3485	3862	4273	4702	5113	5227	5361
	5	3423	3739	4078	4443	4846	5293	5772	6250	6456
	6	4044	4347	4675	5027	5415	5852	6342	6876	7558
	7	4669	4960	5274	5614	5986	6403	6880	7422	8664

### Orientation of the Maximum Principal Stress

The Orientation of the maximum principal stress is an important factor determining the direction of roof failure. For example, the failure direction can be determined by using the Mohr-Coulomb criterion when the orientation of the maximum principal stress is known. Fig. 6-36 shows the angle between the maximum principal stress and the horizontal direction for different cases. It indicates that the orientation of the maximum principal stress is influenced by both the stress ratio (R) and the coefficient of friction in the interface between the coal seam and the roof/floor. The angle ( $\alpha$ ) between the maximum principal stress and the horizontal direction increases with the coefficient of friction at the entry rib sides when the stress ratio (R) is fixed. However, the angle decreases with the stress ratio (R) when the coefficient of friction is constant. Generally, at the entry center, the angle ( $\alpha$ ) is about  $0^{\circ}$ . At the two rib sides, the angle ( $\alpha$ ) ranges from  $6^{\circ}$  to  $25^{\circ}$ , as shown in Fig. 6-37 and Table 6-5.

Suppose that the Mohr-Coulomb failure criterion be used to determine the direction of cutter roof. The failure angle ( $\beta$ ), as shown in Fig. 6-38 is about

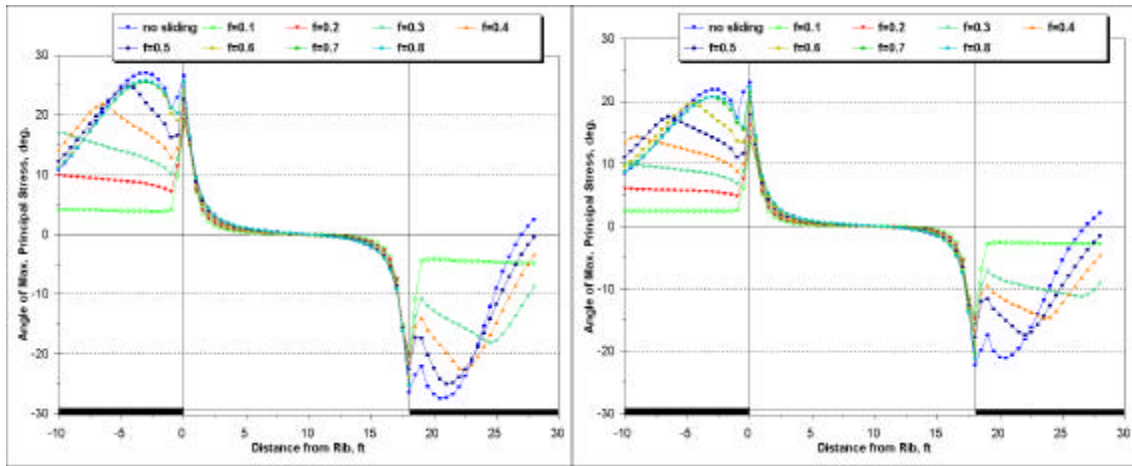
$$\mathbf{b} = (6^{\circ} \sim 25^{\circ}) + (45^{\circ} + \frac{\theta}{2})$$

where  $\theta$  - Friction angle of roof material.

Assume that the friction angle of roof ( $\theta$ ) is  $30^{\circ}$ , the failure angle ( $\beta$ ) ranges from  $66^{\circ}$  to  $85^{\circ}$ .

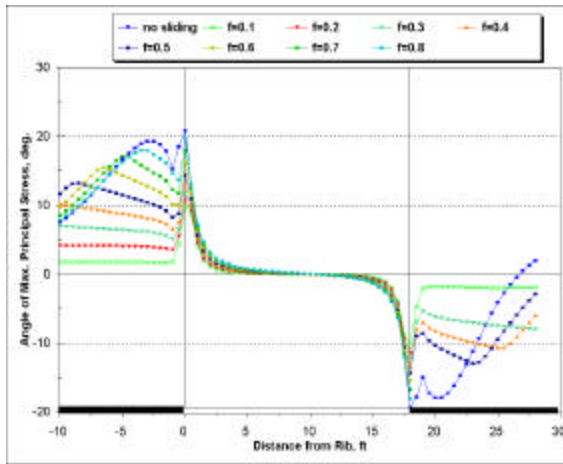
**Table 6-5 Orientations of Max. Principal Stress Near Rib Side (degree)**

Point	Stress Ratio (R)	Coefficient of Friction between Coal and Roof/Floor (f)								No interfaces
		0.1	0.2	0.3	0.4	0.5	0.6	0.7	0.8	
P1	3	19.06	19.28	19.96	21.17	22.63	24.15	25.47	25.52	26.59
	4	13.31	14.19	15.13	16.39	17.95	19.67	21.41	22.26	23.00
	5	9.79	10.82	11.85	13.02	14.45	16.14	17.98	19.86	20.83
	6	7.50	8.48	9.48	10.57	11.83	13.35	15.10	17.02	19.18
	7	5.91	6.79	7.72	8.71	9.83	11.15	12.72	14.55	17.95
P2	3	15.07	14.87	15.00	15.44	15.93	16.33	16.44	16.45	16.22
	4	11.15	11.51	11.86	12.42	13.09	13.76	14.32	14.46	14.30
	5	8.68	9.24	9.73	10.28	10.97	11.72	12.45	13.08	13.03
	6	7.01	7.62	8.17	8.72	9.36	10.09	10.87	11.62	12.14

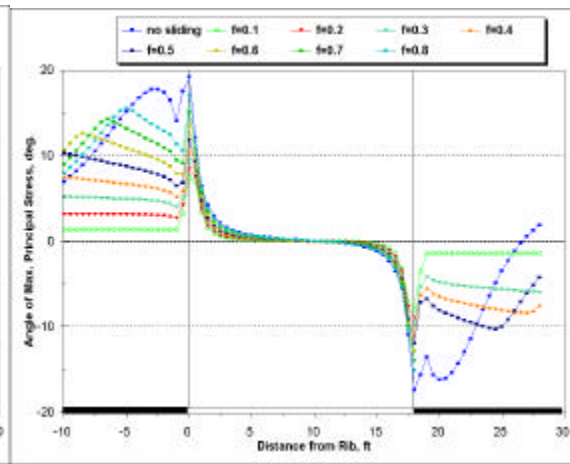


(a) R=3

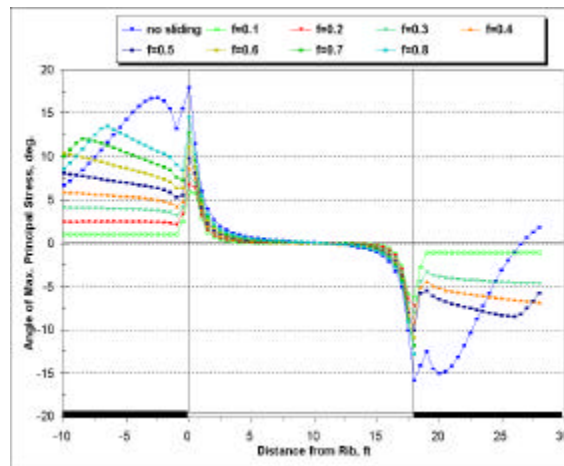
(b) R=4



(c) R=5



(d) R=6



(e) R=7

Fig. 6-36 Orientation of the Maximum Principal Stress with Interface Sliding

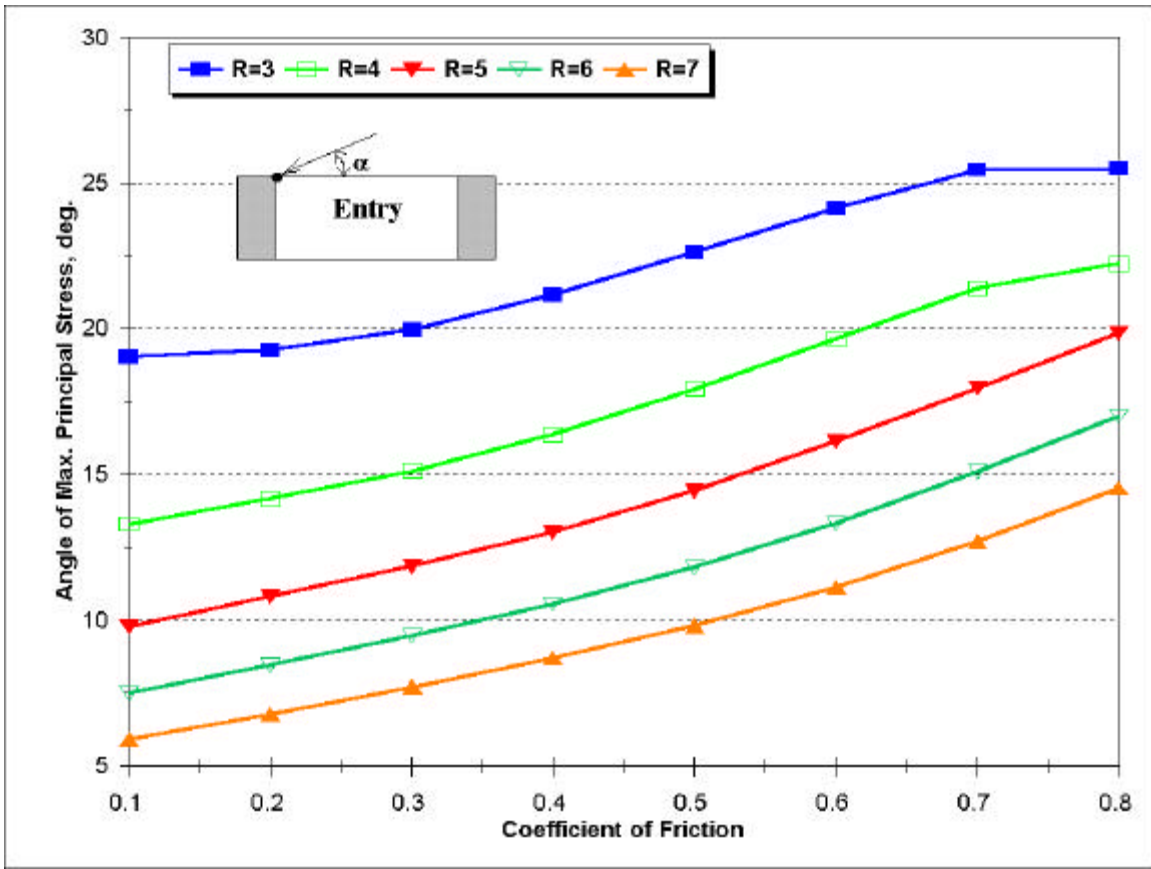


Fig. 5-37 Orientation of the Max. Principal Stress vs. Coefficient of Friction

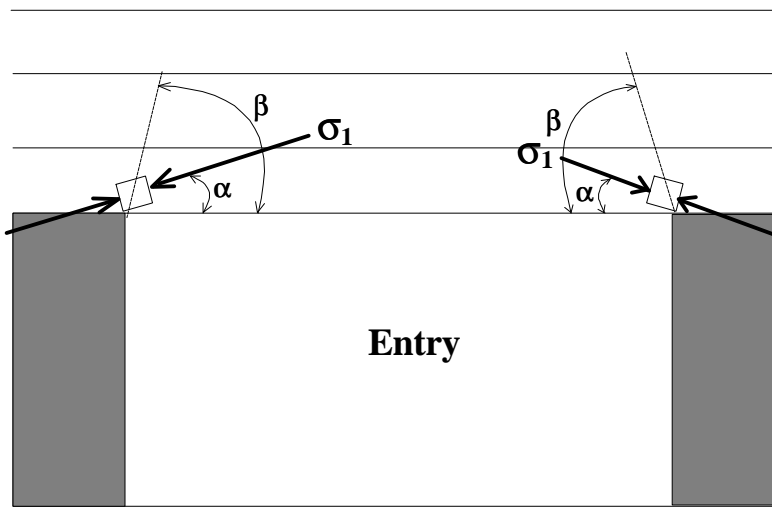


Fig. 5-38 Direction of Roof Failure Plane

### Minimum Principal Stress

As discussed in the previous section, the minimum principal stress at the roof line level changes very slightly with the stress ratio (R) and the coefficient of friction (f), as shown in Fig. 6-39. Generally, the minimum principal stress at the entry center and near the rib sides is smaller when there is no interface sliding between the coal seam and the roof/floor. When the interface sliding occurs, the minimum stress of the minimum principal stress occurs at the entry center. Table 6-6 lists the minimum principal stress at points P1 and P2. It also indicates that the stress changes slightly with the stress ratio (R) and the coefficient of friction (f).

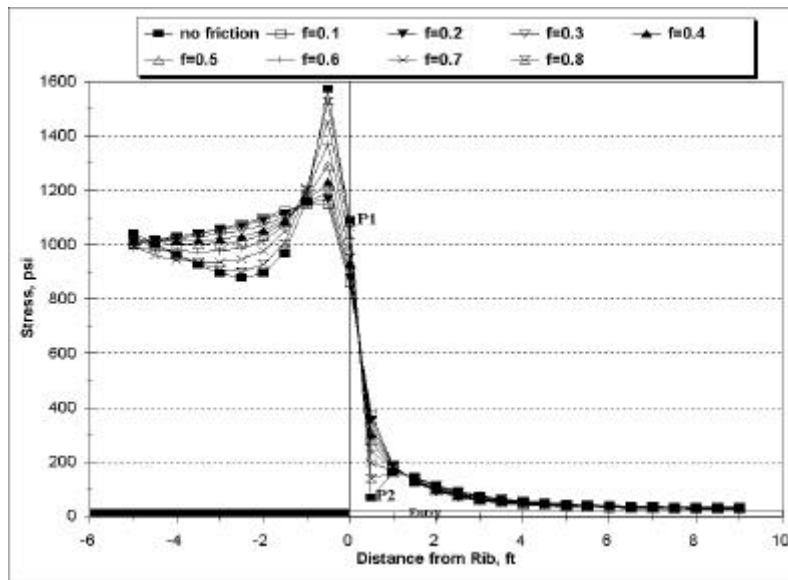


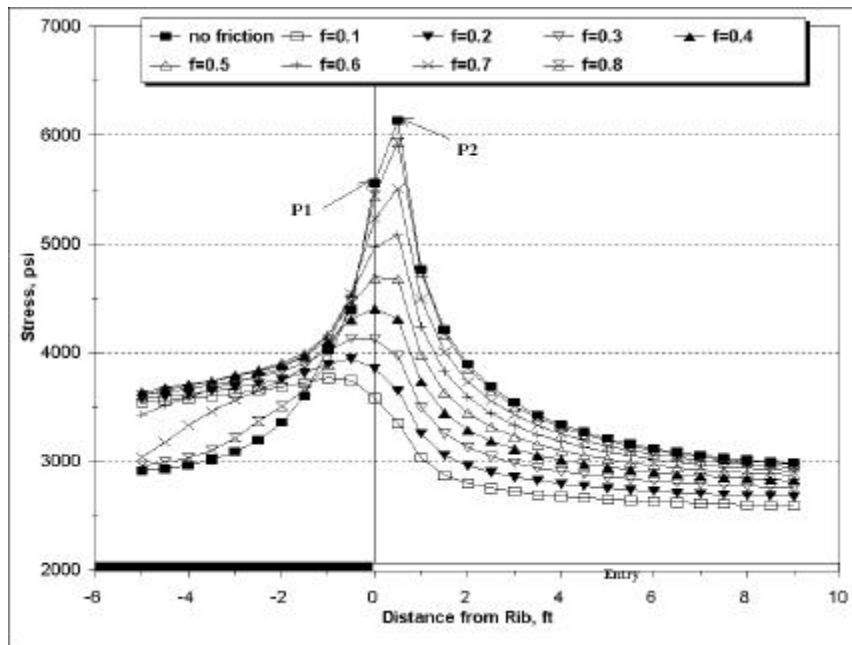
Fig. 6-39 Typical Min. Principal Stress at the Roof Line Level

Table 6-6 Min. Principal Stress Near Rib Side

Point	Stress Ratio (R)	Coefficient of Friction between Coal and Roof/Floor (f)								No interfaces
		0.1	0.2	0.3	0.4	0.5	0.6	0.7	0.8	
P1	3	796	807	827	856	877	877	858	858	841
	4	842	857	876	907	946	977	988	982	920
	5	858	879	901	932	975	1023	1064	1084	1090
	6	860	885	911	942	985	1039	1097	1146	1192
	7	854	881	910	944	985	1039	1104	1171	1287
P2	3	413	403	250	222	187	145	120	119	57
	4	301	276	294	268	237	198	150	131	59
	5	345	322	329	303	275	241	196	141	68
	6	375	355	359	333	306	275	236	184	68
	7	397	382	386	361	334	305	270	224	64

**Stress along Horizontal Direction**

The stress along the horizontal direction is similar to the maximum principal stress at the roof line level. It is concentrated at the rib sides, as shown in Fig. 6-40. Generally, the maximum stress occurs at point P1 when the stress ratio (R) is equal to or less than 3. When the stress ratio (R) is larger than 3 and the coefficient of friction (f) is larger than 0.5, it occurs at point P2. The stress at points P1 and P2 is listed in Table 6-7. Usually, the stress along the horizontal direction is relieved when the interface sliding between the coal seam and the roof/floor occurs.



**Fig. 6-40 Typical Stress along the Horizontal Direction**

**Table 6-7 Stress along Horizontal direction Near Rib Side**

Point	Stress Ratio (R)	Coefficient of Friction between Coal and Roof/Floor (f)								No interfaces
		0.1	0.2	0.3	0.4	0.5	0.6	0.7	0.8	
P1	3	2328	2618	2905	3183	3428	3596	3557	3561	3598
	4	2956	3236	3521	3805	4084	4337	4529	4520	3725
	5	3584	3853	4129	4409	4693	4974	5235	5445	5561
	6	4213	4469	4734	5005	5283	5567	5850	6118	6546
	7	4841	5086	5339	5598	5866	6141	6426	6713	7532
P2	3	2082	2397	2724	3065	3407	3709	3816	3826	3948
	4	2718	3025	3351	3696	4066	4448	4810	4909	5039
	5	3354	3652	3971	4311	4681	5085	5513	5937	6132
	6	3989	4278	4588	4919	5280	5681	6125	6605	7227
	7	4625	4903	5202	5524	5874	6261	6698	7191	8324

Based on the above stress analysis, it is found that the stress in the roof is relieved to some degree when the interface sliding occurs between the coal seam and the roof/floor. If the coefficient of friction in the interfaces is small, the stress in the roof reduces significantly. This will benefit the roof stability. In addition, the stress in the entry roof increases with the coefficient of friction in the interfaces. When the coefficient of friction is larger than 0.6, the stress relief is not significant. However, the maximum stresses of the Von-Mises stress, the maximum principal stress and the stress along the horizontal direction often occur near the entry rib sides.

### **6.5.2 Sliding and Roof Separating**

When the roof separations occur, the stress distributions in the roof are totally different from those without separations. Because of roof separations, the roof actually consists of more layers. Each layer is subjected to high horizontal stress and the friction force between the layers. In this situation, the stress in the roof is larger than that without separations. Generally, the first roof layer is subjected to the largest loading and the roof failure will begin at the first layer. Therefore, the stress in the first layer is mainly analyzed in the following.

#### **Von-Mises Stress**

The typical distribution of the Von-Mises stress is shown in Fig. 6-41. On the lower surface of the first layer, the maximum stress occurs at point P2, near the entry rib sides. The stresses at the two rib sides are not the same. On the upper surface, the maximum stress occurs at the entry center. Since the Von-Mises stress at the rib sides is larger than that at the entry center, the layer may first yield at one rib side.

The Von-Mises stress increases with the stress ratio ( $R$ ) of the horizontal to the vertical stress. As analyzed above, it also increases with the coefficient of friction ( $f_1$ ) in the interfaces between the coal seam and the roof/floor. But it reduces slightly with the coefficient of friction ( $f_2$ ) in the interfaces between the roof layers (Fig. 6-19). Generally, the influence of the coefficient of friction ( $f_2$ ) on the Von-Mises stress is not as significant as that of the coefficient of friction ( $f_1$ ). The Von-Mises stress at points P1 and P2 on the lower surface of the first layer is listed in Table 6-8. The stress in the roof

with roof separation is larger than that without roof separation, especially when the stress ratio is large and the coefficient of friction ( $f_2$ ) in the interfaces between the roof layer is small.

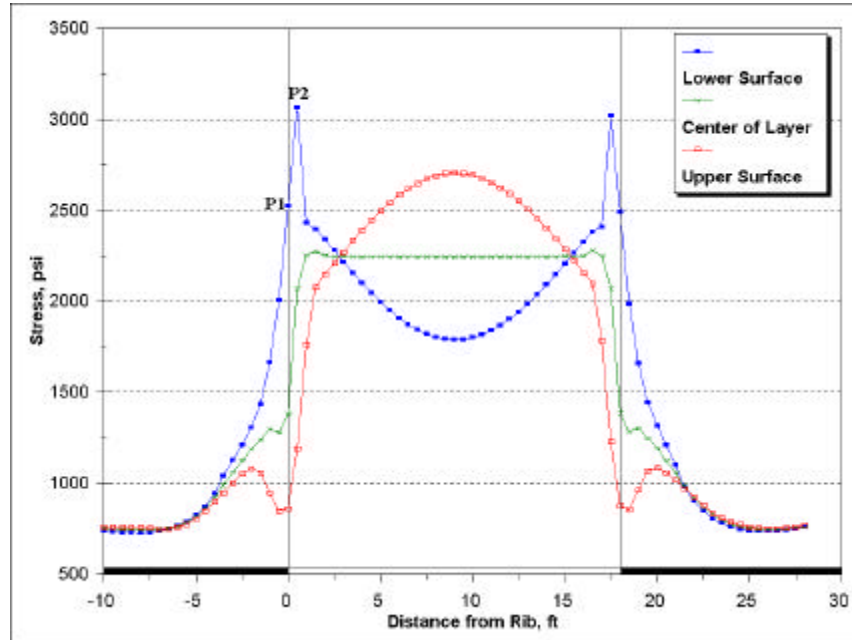


Fig. 6-41 Typical Von-Mises Stress in the First Roof Layer

Table 6-8 Von-Mises Stress at Points P1 and P2

Point	Stress Ratio (R)	Coefficient of Friction ( $f_1$ )	No Separation in Roof	Coefficient of Friction ( $f_2$ )				
				0.2	0.3	0.4	0.5	0.6
P1	3	0.2	1982	2103	2009	1933	1889	1864
		0.4	2564	2524	2444	2414	2377	2364
		0.6	3094	2769	2749	2777	2786	2806
	5	0.2	2931	3234	3094	2986	2921	2878
		0.4	3460	3923	3583	3479	3402	3361
		0.6	4031	4186	3985	3881	3847	3823
	7	0.2	3989	4548	4317	4166	4078	4015
		0.4	4448	5987	4885	4624	4489	4411
		0.6	4947	7210	5564	5120	4889	4828
P2	3	0.2	2089	2491	2362	2282	2218	2171
		0.4	2790	3066	2924	2857	2809	2763
		0.6	3509	3454	3354	3321	3313	3305
	5	0.2	3104	3724	3548	3429	3340	3275
		0.4	3776	4700	4226	4074	3987	3921
		0.6	4589	5205	4885	4703	4622	4583
	7	0.2	4168	5155	4871	4695	4585	4494
		0.4	4788	7312	5730	5358	5175	5048
		0.6	5541	9472	6921	6177	5812	5727

### Maximum Principal Stress

The maximum principal stress in the first layer is similar to the Von-Mises Stress, as shown in Fig. 6-42. On the lower surface of the layer, the maximum stress occurs at point P1, near the entry rib sides, when the stress ratio ( $R$ ) and the coefficient of friction ( $f_1$ ) in the interfaces between the coal seam and the roof/floor are small. Otherwise, it occurs at point P2. On the upper surface, the maximum stress occurs at the entry center.

The maximum principal stress increases with the stress ratio ( $R$ ) of the horizontal to the vertical stress and the coefficient of friction ( $f_1$ ). But it decreases slightly with the coefficient of friction ( $f_2$ ) in the interfaces between the roof layers. Generally, the influence of the coefficient of friction ( $f_2$ ) on the Von-Mises stress is not as significant as that of coefficient of friction ( $f_1$ ). The maximum principal stress at points P1 and P2 on the lower surface of the first layer is listed in Table 6-9. The stress in the roof with roof separation is larger than that without roof separation, especially when the stress ratio is large and the coefficient of friction ( $f_2$ ) in the interfaces between the roof layer is small.

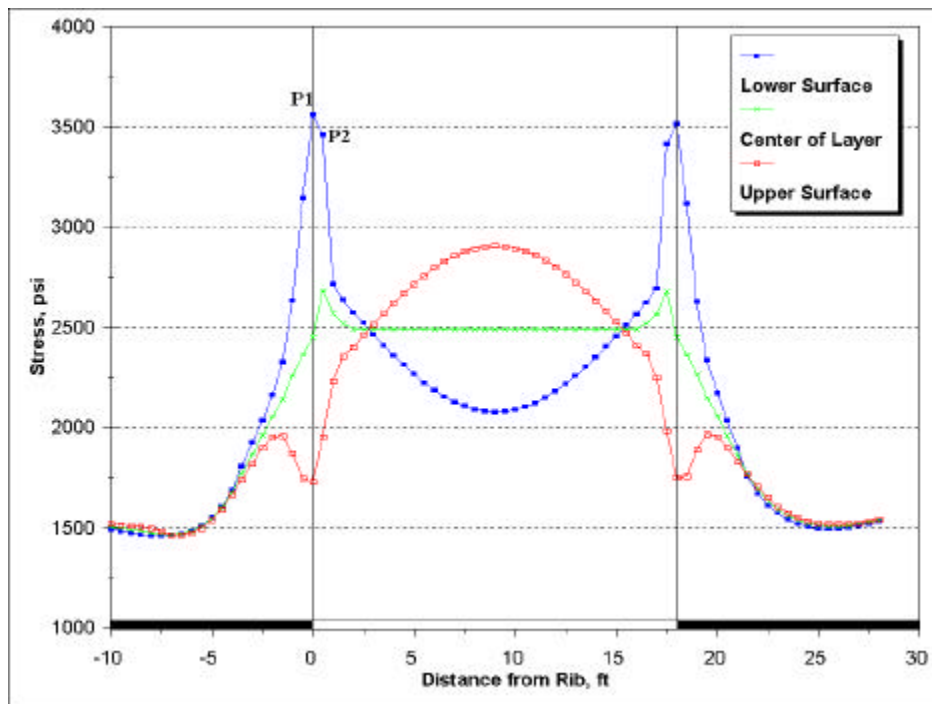


Fig. 6-42 Typical Max. Principal Stress in the first Layer

Table 6-9 Max. Principal Stress at Points P1 and P2

Point	Stress Ratio (R)	Coefficient of Friction ( $f_1$ )	No Separation in Roof	Coefficient of Friction ( $f_2$ )				
				0.2	0.3	0.4	0.5	0.6
P1	3	0.2	2839	3040	2931	2859	2817	2796
		0.4	3532	3560	3458	3432	3410	3407
		0.6	4142	3823	3794	3830	3861	3898
	5	0.2	3962	4292	4144	4047	3989	3953
		0.4	4595	5138	4753	4649	4590	4562
		0.6	5304	5492	5278	5170	5150	5153
	7	0.2	5145	5676	5446	5313	5237	5186
		0.4	5707	7247	6140	5889	5779	5718
		0.6	6339	8513	6981	6535	6309	6278
P2	3	0.2	2546	2857	2724	2645	2586	2545
		0.4	3281	3460	3305	3239	3196	3160
		0.6	4014	3855	3747	3715	3714	3716
	5	0.2	3739	4229	4054	3942	3862	3806
		0.4	4443	5243	4760	4609	4530	4474
		0.6	5293	5772	5450	5263	5188	5160
	7	0.2	4960	5772	5499	5336	5239	5160
		0.4	5614	7854	6375	6025	5864	5756
		0.6	6403	9832	7568	6871	6525	6456

**Orientation of Maximum Principal Stress**

The angle ( $\alpha$ ) between the maximum principal stress and the horizontal direction is shown in Fig. 6-43. It indicates that the angle increases slightly with the coefficient of friction ( $f_2$ ) in the interfaces between the roof layers. The angle is also influenced by the stress ratio (R) and the coefficient of friction ( $f_1$ ) in the interfaces between the coal seam and the roof/floor. Fig. 6-44 and Table 6-10 show the angles in the different cases at one rib side.

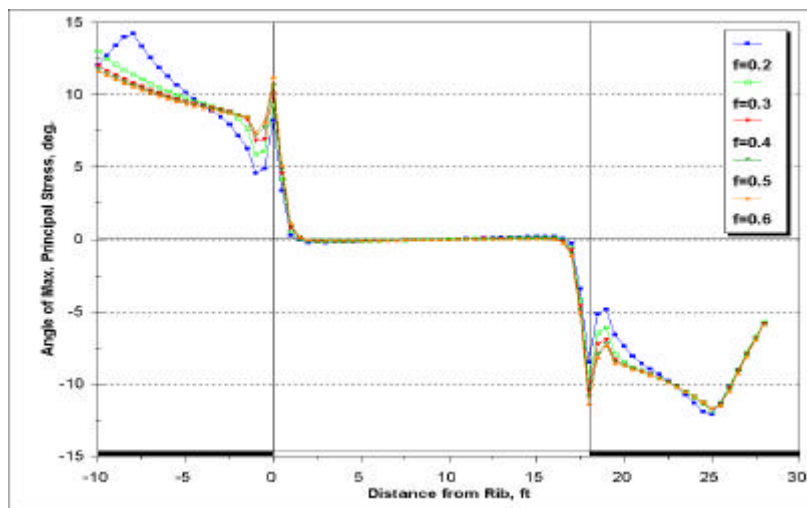
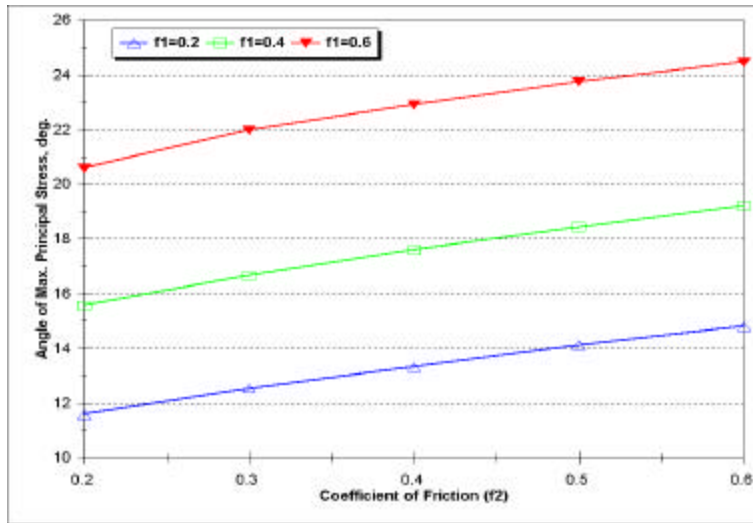
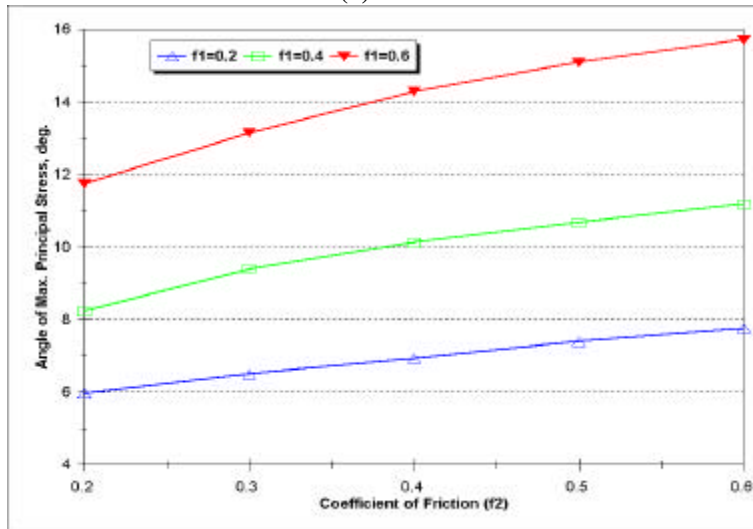


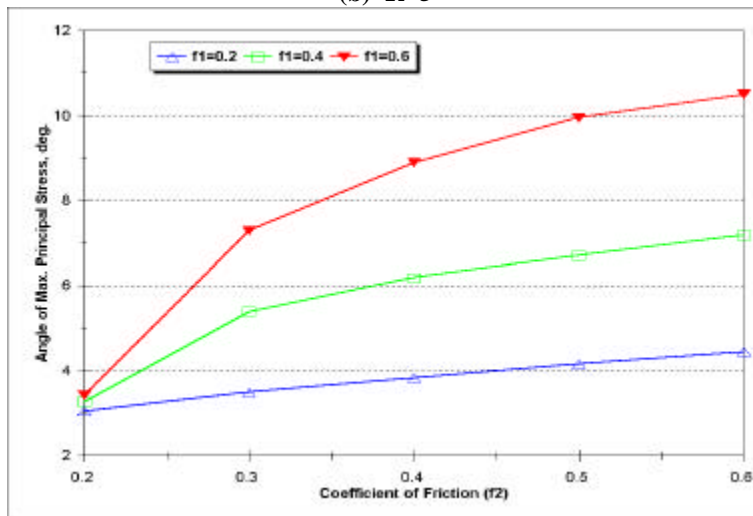
Fig. 43 Orientation of the Max. Principal Stress (R=5,  $f_1=0.4$ )



(a) R=3



(b) R=5



(c) R=7

Fig. 6-44 Orientation of Max. Principal Stress at One Rib Side

**Table 6-10 Orientation of Max. Principal Stress at Points P1 and P2 (degree)**

Point	Stress Ratio (R)	Coefficient of Friction ( $f_1$ )	No Separation in Roof	Coefficient of Friction ( $f_2$ )				
				0.2	0.3	0.4	0.5	0.6
P1	3	0.2	19.28	11.59	12.54	13.32	14.13	14.80
		0.4	21.17	15.57	16.66	17.60	18.44	19.23
		0.6	24.15	20.60	21.99	22.90	23.76	24.46
	5	0.2	10.82	5.96	6.50	6.93	7.40	7.76
		0.4	13.02	8.23	9.40	10.12	10.67	11.19
		0.6	16.14	11.75	13.14	14.28	15.08	15.71
	7	0.2	6.79	3.04	3.48	3.83	4.15	4.44
		0.4	8.71	3.26	5.38	6.19	6.71	7.18
		0.6	11.15	3.41	7.29	8.90	9.96	10.51
P2	3	0.2	14.87	5.72	6.17	6.55	6.82	7.04
		0.4	15.44	6.21	6.78	7.22	7.66	7.96
		0.6	16.33	6.87	7.54	8.05	8.46	8.75
	5	0.2	9.24	3.33	3.61	3.90	4.08	4.25
		0.4	10.28	3.40	4.17	4.57	4.90	5.11
		0.6	11.72	4.05	4.78	5.36	5.80	6.15
	7	0.2	6.41	1.82	2.06	2.31	2.42	2.55
		0.4	7.53	1.14	2.36	2.92	3.33	3.58
		0.6	8.79	0.60	2.23	3.36	4.10	4.43

**Minimum Principal Stress**

The minimum principal stress in the first layer is distributed in a different way, as shown in Fig. 3-45. On the lower surface of the layer, the stress near the entry rib sides is small. At the entry center, the minimum principal stress is larger than that near the rib sides. Because of the high horizontal stress, the entry center is in compression. Without the high horizontal stress, it is in tension. On the upper surface of the layer, the minimum principal stress is the minimum at the entry center. It is totally different from the stress distribution without the horizontal stress. The reason is because the layer deforms along the vertical direction under the horizontal stress. Since roof separation between the first layer and the second layer occurs, a tensile stress along the vertical direction occurs. Fig. 6-46 shows the vertical stress in the first layer. It indicates that a tensile stress occurs at the center of the upper surface. This tensile stress will worsen the roof condition.

Generally, the influence of the stress ratio (R) and the coefficients of friction in the interfaces between the coal seam and the roof/floor and between the roof layers on the minimum principal stress is not significant. Table 6-11 lists the minimum principal stress near the rib sides.

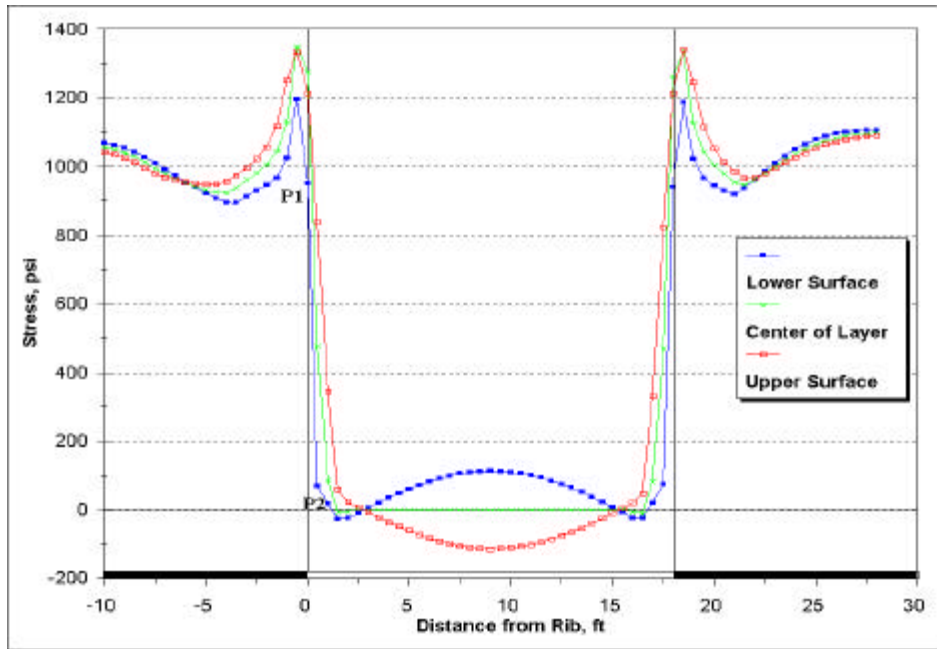


Fig. 6-45 Typical Min. Principal Stress in the First Layer

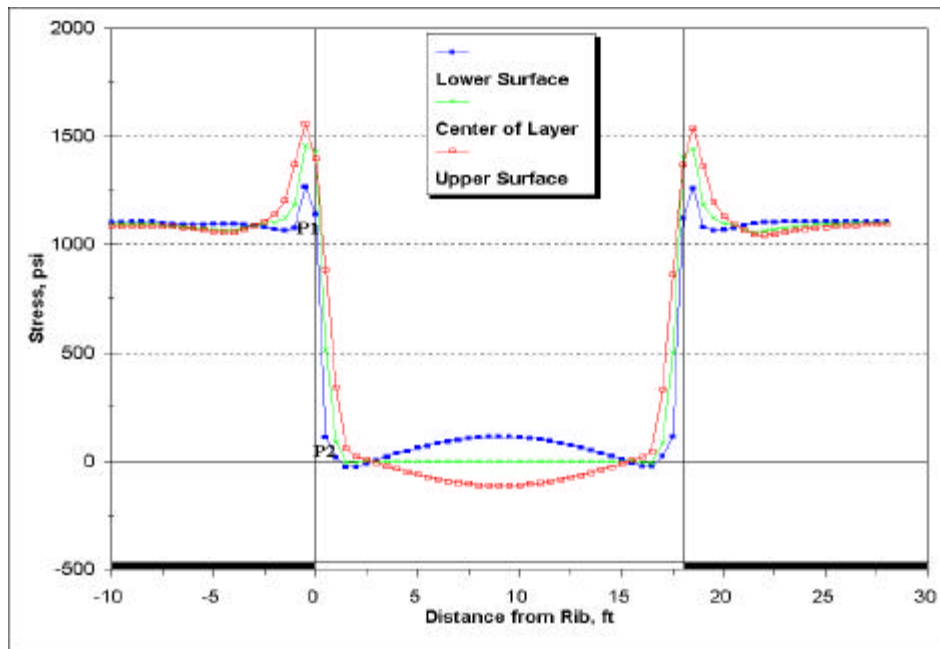


Fig. 6-46 Typical Vertical Stress in the First Layer

**Table 6-11 Min. Principal Stress at Points P1 and P2**

Point	Stress Ratio (R)	Coefficient of Friction ( $f_1$ )	No Separation in Roof	Coefficient of Friction ( $f_2$ )				
				0.2	0.3	0.4	0.5	0.6
P1	3	0.2	807	893	890	909	922	932
		0.4	856	952	937	948	975	990
		0.6	877	935	929	934	961	980
	5	0.2	879	867	879	909	930	945
		0.4	932	964	957	974	1010	1033
		0.6	1023	1042	1055	1066	1090	1128
	7	0.2	881	765	799	843	872	895
		0.4	944	729	875	924	977	1009
		0.6	1039	615	981	1043	1083	1130
P2	3	0.2	403	112	123	135	150	163
		0.4	222	70	73	82	95	112
		0.6	145	26	30	36	45	59
	5	0.2	322	117	140	164	187	206
		0.4	303	34	85	106	127	148
		0.6	241	-3	36	54	71	90
	7	0.2	382	62	112	152	181	208
		0.4	361	-303	21	95	145	184
		0.6	305	-788	-129	22	92	121

**Stress along the Horizontal Direction**

The stress along the horizontal direction in the first layer is similar to the maximum principal stress, as shown in Fig. 6-47. The maximum stress occurs near the entry rib sides. Table 6-12 lists the stress along the horizontal direction at points P1 and P2.

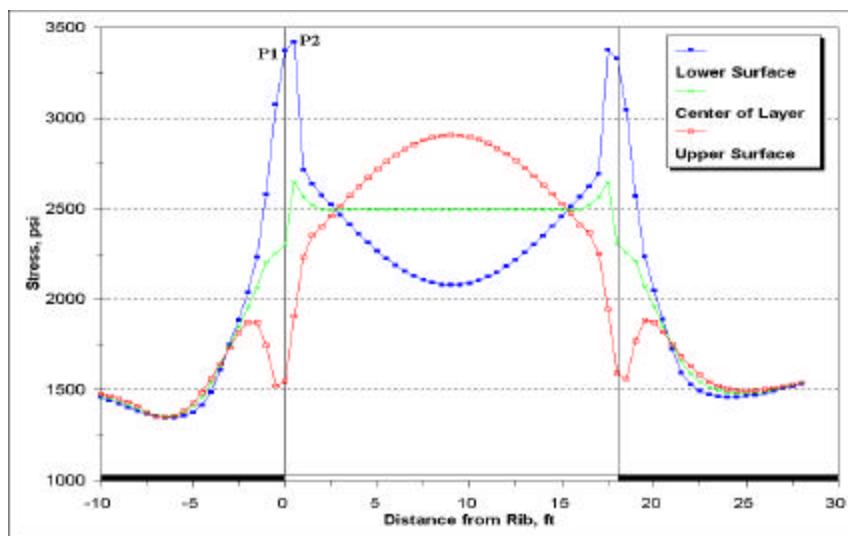


**Fig. 6-47 Typical Stress along the Horizontal Direction in the First Layer**

**Table 6-12 Stress along Horizontal Stress at Points P1 and P2**

Point	Stress Ratio (R)	Coefficient of Friction ( $f_1$ )	No Separation in Roof	Coefficient of Friction ( $f_2$ )				
				0.2	0.3	0.4	0.5	0.6
P1	3	0.2	2618	2953	2835	2755	2705	2674
		0.4	3183	3372	3251	3205	3167	3145
		0.6	3596	3466	3393	3392	3391	3399
	5	0.2	3853	4255	4103	4001	3938	3898
		0.4	4409	5052	4652	4535	4467	4429
		0.6	4974	5308	5060	4921	4876	4858
	7	0.2	5086	5662	5429	5293	5215	5160
		0.4	5598	7226	6094	5831	5714	5644
		0.6	6141	8485	6884	6404	6153	6107
P2	3	0.2	2397	2830	2694	2612	2551	2509
		0.4	3065	3420	3260	3189	3141	3102
		0.6	3709	3800	3683	3643	3634	3632
	5	0.2	3652	4215	4039	3924	3844	3786
		0.4	4311	5225	4735	4580	4498	4440
		0.6	5085	5743	5412	5217	5135	5102
	7	0.2	4903	5766	5492	5328	5230	5151
		0.4	5524	7851	6364	6009	5844	5734
		0.6	6261	9831	7556	6848	6492	6418

When roof separations occur, the Von-Mises stress, the maximum principal stress and the stress along the horizontal direction are concentrated at the entry rib sides. Generally, the stresses at the first layer are larger. Because of roof separations the stresses are much larger than those without separation, especially when the stress ratio (R) of the horizontal to the vertical stress is large and the coefficient of friction in the interfaces between the roof layers is small. In addition, at the center of the upper surface of the first layer a tensile stress occurs along the vertical direction. These are the reasons why the roof failure often occurs in the weak laminated roof.

Roof supports, such as roof bolts, can reduce or eliminate the roof separation. This can decrease the stress in the roof and enhance the roof stability.

## **CHAPTER 7**

### **CONCLUSIONS AND RECOMMENDATIONS**

In this research, the stress distributions in the entry roof in longwall mining have been studied when a high horizontal stress occurs. A special emphasis has been placed upon the influences of the stress angle between the orientation of the maximum horizontal stress and the entry/mining face direction on the stresses in the weak entry roof in the longwall mining. In addition, the effects of the interfaces between the coal seam and the roof/floor and between the roof layers have been analyzed in detail.

The information available in the literature has been reviewed. Using a three-dimensional finite element method, the stresses in the entry roof have been analyzed. The influences of the stress angle, the stress ratio of the maximum horizontal stress to the minimum horizontal stress, and other parameters, such as different overburden depth, on the stress distributions have been investigated through parametric studies. In addition, the influence of the interfaces between the coal seam and the roof/floor on the roof stress has been analyzed when the stress ratio of the horizontal to the vertical stress ranges from 3.0 to 7.0. Roof separations have also been considered in the research. In this case, sliding between the coal seam and the roof/floor and separations in the laminated roof have been taken into account.

#### **7.1 Conclusions**

Based on the results of this research, the following conclusions can be made about the stress distributions in the entry roof during entry development:

- (1) Generally, some factors, such as the stress angle between the orientation of maximum horizontal stress to entry direction, the stress ratio of maximum horizontal stress to minimum horizontal stress and sequence of entry development, can control the effects of high horizontal stress on the entry roof stability. Among these factors, the stress angle is the most important factor.

- (2) In a high horizontal stress field, the stress in the entry roof is much larger than that without the horizontal stress. In addition, the stresses in the roof are not symmetric. Usually, the stresses at one rib side are larger than those at the other rib side.
- (3) During a three-entry development, the Von-Mises stress and the maximum principal stress are concentrated at the entry rib sides. They increase with the stress angle from  $0^{\circ}$  to  $60^{\circ}$ , and then decrease slightly from  $60^{\circ}$  to  $90^{\circ}$ . Generally, they reach the maximum when the angle is about  $60^{\circ} \sim 75^{\circ}$ . The influence of the angle on the minimum principal stress is not significant. Therefore, the angle between the mining direction and the maximum horizontal stress should be less than  $30^{\circ}$ , when a longwall panel is designed. In this case, the roof stress is small, although the stress is slightly larger than that when the angle is  $0^{\circ}$ .
- (4) The patterns of the Von-Mises stress distributions along entry rib sides are also affected by the stress angle. When the angle is less than  $45^{\circ}$ , the maximum stress occurs near the entry face during the entry development. When the angle is equal to or larger than  $45^{\circ}$ , the roof stress along the whole entry is large. At the entry center, the maximum stress of the Von-Mises stress always occurs near the entry face.
- (5) At the intersections between an entry and a crosscut, the stresses are larger at the pillar corners. The Von-Mises stress and the maximum principal stress increase with the angle between the maximum horizontal stress and the axial direction of the crosscut. In a cross section, the Von-Mises stress at one pillar corner is larger than that at the other corner when the angle is less than  $45^{\circ}$ , but it reverses when the angle is equal to or larger than  $45^{\circ}$ .
- (6) The stress ratio of the maximum to the minimum principal stresses has little influence on the roof stress. Its effect depends on the stress angle. When the angle is equal to or less than  $45^{\circ}$ , the Von-Mises stress decreases with the ratio from 1.0 to 2.0, and then very slightly from 2.0 to 3.0. When the angle is larger than  $45^{\circ}$ , the influence of the stress ratio on the Von-Mises stress can be ignored.

- (7) In a high horizontal stress field, the overburden depth is not an important factor. Since the vertical stress is much less than the horizontal stress, the influence of the overburden depth on the Von-Mises stress and the maximum principal stress in the roof is not significant. But, as the overburden depth increases, the minimum principal stress at the entry center decreases.

In a longwall mining system, the entries near the mining face are subjected to the large front abutment pressure caused by the mining face. Without a high horizontal stress, the entries at the T-junctions are generally in a worse condition. When a high horizontal stress occurs, the stresses in the entry roof at the T-junctions increase. The stresses at the T-junctions are distributed in the following ways:

- (1) The Von-Mises stress and the maximum principal stress at the T-junctions in a single panel increases with the stress angle between the maximum horizontal stress and the mining direction. Generally, the T-junctions are in the worst stress conditions when the stress angle is equal to or more than  $60^{\circ}$ .
- (2) When the maximum horizontal stress is from the headgate side in a single panel, the stresses, such as the Von-Mises stress and the maximum principal stress, at the T-junction in the headgate is larger than that in the tailgate.
- (3) In a multiple-panel system, the tailgate entries in the current mining panel will be heavily affected by the adjacent mined-out panel. Since the tailgate entries are subjected to the side abutment pressure caused by the mined-out panel, the tailgate entries are generally in the worst conditions. The stresses in the headgate entries are smaller than those in a single panel. Therefore, the headgate entries are in a better condition as compared to the tailgate entries.
- (4) The stress angle between the maximum horizontal stress and mining direction also has a significant effect on the entry roof stability in a multiple-panel system. However, the entries in a multiple-panel system are less sensitive to the stress angle than those in a single panel. In a single panel, the stress increases with the stress angle rapidly, especially when the angle is less than  $60^{\circ}$ . But in a multiple-panel system, the stress increases with the stress angle gradually.

- (5) The direction of the maximum horizontal stress has some effects on the stresses in the entry roof. In a multiple-panel system, when the horizontal stress is from the gob side (the mined-out panel side), the stress at the T-junction in the headgate is larger than that from the solid coal side. For the tailgate entries, it reverses.
- (6) The influence of the stress angle on the minimum principal stress on the roof is small. Generally, the minimum principal stress in the roof increases under a high horizontal stress. In addition, the minimum stress occurs at the entry center.

When the interface sliding between the coal seam and the roof/floor and between the roof layers occurs, the pillar moves toward the entry and roof separations occur. In this situation, the roof stresses have the following characteristics:

- (1) Once the sliding between the coal seam and the roof/floor occurs, the stresses, such as the Von-Mises stress and the maximum principal stress will be reduced to some degrees. If the coefficient of friction in the interfaces is small, the stresses in the roof are reduced significantly. This will benefit the roof stability. In addition, the stress magnitude depends both on the stress ratio of the horizontal to the vertical stress and on the coefficient of friction in the interfaces. The roof stresses increase with the stress ratio and the coefficient of friction.
- (2) The patterns of the stress distributions in the entry roof do not change, when the interface sliding between the coal seam and the roof/floor occurs. Without the interface sliding, the Von-Mises stress and the maximum principal stress are concentrated at the entry rib sides. When the interface sliding occurs, the maximum stresses of the Von-Mises stress and the maximum principal stress also occur near the rib sides.
- (3) The minimum principal stress at the roof line level changes very slightly with the stress ratio and the coefficient of friction.
- (4) When roof separations occur, the lowest layer is subjected to the largest loading. In this case, the stresses on the two opposing surface of the layer are

different. Generally, the maximum stress occurs near the entry rib sides on the lower surface. The roof stresses with roof separations are larger than those without roof separations.

- (5) The roof stresses increase with the stress ratio of the horizontal to the vertical stress and the coefficient of friction in the interfaces between the coal seam and the roof/floor. But the influence of the interface sliding between the roof layers on the roof stresses is not significant. Usually, the roof stresses reduce slightly with the coefficient of friction in the interfaces between the roof layers.
- (6) The minimum principal stress in the first layer is distributed in a different way. On the lower surface of the layer, the stress near the entry rib sides is small. At the entry center, the minimum principal stress is larger than that near the rib sides. On the upper surface of the layer, the minimum principal stress is the minimum at the entry center. The reason is because the layer deforms along the vertical direction under the horizontal stress. Since roof separation between the first layer and the second layer occurs, a tensile stress at the center of the upper surface occurs along the vertical direction. This tensile stress will worsen the roof condition.
- (7) Generally, the influence of the stress ratio and the coefficients of friction in the interfaces between the coal seam and the roof/floor and between the roof layers on the minimum principal stress is not significant.

## 7.2 Recommendations for Panel Design and Entry Roof Support

The headgate entries are the most important entries in a longwall panel. They are used for the coal transportation, material transportation, ventilation and mantrip. Any roof problems in the belt entry will delay coal production. Therefore, a good longwall panel design should have a good roof condition in the headgate entries.

As analysis previously, the longwall entries and face will be in a good condition when the mining direction is parallel to the maximum horizontal stress. In addition, in a multiple-panel system, when a maximum horizontal stress is from the solid coal side, the roof stresses at the T-junctions are smaller than those when the horizontal stress is from the gob side. Therefore, based on the knowledge gained through this investigation, it is recommended that:

- (1) The angle between the orientation of the maximum horizontal stress and the direction of longwall face retreat should be kept to a minimum if possible. When the angle is  $0^{\circ}$ , namely the maximum horizontal stress is perpendicular to the mining direction, the longwall entries will be in the best stress conditions. If the mining direction must be biased to the maximum horizontal stress, the angle should be less than  $30^{\circ}$ . Because the stress in the entry roof increases rapidly when the angle is larger than  $30^{\circ}$ .
- (2) If a longwall panel is angled to the orientation of the maximum horizontal stress, the panel retreat should be sequenced as shown in Fig. 7-1. The maximum horizontal stress ( $\sigma_{hmax}$ ) is always from the tailgate side. In this case, the roof stress in the headgate entries is smaller. When panel 1 is being mined, the roof stress in the headgate entries is slightly larger than that in the tailgate entries. However, after panel 1 is mined out, the roof stress in the headgate entries reduces. The headgate entries will be in better condition. For panels 4~6, panel 4 should be mined out first, and then panels 5 and 6.
- (3) Once the crosscuts have roof problems because they are perpendicular to the maximum horizontal stress, they can be angled to the entries.

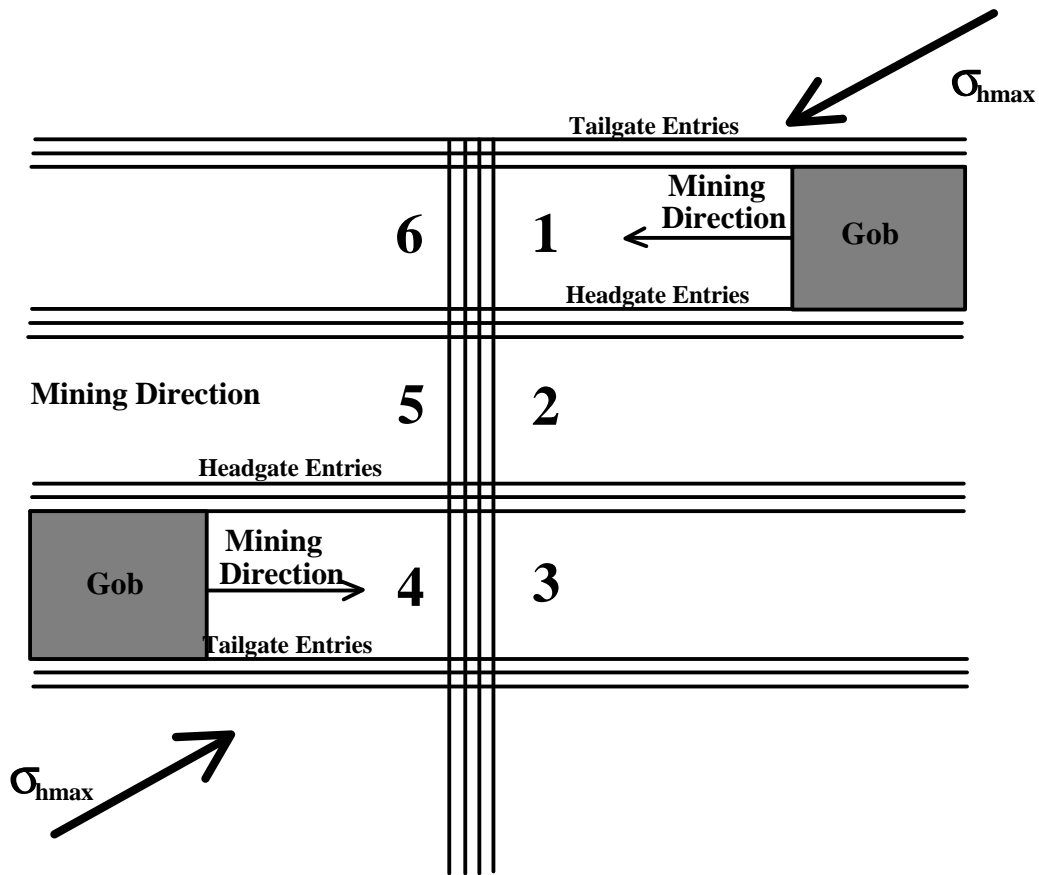


Fig. 7-1 Recommendation of Longwall Panel Design

In a high horizontal stress field, the roof stresses in longwall entries, such as the Von-Mises stress and the maximum principal stress are concentrated along the two entry rib sides, and the stress distributions are not symmetrical. Generally, the stresses at one rib side are larger than those at the other side. Under the high horizontal stress, tensile stress may occur in the entry roof. In addition, the roof stress without roof separations is less than that with roof separations. Therefore, the suitable roof support should

- (1) prevent entry roof from separating;
- (2) reduce or eliminate the tensile stress in the entry roof; and
- (3) choose the support parameters according to roof stress distributions.

## REFERENCES

1. Agapito, J.F.T., Mithcell, S.J., Hardy, M.P., Aggson, J.R., and Hoskins, W.N., "A Study of Ground Control Problems in Coal Mines With High Horizontal Stresses", The State of the Art in Rock Mechanics, Proceedings, 21<sup>st</sup> US Symposium on Rock Mechanics ,Rolla, MO, 1980, p.185~825.
2. Ahola, M. and Kripakov, N., "Analysis of Cutter Roof Using the Boundary-Element Method", Proceeding, 6<sup>th</sup> Conference on Ground Control in Mining, WV University, Morgantown, WV, 1987, p.107~117.
3. Bieniawski, Z.T., "Strata Control in Mineral Engineering", John Wiley & Sons, 1987, p.111~146.
4. Blevins, C.T., "Coping with High Lateral Stresses in an Underground Illinois Coal Mine", Proceeding, 2<sup>nd</sup> Conference on Ground Control in Mining, WV University, Morgantown, WV, 1982, p.137~141.
5. Blevins, C.T., "Ground Control Experience in a High Horizontal Stress Field at Inland Steel Coal Mine No. 2", Proceeding, 4<sup>th</sup> Conference on Ground Control in Mining, WV University, Morgantown, WV, 1985, p.227~233.
6. Chang, Steve H., "A Finite Element Simulation of Elasto-Plastic Contact Problems" West Virginia University, Dissertation, 1985, p.4~35.
7. Chen, H.J. and Peng, S.S., "Mechanism of Roof Failure in Longwall Entry System under High Horizontal Stress Condition", 1998 SME meeting, preprint No. 98-163.
8. Chen, H.J. and Peng, S.S., "Stress Distributions in Three-Entry Development Under High Horizontal Stress", 1999 SME meeting, preprint No. 99-149.
9. Cassie, J. and McLennan, A., "Formation of Face Headings Using Stress Relief at Asfordby Mine", Proceeding, 16<sup>th</sup> Conference on Ground Control in Mining, WV University, Morgantown, WV, 1997, p.58~67.
10. Dahl, H.D. and Parsons, R.C., "Ground Control Studies in the Humphrey No.7 Mine, Christopher Coal Div., Consolidation Coal Co.", SME Transactions, Vol. 252, 1972, p.211~222.
11. Farmer, I., "Coal Mine Structures", Chapman and Hall Ltd, 1985, p.153~215.

12. Gale, W.J., Nemcik, J.A., and Upfold, R.W., "Application of Stress Control Methods to Underground Coal Mine Design in High Lateral Stressfield", Proceeding, 6<sup>th</sup> International Congress on Rock Mechanics, International Society for Rock Mechanics, 1987, p.897~900.
13. Gale, W.J., "Strata Control Utilising Rock Reinforcement Techniques and Stress Control Methods, in Australian Coal Mines", The Mining Engineer, Jan. 1991, Vol. 150, No. 352, p.247~253.
14. Gercek, H., "Stability of Intersections in Room-and-Pillar Coal Mining", Pennsylvania State University, Dissertation, 1982, p.47~125.
15. Hanna, K., Haramy, K., Conover, D., and Dopp, D., "Effect of High Horizontal Stress on Coal Mine Entry Intersection Stability", Proceeding, 5<sup>th</sup> Conference on Ground Control in Mining, WV University, Morgantown, WV, 1986, p.167~182.
16. Hart, W.M., Schissler, A., and Chen, J.S., "Analysis of Entry Roof Failure and Falls at Springvale Colliery", Proceeding, 15<sup>th</sup> Conference on Ground Control in Mining, Colorado School of Mines, Golden, CO, 1996, p.193~207.
17. Herget, G., "High Stress Occurrences in the Canadian shield", Proceedings, 23<sup>d</sup> US Symposium on Rock Mechanics, Rolla, MO, 1982, p.203~210.
18. Hill, J.L. and Bauer, E.R., "An Investigation of the Cutter Roof Failure in a Central Pennsylvania Coal Mine: A Case Study", Rock Mechanics in Productivity and Protection 25<sup>th</sup> Symposium on Rock Mechanics, 1984, p.603~614.
19. Hoek, E. and Brown, E.T., "Underground Excavations in Rock", Institute of Mining and Metallurgy, London, 1980
20. Jaeger, J.C. and Cook, N.G.W., "Fundamentals of Rock Mechanics" Third Edition, London, 1979, p.25~231.
21. Jeremic, M.L., "Coal Mine Roadway Stability in Relation to Lateral Tectonic Stress - Western Canada", Mining Engineering, June 1981, p.704~709.
22. Jeremic, M.L., "Strata Mechanics in Coal Mining" A.A. Balkema Publisher, 1985, p.97~430.

23. Khair, A.W., "Failure Criteria Applicable to Pressurized Cavities in Geologic Materials under In-Situ Stress Conditions", The Pennsylvania State University, Dissertation, 1972, p.166~183.
24. Kripakov, N.P., "Alternatives for Controlling Cutter Roof in Coal Mines", Proceeding, 2<sup>nd</sup> Conference on Ground Control in Mining, WV University, Morgantown, WV, 1982, p.142~151.
25. Krupa, E.D. and Khair, A.W., "Assessment of Underground Structural Design", Proceeding, 10<sup>th</sup> Conference on Ground Control in Mining, WV University, Morgantown, WV, 1991, p.14~25.
26. Laursom, P.G. and Cox, W.J., "Mechanics of Materials" John Wiley & Sons, INC., 1954, p.35~150.
27. Mark, C., "Horizontal stress and its effects on longwall ground control", Mining Engineering, November 1991, p.1356~1360.
28. Mark, C., Mucho, T.P., and Dolinar, D., "Horizontal Stress and Longwall Headgate Ground Control", Mining Engineering, January 1998, p.61~68.
29. Mucho, T.P. and Mark, C., "Determining the Horizontal Stress Direction Using the Stress Mapping Technique", Proceeding, 13<sup>th</sup> Conference on Ground Control in Mining, WV University, Morgantown, WV, 1994, p.277~289.
30. Mucho, T.P., "Roof Control Problems on Development and Longwall Gateroads at a Southwestern PA Coal Mine", Proceeding, 5<sup>th</sup> Conference on Ground Control in Mining, WV University, Morgantown, WV, 1986, p.278~282.
31. Oyler, D.C., Campoli, A.A., and Chase, F.E., "Factors Influencing the Occurrence of Coal Pillar Bumps at the 9-Right Section of the Olga Mine", Proceeding, 6<sup>th</sup> Conference on Ground Control in Mining, WV University, Morgantown, WV, 1987, p.10~17.
32. Peng, S.S. and Wang, Y.J., "Cutter Roof Initiation and Propagation in Multiple-Entry Development Subject to High Horizontal Stress", 1996 SME meeting, preprint No. 96-172.
33. Plumb, R.A. and Cox, J.W., "Stress Directions in Eastern North America Determined to 4.5 km From Borehole Elongation Measurement" Journal of Geophysical Research, Vol. 92, No. B6, May 1987, p.4905~4816.

34. Roley, R.W., "Pressure cutting: A Phenomenon of Coal Mine Roof Failure", *Mechanization*, Vol. 12, No. 12, 1948, p.69~74.
35. Schissler, A.P. and Chen, J.S., "Horizontal Stress Multiplier on Coal Mine Ground Control", presented at 1998 SME Annual Meeting, Orlando, FL, March 1998.
36. S.C.T. "What is Roof Bolting ?", *Strata Control Technology (Training Program)*
37. Siddal, R.G., "Stress Effects Within the Selby Coalfield", *Technology in Mining*, Institute of Mining Elec. and Mining Mechanics Engineering, 1989, p13.
38. Su, W.H. and Peng, S.S., "Cutter Roof and Its Causes", *Mining Science and Technology*, Vol.4, 1987, p.113~132.
39. Su, D.W.H. and Hasenfus, G.J., "Regional Horizontal Stress and Its Effect on Longwall Mining in the Northern Appalachian Coal Field", *Proceeding, 14<sup>th</sup> Conference on Ground Control in Mining*, WV University, Morgantown, WV, 1995, p.39~45.
40. Sun, S.F., Fang, X.S., and Lu, Y.H., "Mechanics of Materials" The Education Publishing Press, 1965, p.314~321 (in Chinese).
41. Wang, Y.J. and Peng, S.S., "High Horizontal Stress Effects on Longwall Gate Entry Stability", *Proceeding, 15<sup>th</sup> Conference on Ground Control in Mining*, Colorado School of Mines, Golden, CO, 1996, p.179~191.
42. Zoback, M.L. and Zoback, M.D., "Tectonic StressField of the United States" *Geophysical Framework of the Continental U.S.*, Geol. Soc. Am., Memoir 172, p.523~539.



## VITA

Hanjie Chen was born on August 13, 1958 in Shaanxi, People's Republic of China. He obtained his Bachelor of Science Degree in Mining Engineering in 1982 and Master of Science Degree in Mining Engineering in 1984 from Xi'an Mining Institute, China.

After graduation, he worked as a lecturer in the Department of Mining Engineering, Xi'an Mining Institute. From October, 1993 to August 1995 he studied and worked as a visiting scholar in the Department of Structural Engineering, University of Manchester Institute of Science and Technology (UMIST), U.K..

In August 1995, he enrolled in the Ph.D program in Mining Engineering at West Virginia University. Thereafter, he has been working as a graduate research assistant in the Department of Mining engineering, West Virginia University.